JRC Scientific and Technical Reports

Climate and air quality impacts of combined climate change and air pollution policy scenarios

John van Aardenne, Frank Dentener, Rita Van Dingenen, Greet Maenhout, Elina Marmer, Elisabetta Vignati, Peter Russ, Laszlo Szabo and Frank Raes

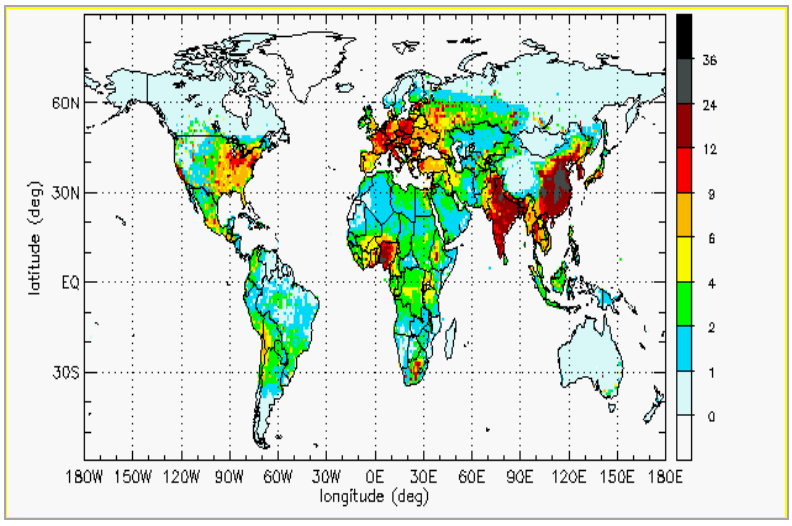

LOSS OF LIFE EXPECTANCY in the year 2000 due to Particulate Matter (months)

EUR 24572 EN - 2010

JRC EUROPEAN COMMISSION

ies Institute for Environment and Sustainability

European Commission
Joint Research Centre
Institute for Environment and Sustainability

Contact information
Frank Dentener
Address: Via E. Fermi 2749, I-21027 Ispra (VA),Italy
E-mail: frank.dentener@jrc.ec.europa.eu
Tel: +390332786392
Fax: +390332785837

http://ies.jrc.ec.europa.eu/
http://www.jrc.ec.europa.eu/

JRC61281

EUR 24572
ISBN 978-92-79-17454-4
ISSN 1018-5593
doi:10.2788/33719

Luxembourg: Publications Office of the European Union

Printed in Italy

Climate and air quality impacts of combined climate change and air pollution policy scenarios

John van Aardenne, Frank Dentener, Rita Van Dingenen, Greet Maenhout, Elina Marmer, Elisabetta Vignati, Peter Russ, Laszlo Szabo and Frank Raes.

October 2010

Table of contents

1. Introduction

2. Model description

2.1 POLES

2.2 EDGAR

2.3 TM5

3. Scenarios

3.1 Scenario 1: no further climate and air quality policies (BAU)

3.2 Scenario 2: global climate policy only (CARB)

3.3 Scenario 3: global air quality policy (BAP)

3.4 Scenario 4: integrated air quality and climate policy (CAP)

3.5 Scenario 5 and Scenario 6: intermediate global air quality policy in non OECD countries

3.6 Resulting emissions trends

4. Results from impact assessment

4.1 Surface and column concentrations for ozone and particulate matter

4.2 Impacts of ozone on vegetation

4.3 Impacts of nitrogen deposition on vegetation

4.4 Effects of PM and O_3 on human health

4.5 Effects on climate: aerosol and ozone forcing

4.6 CH_4, CO_2 and N_2O concentrations pathway

4.7 Integrated radiative forcing and uncertainties

5. Discussion and conclusions

References

Annex 1: Definitions of geographic areas

Annex 2: Examples of coupling POLES and EDGAR data

Annex 3: Effects of air pollutants on vegetation and health

Annex 4: Calculation of Radiative Forcing for aerosols and ozone

1. Introduction

To improve the capability of DG ENV (Directorate General Environment) to analyze climate change and air pollution policies, swift access to model runs and correct interpretation with existing models and databases used in-house at the European Commission is required. With that in mind DG ENV Directorate C has made an Administrative Arrangement (070402/2006/453771/MAR/C5) with DG JRC-IPTS and DG JRC-IES for consistent and effective technical analysis.

Specifically, we describe the coupling of the global partial equilibrium energy model POLES (Prospective Outlook on Long-term Energy Systems) with the global emissions database EDGAR (Emission Database for Global Atmospheric Research). Scenarios for greenhouse gases and air pollutants are developed, based on the POLES output, and on assumptions on further air pollution emission reductions for the period 2000-2050. The resulting scenarios are subsequently used in the global atmospheric chemistry transport model TM5 (Tracer Model version 5), and impacts on vegetation, human health and climate are evaluated. The focal years of the impact assessment are 2030 and 2050, which is of immediate importance for air quality management in the next decades.

Section 2 describes the models used in this analysis. Section 3 describes the rationale behind the scenario analysis, the construction of different emission scenarios and resulting emission trends. Chapter 4 presents the model results, and an integrated assessment of the impacts on vegetation, human health, and climate. Chapter 5 presents the conclusions.

2. Model description

2.1 POLES

The POLES partial equilibrium energy model (run at JRC IPTS) describes potential trends up to 2050 in global and European energy use and industrial activities taking into account impacts of climate policies on future energy consumption and process technologies. As described in more detail in Russ et al. (2007) the model performs yearly simulations of energy demand and supply by taking into account the effects of income, fuel prices, technology developments and energy policies and calculates resulting greenhouse gases. The POLES model defines 47 world regions for which the model calculated detailed energy balances based on a single world oil market, three regional coal markets (America, Europe and Asia) and a national gas market that follows bilateral trading. The fuel prices are determined endogenously with oil price depends on the reserve to production ratio.

The POLES scenarios applied in this study are based on the baseline scenario and the greenhouse gas reduction scenario, used for the 2009 Communication from the Commission "Towards a comprehensive climate change agreement in Copenhagen" (Russ et al. 2007). In the POLES baseline scenario, energy consumption from 2000 to 2050 is driven by population and economic growth but not by energy efficiency/climate change policies. In the POLES greenhouse gas scenario, energy consumption from 2000 to 2050 is not only driven by population and economic growth but also by climate policies and measures aiming at reducing global greenhouse gas emissions in the energy sector by 25% in 2050 compared to the 1990.

The scenarios provide trends for the sectors electricity production, industry, transport (excluding shipping), residential and services, and production of primary fuel. The following fuel types where considered: coal, coke, electricity, gas, geothermal, heat, hydro, nuclear, oil, renewable, wood and waste fuels. Due to systematic differences in the base year datasets of fuel by sector between POLES and EDGAR, the data provided by IPTS are in the form of annual growth rates by fuel-sector combination for periods 2000-2005, 2005-2010, 2010-2020, etc. These growth rates are subsequently applied to the best current estimates for GHG and air pollution emissions as generated by the more detailed EDGAR database (see section 2.2).

Trends in agriculture, land use and waste are provided from the ADAM project (P. Russ, D. van Vuuren, personal communication, 2008) with emission trends given by world

region for a baseline scenario and a stabilization scenario (450 ppm) based on runs with the IMAGE model.

More details are discussed in section 3.

2.2 EDGAR

The Emission Database for Global Atmospheric Research (EDGAR) is hosted at and further developed by IES in collaboration with the Dutch Environment Assessment Agency (PBL). EDGAR provides historical (1970-2005) global anthropogenic emissions of greenhouse gases CO_2, CH_4, N_2O, HFCs, PFCs and SF_6, of precursor gases CO, NOx, NMVOC and SO_2 and the aerosols BC and OC per source category both at country and region levels as well as on grid. Emissions are calculated by taking into account activity data such as fuel consumption by sector, installed abatement measures, uncontrolled emission factors and emission reduction effects of control measures. Emissions are calculated for ~230 countries for the emission source (sub)groups; (i) combustion/conversion in energy industry, manufacturing industry, transport and residential sectors, (ii) industrial processes, (iii) solvents and other product use, (iv) agriculture, (v) large scale biomass burning, (vi) waste and (vii) miscellaneous sources.

In order to match POLES source-sectors with those of EDGAR, an aggregated emission dataset has been compiled using EDGAR that distinguishes the following emissions groups: industry (IND = combustion in electricity and manufacturing industry), domestic (DOM), land transport (TRA), aviation (AIR), international shipping (SEA), industrial processes (IPR = process and fugitive emissions incl. solvents), agriculture (AGR) and waste handling (WST) for the 47 regions identified in POLES. Annex 1 presents and overview of the link between the EDGAR countries and the POLES regions.

Construction of the base year2000 emissions

For consistence with POLES, the base year 2000 was chosen as a starting point for the scenarios. Emissions from the energy system (IND/DOM/TRA) have been calculated using an emission factor approach. Activity data for the period 2000-2005 have been taken from the EDGARv4_preliminary version dataset where the 94 sector and 64 fuel type combinations have been aggregated into the POLES fuel sector definition. The basis of this activity dataset is formed by the energy balances of OECD (Organisation for Economic development and co-

operation) countries (1960-2005) and non-OECD countries (1971-2005) (OECD, 2007) with modifications of IEA data to account for ~70 individual countries summed under the IEA regions Other Latin America, Other Africa and Other Asia. Furthermore, since the IEA data is known to be weak in covering the residential biofuel combustion in non-OECD countries, data for fuelwood combustion have been taken from FAO data and use of crop residues and dung are taken from the EDGARv4_preliminary version agricultural datasets (e.g. crop residues left on the field).

Reduction percentages on emission factors have been taken from three sources of information. For the EU 27, and to be consistent with the base year emission values used in the NEC directive report number 5 (Amann et al., 2007), detailed emission factors and activity data for the year 2000 from the GAINS model have been transformed into implied emission factors for each of the fuels and sectors defined in POLES fuel. For countries in Asia, implied emission factors from the REAS inventory (Ohara, 2007) have been selected. For those country-sector-fuel combinations where GAINS or REAS did not provide emission factor data, emission factors were taken from EDGAR calculations (Van Aardenne et al., 2005 and EDGARv4 preliminary version) and the EMEP/CORINAIR emission inventory guidebook (EEA, 2006).

Emissions from aviation, international shipping and non-energy emissions were not provided by POLES and included separately. International aviation (AIR) and international ship (SEA) emissions for present and future have been taken from the Quantify project (unpublished results, 2008), see section 3. Emission from industrial processes (IPR) and Waste handling (WST) have been included following Olivier et al. (2005) and Van Aardenne et al.(2005). Emissions from the agriculture sector (AGR) have been taken from EDGARv4 (preliminary version).

The resulting base year emission inventory is presented in Table 1. The table shows the total emissions by EU27[1] and non-EU27 countries (excl. international shipping and aviation) and a comparison with national reported data (EU27) and global emission inventories as used in the AEROCOM/PHOTOCOM experiments. The emissions included in this report are consistent with national inventories for the EU27 with a difference of approximate 5-10% for most compounds, excluding N_2O and NH_3 with a difference of ~20%. This difference is acceptable given the large uncertainty in agricultural emissions.

[1] EU27 is the abbreviation for the 27 member states of the European Union

Table 1. Total emissions for the year 2000 in the EU27 and global total (Unit Tg yr^{-1}). Emission in EU27 excludes international shipping and aviation).

	EU27 (this work)	EU27 (UNFCCC reports)[1]	Global (this work incl. shipping and aviation)	Global (other)
CO_2	3927	4113	26152	25596 [4]
CH_4	23	23	301	300.56 [5]
N_2O	1.2	1.4	6.2	
NH_3	5.7	3.7 [2] / 4.3 [3]	41.11	58.87 [5]
NO_x	12.7	12	106.0	81.41 [5]
NMVOC	13.4	12	117.9	115.77 [5]
CO	42.3	38	600.0	470.43 [5]
SO_2	11.5	10	119.1	100.83 [5]
BC	0.41		4.91	4.4 [5]
OC	0.39		13.59	11.55 [5]

[1]UNFCC, [2]Amann et al., 2007, [3] EMEP expert estimate, [4] Marland et al., [5] ACCENT PHOTOCOMP (Dentener et al., 2006),

2.3 TM5

The modeling of atmospheric levels of pollutants resulting from the respective emission scenarios is done with the two-way nested atmospheric zoom model TM5. The TM5 model is an off-line global transport chemistry model (Krol et al. 2005) that uses meteorological fields, including large-scale and convective precipitation and cloud data, from the European Centre for Medium Range Weather Forecast (ECMWF). Vertical mixing follows the parameterizations by Louis (1979) and Holtslag and Moeng (1991), and convection is parameterized following Tiedtke (1989). The horizontal transport scheme is from Russel and Lerner (1981). The standard version of TM5 employs 25 vertical layers which are derived from the 60 layers of the operational ECMWF model. Roughly 15 of these layers are located in the troposphere, and 7 of them between the surface and 2 km. The model resolution can be chosen flexibly. For this work a similar set-up has been selected as used for simulations performed in the frame of the Task Force Hemispheric Transport. High resolution 1ºx1º zoom regions are utilized over the main centers of pollution North America, Europe, India and China; the resolution for most of the remaining Northern Hemisphere is 3ºx2º, where as a resolution of 6ºx4º in the remaining less polluted regions such as the Southern Hemisphere are used.

The gas phase chemistry is calculated using a modified CBM-IV chemical mechanism (Houweling et al.,1998), solved by means of the Eulerean backward iterative (EBI) method.

(Hertel et al., 1983). Aerosol chemistry includes the oxidation chemistry of SO2, heterogeneous reactions on aerosol (Dentener and Crutzen, 1993) and the formation of aerosol nitrate (Metzger et al., 2002).

Natural emissions of gases and aerosol (precursors) are not included in EDGAR and taken from recommendations by GEIA, and AEROCOM. Anthropogenic emissions were taken from the EDGAR/POLES emissions described in section 2.3.

To avoid calculations on decadal timescales, CH_4 concentrations were prescribed, and the future CH4 concentrations pathways were prescribed following methodology described by Prather et al. (2001) in the IPCC-TAR report (see section 4.6).

The model has been used in numerous applications (Krol et al., 2005; de Meij et al. 2005; Bergamaschi et al., 2007) and in a number of recent intercomparisons (Dentener et al., 2005, 2006, Stevenson et al., 2006, Kinne et al, 2006, Textor et al. 2007, Bergamaschi et al. 2007).

3. Scenarios

As mentioned in section 2.1 the POLES model provided energy growth rates under a greenhouse gas reduction scenario with greenhouse gas emissions reduced by 25% in 2050 compared to 1990. These reductions, together with those in agriculture and in land-use change and forestry (de-forestation), would contribute to achieving a global mean temperature increase of less than 2 degrees above its pre-industrial value (Russ et al, 2007)

Due to increase of fuel efficiency and fuel shifts such a climate policy will have as co-benefit a reduction in air pollutant emissions. In this study six emission scenarios related to the energy system over the period 2000-2050 have been explored and resulting impacts on environment have been analyzed with a focus on 2030. Since air pollution and greenhouse gas policies are often developed independently, the scenarios follow different routes as illustrated in Figure 1.

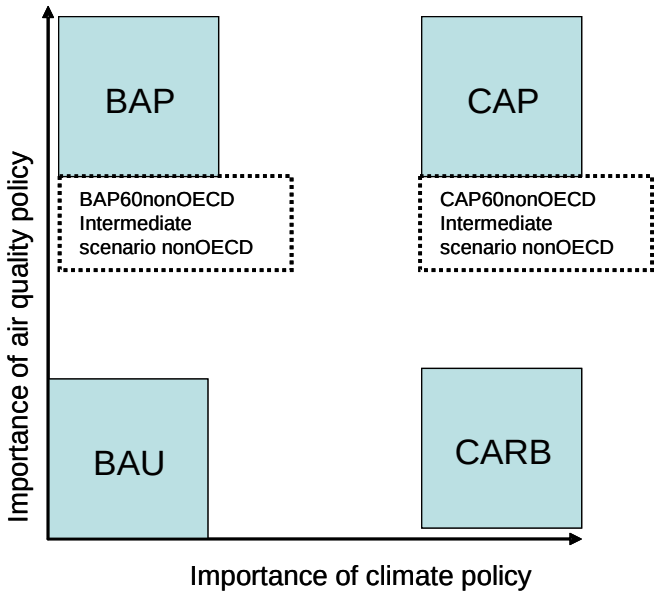

Figure 1: Schematic overview of the six different scenarios analyzed. The scenarios range from no climate and air pollution policy implemented in the energy system in all world countries beyond existing measures (BAU) to an integrated scenario where climate and air pollution measures are implemented on the global scale (CAP). Two intermediate scenarios have been defined in which air pollutant measures are assumed to be implemented with less success than in OECD countries (i.e. 60 % of emission reductions).

The scenarios range from no climate and air pollution policy implemented in the energy system in all world countries beyond existing measures (BAU) to an integrated scenario where climate and air pollution measures are implemented on the global scale (CAP). In addition to these global implementation scenario two intermediate scenarios have been defined in which the air pollution reduction measures in non-OECD countries is assumed to reach 60% of the air pollution measures applied in the OECD countries.

3.1 Scenario 1: no further climate and air quality policies (BAU)

The first scenario named **"Business as Usual"** hereafter referred to as **BAU**, explores a pessimistic situation in which no further climate and air pollution policies are implemented beyond what was in place in the year 2000. This means that energy consumption from 2000 to 2050 is driven by population and economic growth but not by energy efficiency/climate change policies (POLES baseline scenario). The combustion technologies/abatement measures are

assumed not to change beyond the year 2000 technologies. In practice this means that air pollution emission factors for the year 2000–as described in section 2.2- have been applied for the entire period 2000-2050.

Emissions from sectors where no POLES data has been provided (SEA, AIR, AGR and WST) follow the trend from the SRES B2 scenario(Nakicenovic, 2000), which is among the SRES scenarios the most consistent with the characteristics of the POLES greenhouse gas scenario in terms of GDP, population and the concept of global participation. Emissions from aviation and shipping (AIR and SEA) follow the B2 scenario interpretation of the Quantify project (Borken et al., manuscript in preparation). Emissions from agriculture (AGR) follow the SRES B2 interpretation of the IMAGE model whereas CH_4 emissions from the waste sector (WST) are scaled with the population trends as taken from the IMAGE model. Emissions from industrial processes (IPR) are assumed to follow emission trends from industrial combustion calculated using EDGAR-POLES.

3.2 Scenario 2: global climate policy only (CARB)

The second scenario named "Carbon constraint" hereafter referred to as **CARB**, assumes that global climate, but no additional air pollution policies are implemented (see Figure 1). This scenario can be used to study the co-benefits of this policy for air quality. The CARB scenario is described in Figure 13 of Russ et al. (2007). Compared to a BAU CO_2 emission of about 40 Gt CO_2 in 2050, the scenario considers a reduction of about 12 Gton CO_2 through energy savings by 2050, about 5 Gton through fossil fuel switches, and about 1 Gton CO_2 through nuclear energy. Together they lead to a 25 % reduction in energy related emissions in 2050 compared to 1990. These reductions in activities will lead to direct reductions in air pollution emissions. The combustion technologies/abatement measures are assumed not to change beyond the year 2000 technologies. In practice this means constant year 2000 emissions factors –as described in section 2.2- have been applied for the period 2000-2050.

It is noted that for this work some modifications of the scenarios described in Russ et al. (2007) have been used. The most significant difference is the introduction of a detailed model for biomass and biofuels including international trade of raw biomass and biofuels. As a result a stronger trend in biofuels is visible in the energy trends compared to earlier work. The updates were received in October 2008 (L. Szabo, P. Russ)

Emissions from sectors where no POLES data has been provided are treated as follows under this climate policy scenario. Aviation and shipping are taken from the Quantify project 2000 – 2050 emission, corrected for additional energy use consistent with the CARB scenario.. Industrial Processes (IPR) year 2000 EDGARv4_preliminary version emissions scaled with emissions trends in EDGAR-POLES Industrial combustion (IND). Agriculture and waste year 2000 EDGARv4_preliminary version emissions scaled with IMAGE 450 ppm scenario from the ADAM project.

3.3 Scenario 3: global air quality policy (BAP)

The third scenario named "**Business as usual energy with air pollution measures"** hereafter referred to as **BAP**, explores the impacts on air quality and climate if the world countries achieve air pollution abatement in the same order of magnitude as might be achieved in Europe under the National Emission Ceiling Scenarios.

This means that energy consumption from 2000 to 2050 is driven by population and economic growth as in the BAU scenario, and not constrained by energy efficiency/climate change policies (POLES baseline scenario). The combustion technologies/abatement measures, however, are assumed to change globally according to strict air pollution regulation as currently being discussed in Europe under the Thematic Strategy on Air Quality through its so called National Emissions Ceiling scenarios. Between the EU27 countries and the rest of the world a 10 year delay in achieving these air pollution targets is assumed by defining EU27 emission factors under the NEC directive as non EU emission factors in the year 2030. After the year 2030 no further reductions/improvements air pollution targets are assumed. These targets are translated in the selection of emission factors as described hereafter

European Union countries: With Europe already en route with these air quality measures the scenario assumes that in 2020 the EU countries have achieved their respective NEC objective and that in 2030 additional emission reductions can be achieved for those countries that had a lower emission reduction target than the European average. This means that for Europe, emission factors in the year 2020 are consistent with country emission factors as used in the calculation of NEC report number 5 as made available by by the International Institute for Applied System Analysis IIASA for the Current Legislation (CLE) scenario. In the

year 2030 additional emission reductions are assumed within Europe for those countries for which emission factors in 2020 where higher than the EU27 averaged emission factor. The averaged EU27 factor is an implied emission factor based on the sum of emissions by sector-fuel for the EU 27 countries and the sum of energy consumption for these sector-fuel combinations. Emissions for the year 2010 are calculated using linear interpolation of the 2000 and 2020 emission factors.

Non-EU 27 countries: For other countries in the world, including the US and Japan, it assumed that due to the need for improvement of air quality, European standards will be implemented by the year 2030. This means that in the year 2030 emission factors in the non-EU countries equal the average EU27 emission factors as described above. After 2030 no further abatement is assumed (emission factors for the years 2040 and 2050 are the same as for 2030). Emission factors for the years 2010 and 2020 are calculated by linear interpolation of the 2000 and 2030 emission factors. While realistic for the US and Japan, this scenario is an optimistic view of the development of air pollution control policy in other countries.

Emissions from sectors where no POLES data has been provided are treated like in Scenario 1

One of the characteristics of the BAP scenario is that the European NEC are partly achieved by fuel shifts, and more fuel efficient technologies, leading to lower emissions of the greenhouse gases CO_2, and CH_4. This is clearly beyond conventional end-of-pipe technologies to reduce air pollution. The BAP scenario thus can evaluate the co-benefits for climate from progressive air pollution abatement measures for Greenhouse Gas emissions, and –as will be shown later- dis-benefits for climate with regard to the cooling effect of aerosol on climate.

3.4 Scenario 4: integrated air quality and climate policy (CAP)

The fourth scenario named “Combined climate and air pollution policy” hereafter referred to as CAP, explores the optimistic case that climate and air pollution policies are integrated. Energy consumption from 2000 to 2050 is not only driven by population and economic growth but also by climate policies and measure aiming at reducing global greenhouse gas emissions by 25% in 2050 compared the reference year 1990 (excluding emissions from agriculture and land use change). The combustion technologies/abatement measures are assumed to change globally according to the BAP case.

A characteristic of CAP is that it places stringent air pollution reduction measures (as in BAP) on top of decreasing fuel use. The design of the scenario has not considered the costs of the technology implementation, and it is likely that optimization of the specific fuel-air pollution technology choice, may lead to drastically lower costs for implementation of add-on air pollution as shown in previous reports (CEC, 2008).

3.5 Scenario 5 and Scenario 6: intermediate global air quality policy in non OECD countries

Both the BAP and CAP scenarios represent a positive view on the possible achievement of air pollution abatement in developing countries. To analyze the impact on environment and climate when developing countries are less successful in achieving abatement measures (e.g. due high costs of abatement measures or technical infeasibility) two intermediate scenarios have been defined. These are:

- BAP-60: Global air quality scenario with non-OECD countries achieving 60% of the reductions achieved in 2020 under the NEC directive in the EU countries. This scenario is calculated as described under CAP with as sole difference the application of emission factors in 2030 to non-OECD countries representing only a 60% reduction compared to the reduction achieved under NEC in European countries.
- CAP-60: global integrated air quality and climate policy in which the energy system follows the CARB scenario combined emission factors in 2030 to non-OECD countries representing only a 60% reduction compared to the reduction achieved under NEC in European countries.

Table 2: Main characteristics of the six emissions scenarios

	BAU	**CARB**	**BAP**	**CAP**	**BAP-60non-OECD**	**CAP-60non-OECD**
Name	Business as usual	Climate policy (carbon constraint)	Business as usual energy with air pollution measures	Combined climate and air pollution policy	As BAP where air pollution abatement in non-OECD countries is less successful (60%) than in OECD countries	As CAP where air pollution abatement in non-OECD countries is less successful (60%) than in OECD countries
Rationale	No policy scenario: Exploration of "worst case" scenario	Climate policy only: Exploration of co-benefits of climate policy for air quality	Air quality policy only: Exploration of magnitude of co-benefits in CARB compared to pure air quality policies	Exploration of additional benefits of combining climate and air quality policies.	Exploration of differences in success of air pollution abatement between world regions	Exploration of differences in success of air pollution abatement between world regions under a global climate policy
Activity data from POLES	Baseline scenario	GHG reduction scenario	Baseline scenario	GHG reduction scenario	Baseline scenario	GHG reduction scenario
Emission factors for energy system	**Constant year 2000 emissions factors:** **Europe**: consistent with CAFÉ/NEC **Asia**: consistent with REAS inventory **Other** and emission factors not covered by CAFÉ/NEC, REAS taken from EDGARFT2000 inventory and EMEP/CORINAIR emission inventory guidebook		**Year 2000**: see BAU and CARB **Year 2010**: EU27: linear interp. 2020 EF Other: linear interp. 2030 EF **Year 2020**: EU27: as used in NEC national baseline Other: linear interp. 2030 EF **Year 2030:** EU27: average EU27 EF year 2020 NEC + country data when country EF < averaged EU27 EF Other: average EU 27 EF of year 2020. **Year 2040 and 2050**: EU27: constant year 2030 EF Other: constant year 2030 EF		**Year 2000**: see BAU and CARB **Year 2010**: EU27: linear interp. 2020 EF Other: linear interp. 2030 EF **Year 2020**: EU27: as used in NEC national baseline Other: linear interp 2030 EF **Year 2030: OECD**: average EU27 EF year 2020 NEC + country data whencountry EF < averaged EU27 EF **Year 2030: non-OECD**: 60% emission reduction of the averaged EU27 EF of the year 2020. **Year 2040 and 2050**: EU27: constant year 2030 EF Other: constant year 2030 EF	
Other emissions	**Aviation/shipping**: BAU, BAP, BAP60non-OECD emissions from Quantify project 2000-2050 **Aviation/shipping**: CARB, CAP, CAP60non-OECD: energy reduction factor applied to emissions from Quantify project 2000-2050 **Industrial processes**: year 2000 emissions scaled with emission trend in industrial combustion as calculated in scenarios **Agriculture/waste:** BAU, BAP, BAP60non-OECD: year 2000 EDGARv4_preliminary emissions scaled with IMAGE baseline scenario ADAM project CARB, CAP, CAP60non-OECD: year 2000 EDGRv4_preliminary emissions scaled with IMAGE 450 ppm scenario ADAM project					
Compounds included	**GHG**: Carbon dioxide (CO_2), Methane (CH_4), Nitrous oxide (N_2O) **AP**: Ammonia (NH_3), Carbon monoxide (CO), Nitrogen oxides (as NO_2), Non methane volatile organic compounds (NMVOC), Sulfur dioxide (as SO_2). **Aerosol**: black carbon (BC) and organic carbon (OC). PM emissions calculated within TM5 model.					
Gridded emissions	EDGARv3 spatial allocation maps on 1x1 degree: population, industrial combustion, power plants, fuel production, arable land/crop production, animal density.					

More details on the methodology for projecting the emissions following POLES and IMAGE projections are given in Doering et al (2009). Annex 2 gives an example of coupling the POLES growth rate to EDGAR for the power generation section.

3.6 Resulting emissions trends.

The calculated emissions under the four different scenarios are shown by compound and POLES world region in Figures 2 to11.

Carbon dioxide emissions (2000-2050)

Main features: Strong emission reductions under the CARB and CAP and CAP60_non-OECD scenarios, no significant reduction in the BAP and BAP_non-OECD scenarios.

As shown in Figure 2, global CO_2 emissions increase from 25 Pg yr^{-1} in 2000 to 54 Pg yr^{-1} in 2050 when no further climate and air quality policies are implemented (BAU). Under a global climate policy scenario (CARB), emissions from CO_2 show a continuing growth from 2000 to 2020 followed by stabilization in 2030 and decline after 2030 to about 20 Pg yr^{-1} in 2050. The emissions in Figure 2 are gross emissions, and Carbon Capture and Sequestration (as in CARB and CAP) reduces the net emissions. The assumption of less success in air pollution abatement does not lead to substantially different emissions.

Methane emissions (2000-2050)

Main features: Strong emission reductions under the CARB and CAP and CAP60_non-OECD scenarios, no reduction in the BAP and BAP_non-OECD scenarios.

As shown in Figure 3, global CH_4 emissions increase from 301 Tg yr^{-1} in 2000 to 550 Tg yr^{-1} in 2050 when no further climate and air quality policies are implemented (BAU). Due to decrease in demand of fossil fuel, fuel shifts, and measures in the agricultural sector a global climate policy (CARB, CAP and CAPnon-OECD) results in a reduction of about 300 Tg yr^{-1} CH_4 compared to BAU. Air quality policies (BAP) results in a small additional reduction of methane related to fuel shifts.

Nitrous oxide emissions (2000-2050)

Main features: Significant emission reductions under the CARB and CAP and CAP60_non-OECD scenarios, no reduction in the BAP and BAP_non-OECD scenarios.

In Figure 4, global anthropogenic N_2O emissions increase from 6 Tg N_2O yr^{-1} in 2000 to 12 Tg N_2O yr^{-1} in 2050 when no further climate and air quality policies are implemented

(BAU). No large impacts of the energy sector related emission inventories are seen, since N_2O emissions are dominated by the agricultural sector. Under a climate scenario agricultural emissions are reduced by about 2 Tg in 2050.Due to implementation of catalytic reduction measures aimed at reduction of NO_x, emissions of N_2O are increasing which is visible in a small increase of N_2O emissions in the scenarios that include air quality policies (BAP and CAP and CAP60non-OECD) compared to BAU and CARB in 2040 and 2050.

Carbon monoxide emissions (2000-2050)

Main features: Strong reduction in the BAP and CAP scenarios, significant reductions in the CARB, and BAP60non-OECD and CAP60non-OECD.

Global anthropogenic CO emissions (Figure 5) increase from 610 CO Tg yr^{-1} in 2000 to 950 Tg yr^{-1} in 2050 when no further climate and air quality policies are implemented (BAU). Under CARB, CO emissions initially show a comparable emission trend as for BAU, followed by a decrease of emissions after 2020 down to 600 Tg yr^{-1} in 2050 due to a strong decrease in the use of coal in industrial combustion as of 2030. Especially in non developed countries small scale industrial combustion is a large source of carbon monoxide. The implementation of air quality measures (BAP) therefore results in a strong reduction of CO emissions due to improvement of combustion technologies/abatement measures with a reduction of emissions to 300 Tg yr^{-1} in 2050. Like for CARB, additional CO emission reductions result from a combined climate air quality policy (CAP) leading to emissions of 280 Tg yr^{-1} in 2050. The importance of developing countries for CO emissions is shown by comparison of BAP60 and BAP: CO emissions are reduced much less in BAP60 due to higher use of coal and less efficient abatement measures.

Nitrogen oxide emissions (2000-2050)

Main features: Strong reduction in all scenarios.

As shown in Figure 6, global NO_x emissions soar from 100 Tg NO_2 yr^{-1} in 2000 to 190 Tg yr^{-1} in 2050 when no further climate and air quality policies are implemented (BAU). The reduction of fuel consumption and fuel shifts in CARB in 2050 diminish NO_x emissions from 2020 onwards to 80 Tg NO_2 yr^{-1}.. Emission abatement measures under an air quality policy (BAP) would reduce NOx emissions to 100 Tg NO_2 yr^{-1} in 2050. Under the combined climate and air pollution scenario (CAP) even further emission reduction are achieved to reduction in the amount of fossil fuels applied after 2030. Even if less efficient abatement measures are

foreseen in the CAP60non-OECD scenario, the fuel shifts and energy efficiency still leads to a reduction of emissions comparable to an air pollution scenario.

Non-methane volatile organic compound emissions (2000-2050)

Main features: Strong reduction in BAP and CAP scenarios, significant reduction in CARB, BAP60non-OECD and CAP60non-OECD.

Figure 7 demonstrate that global VOC emissions increase from 115 Tg yr^{-1} in 2000 to 160 Tg yr^{-1} in 2050 when no further climate and air quality policies are implemented (BAU). Comparable to NO_x emissions, reductions of fuel consumption and fuel shifts due to climate policies in the energy sector (CARB) reduce NMVOC emissions to 120 Tg yr^{-1} in 2050. Due to abatement measures in the air quality policy scenario (BAP), emissions of NMVOC are declining strongly from 2010 onwards (to 54 Tg yr^{-1} in 2050). Under a combined scenario only minor further reductions can be achieved due to a smaller amount of fossil fuels applied after 2030.

Ammonia emissions (2000-2050)

Main features: Significant reductions under CARB and CAP and CAP60non-OECD scenario. Increase in emissions under BAP and BAP60non-OECD scenarios.

As shown in Figure 8, global NH_3 emissions increase from 41 Tg yr^{-1} in 2000 to 55 Tg yr^{-1} in 2050 when no further climate and air quality policies are implemented (BAU scenario). Climate measures in the agricultural sector lead to an emission reduction of 10 Tg in 2050 (40 Tg y^{-1}). Due to implementation of air pollution control measures some sectors show an increase of NH_3 emissions.

Sulfur dioxide emissions (2000-2050)

Main features: Strong reductions in all scenarios

As shown in Figure 9, global SO_2 emissions increase from 119 to ca. 270 Tg yr^{-1} in 2050 (BAU). As a result of fuel shifts and reduction in fuel use the climate policy scenario (CARB) results in large reduction of SO_2 emissions from 2020 onwards, resulting in global emissions similar or less to levels in the year 2000. The resulting emission reductions are stronger than emission reductions achieved under end-of-pipe measure in an air quality policy (BAP) where emissions are reduced to 100 Tg yr^{-1} in 2050. Under the combined air pollution

climate (CAP) scenario SO_2 emissions are even further reduced to 35 Tg yr^{-1} in 2050. The largest emission reductions (both under the CARB, BAP and CAP) scenarios are achieved in continental China and North America.

Black carbon emissions (2000-2050).

Main features: Strong reduction in the air pollution scenarios, significant reductions in the climate scenarios.

As shown in Figure 10, global BC emissions increase from around 5 Tg yr^{-1} to 7 Tg in the period 2000-2050. The BAU trend of BC is dominated by developments in Asia with a combination of reduced combustion of coal fuels in the residential sector and increased combustion of liquid fuels in the transport sector. Under a climate scenario the amount of fuels is reduced but also the amount of biofuels increases leading to a relatively small reduction of BC under the CARB scenario. When air pollutant abatement measures are introduced under the air quality scenario (BAP) emissions are reduced significantly down to 3 Tg yr^{-1} in 2050. Combined air quality and climate policies (CAP) result only in minor additional emission reductions. We note that the uncertainty on black carbon emissions is very high.

Organic carbon emissions (2000-2050)

Main features: Strong reduction in the air pollution scenarios, significant reductions in the climate scenarios.

Figure 11 displays global anthropogenic OC emissions increases from about 14 Tg OC yr^{-1} to 21 Tg in the period 2000-2050. Emissions of organic carbon are dominated by emissions from wood and wood waste fuels Under a climate scenario the amount of fuels is reduced but also the amount of biofuels increases leading to a relatively small reduction of OC under the CARB scenario. When air pollutant abatement measures are introduced under the air quality scenario (BAP) emissions are reduced significantly down to 10 Tg yr^{-1} in 2050. Combined air quality and climate policies (CAP) result in minor additional emission reductions. The less efficient air pollutant reductions in non-OECD (BAP60&CAP60) countries show emission reductions of 30% by 2050.

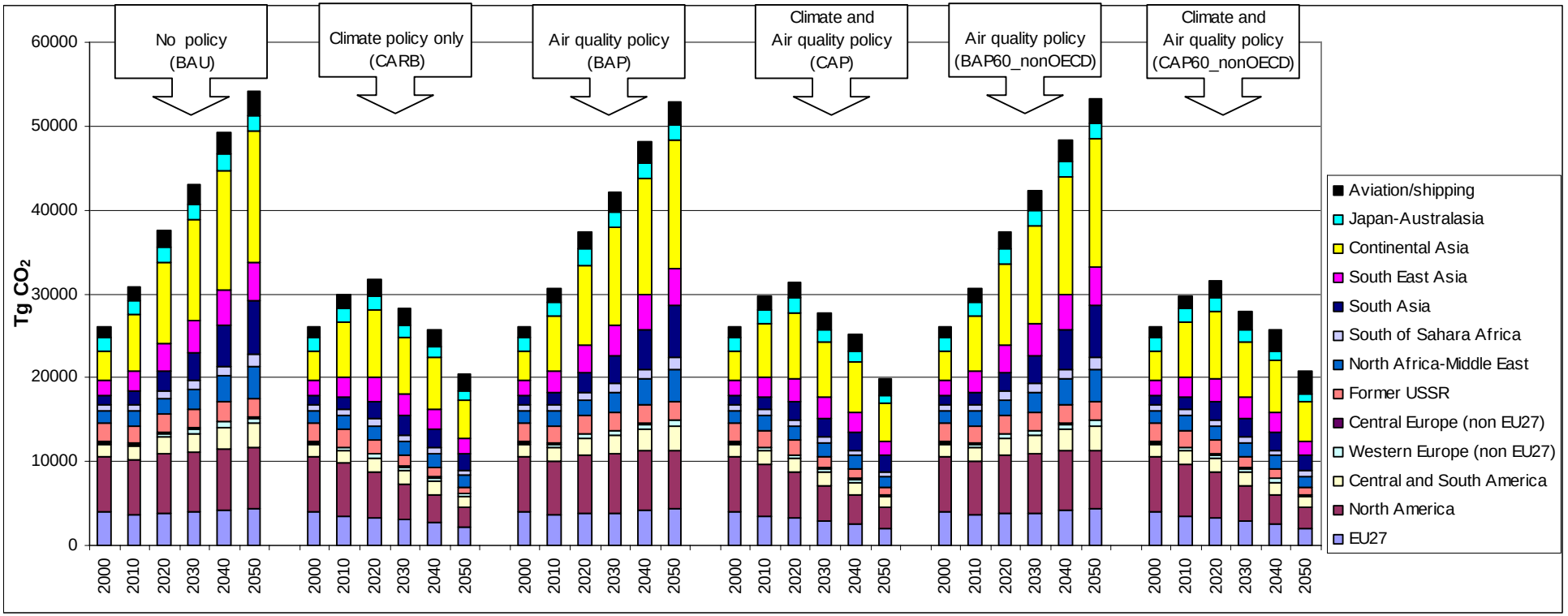

Figure 2: Carbon dioxide emissions by world region in the period 2000-2050 under the four scenarios (Unit: Tg yr^{-1} CO_2

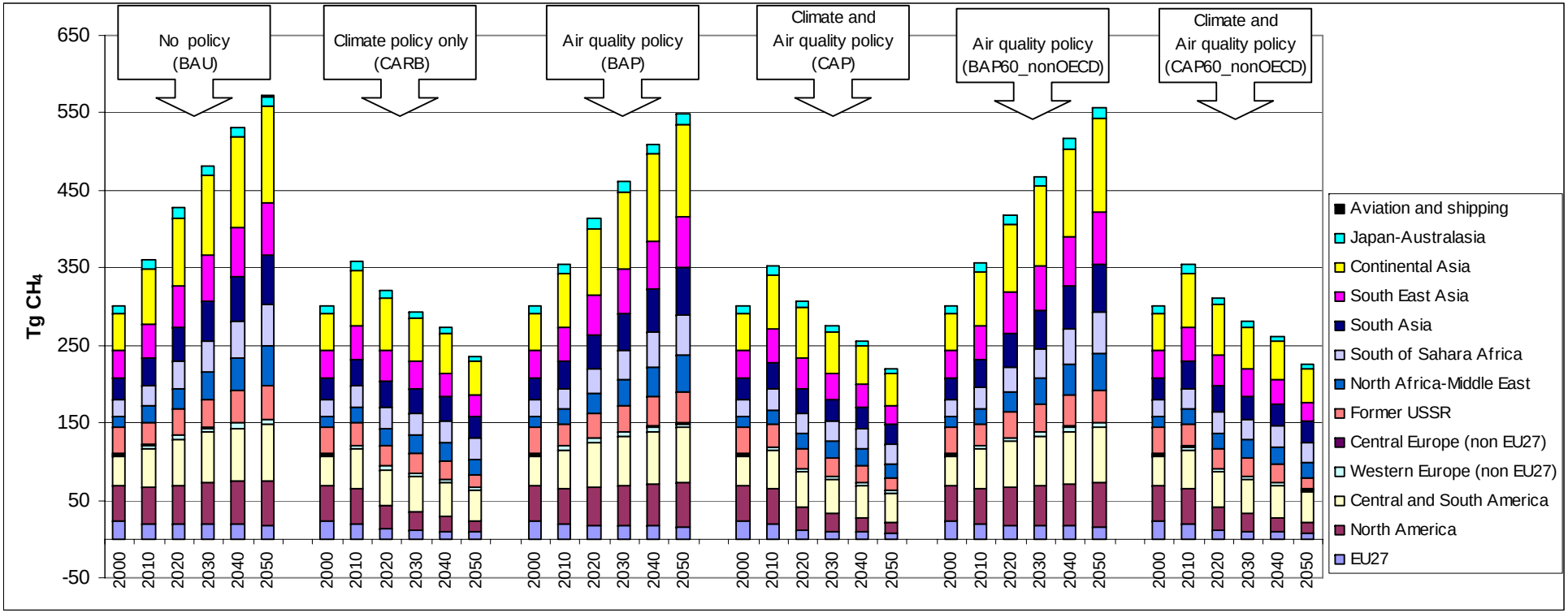

Figure 3: Methane emissions by world region in the period 2000-2050 under the four scenarios (Unit: Tg yr^{-1} CH_4)

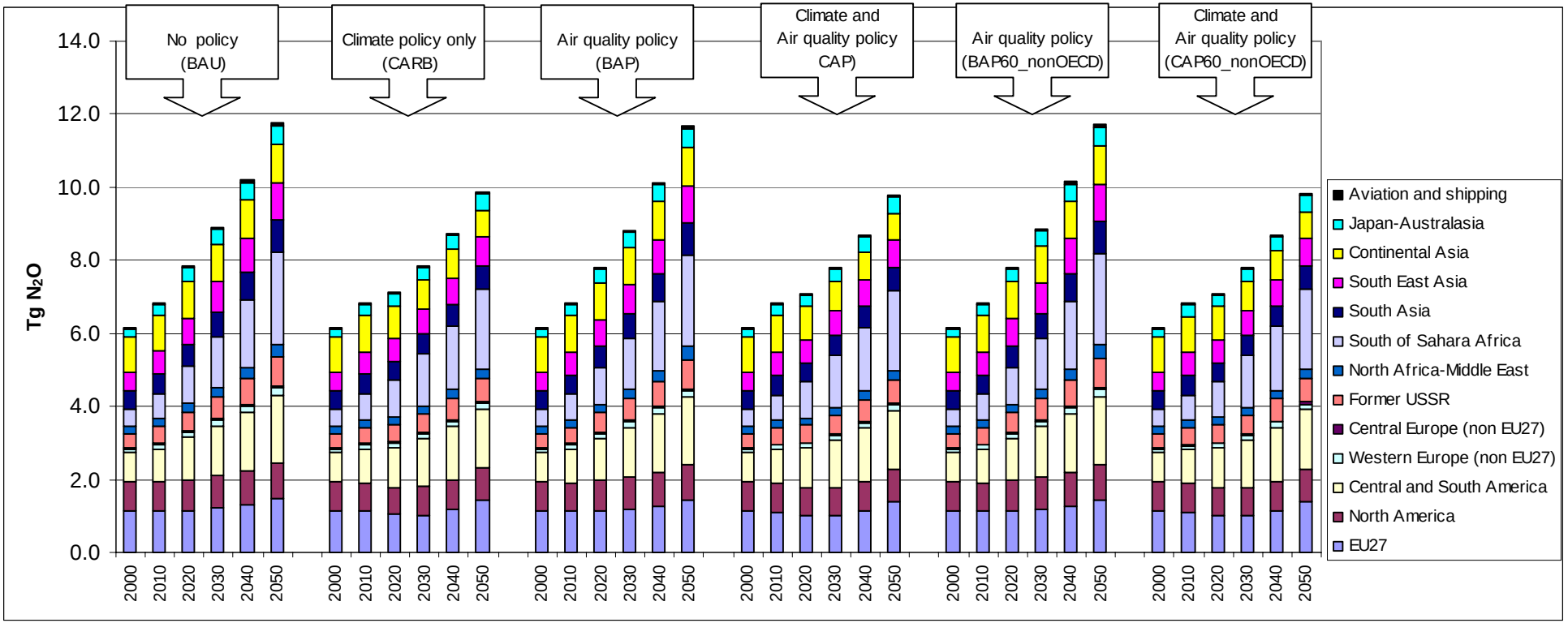

Figure 4: Nitrous oxide emissions by world region in the period 2000-2050 under the four scenarios (Unit: Tg yr^{-1} N_2O)

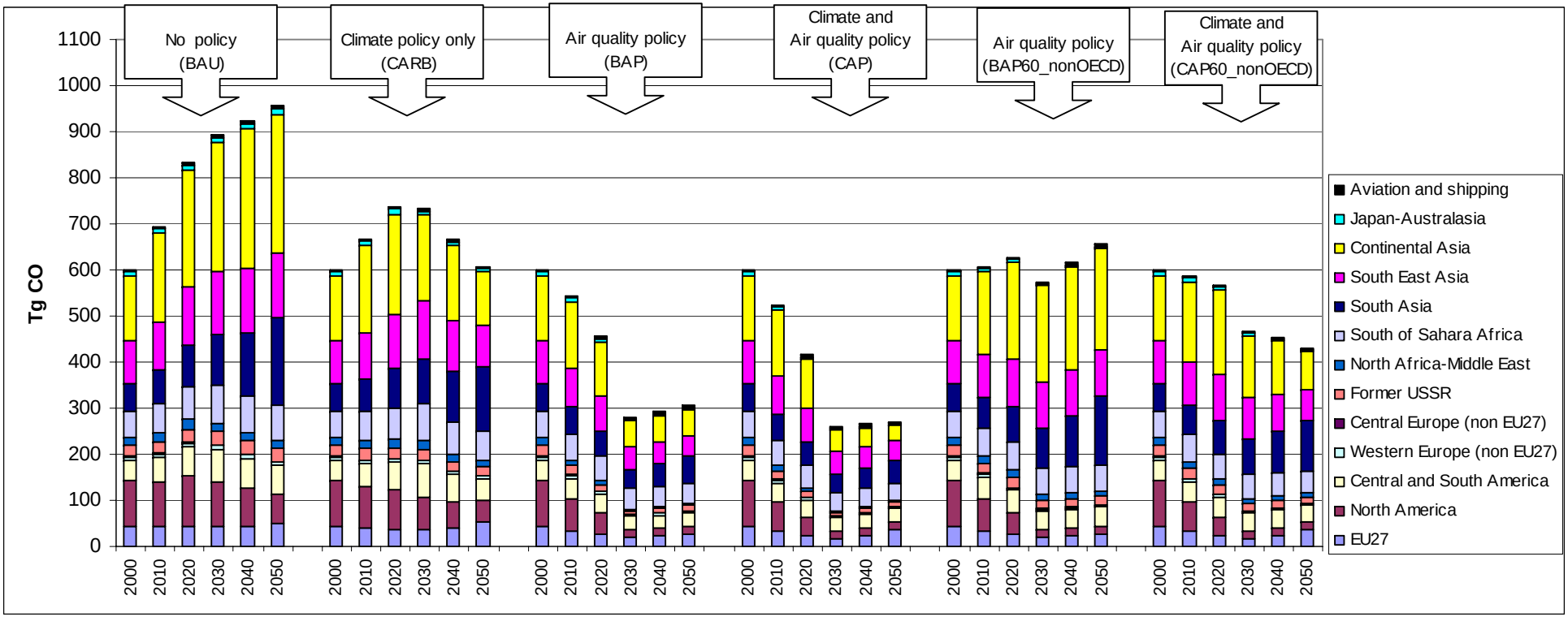

Figure 5: Carbon monoxide emissions by world region in the period 2000-2050 under the four scenarios (Unit: Tg yr^{-1} CO)

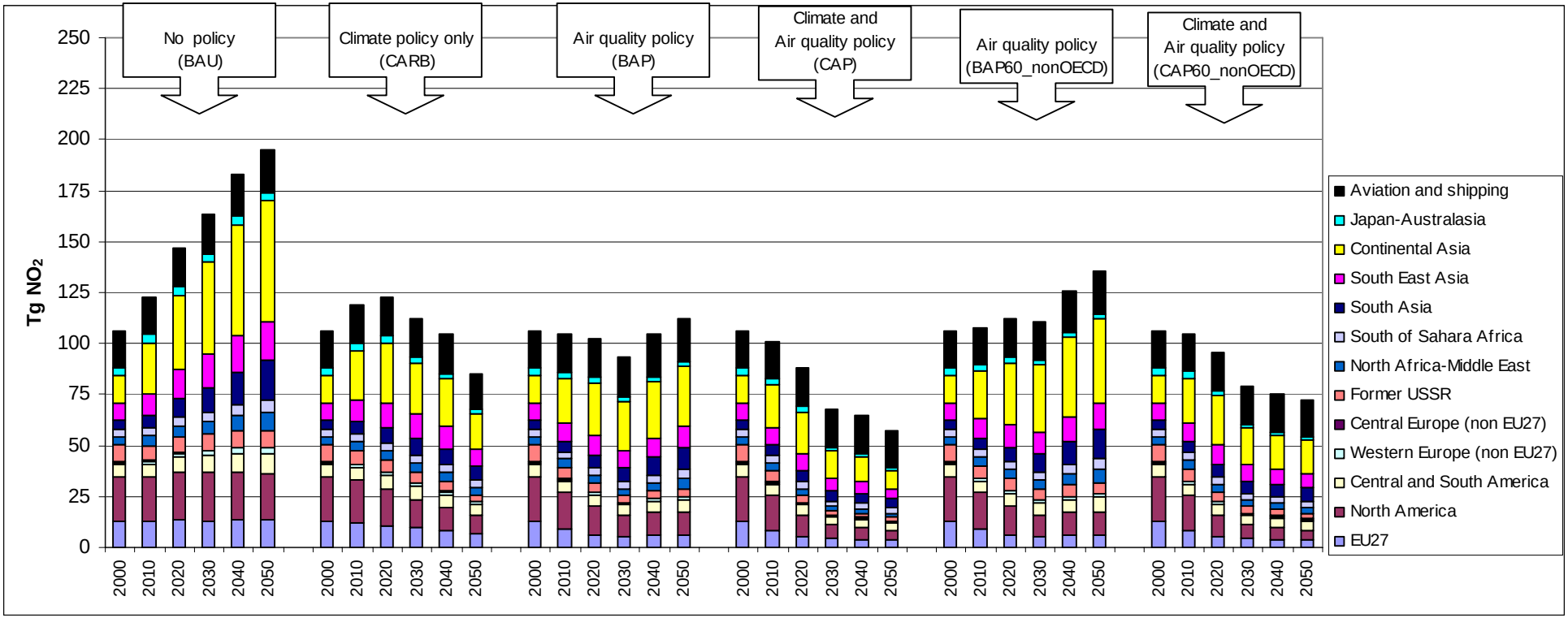

Figure 6: Nitrogen oxide emissions by world region in the period 2000-2050 under the four scenarios (Unit: Tg yr^{-1} NO_2)

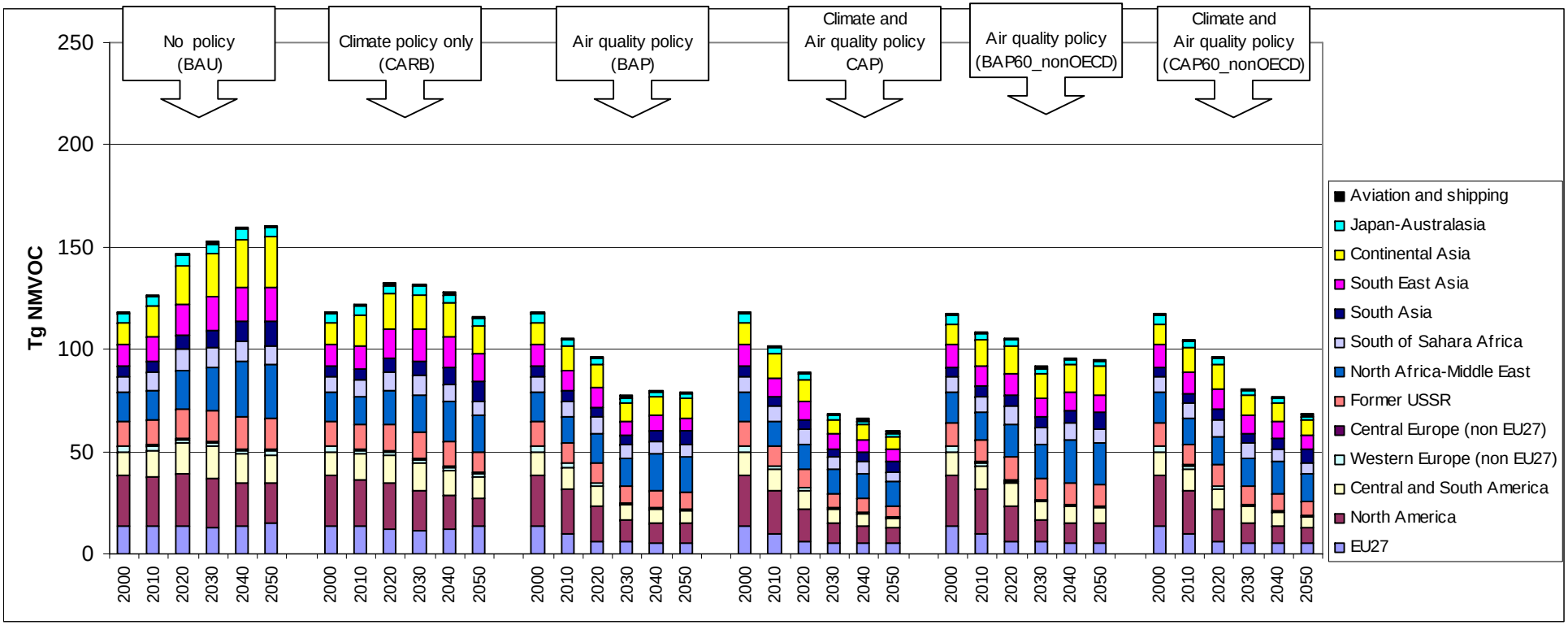

Figure 7: Non-methane volatile organic compound emissions by world region in the period 2000-2050 under the four scenarios (Unit: Tg yr^{-1} NMVOC)

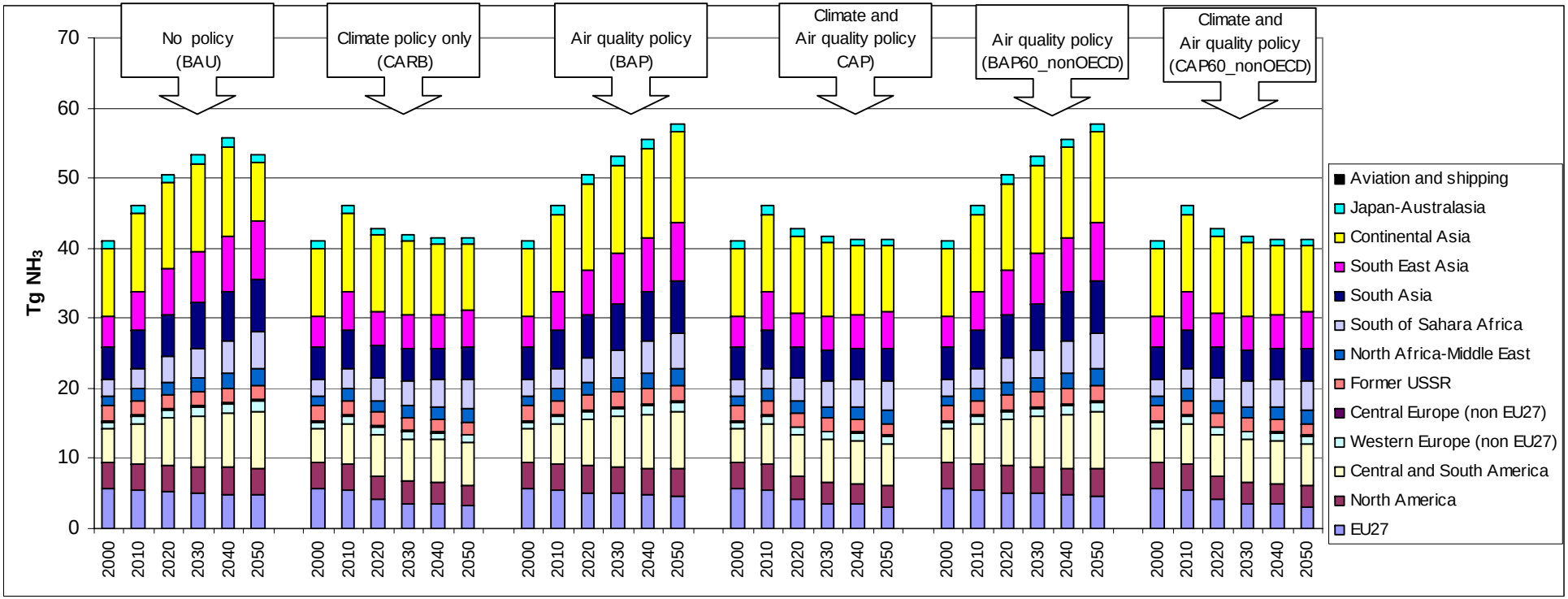

Figure 8: Ammonia emissions by world region in the period 2000-2050 under the four scenarios (Unit: Tg yr^{-1} NH_3)

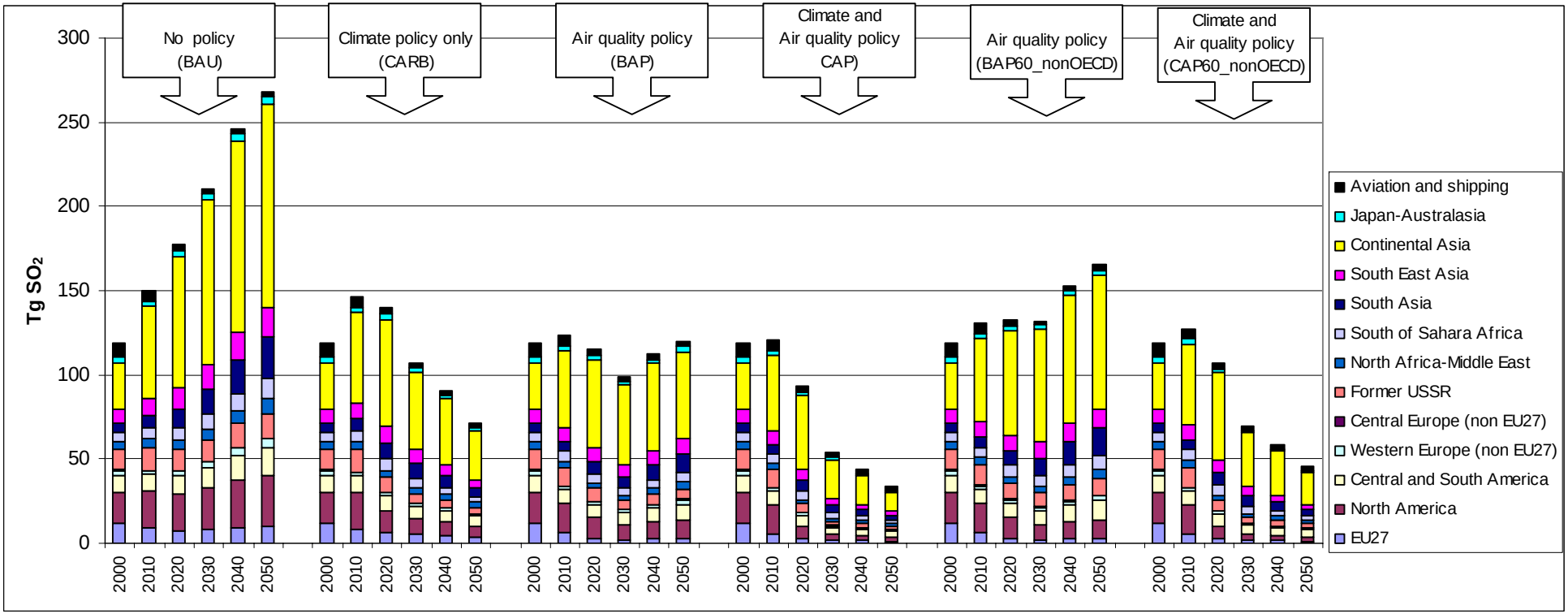

Figure 9: Sulfur dioxide emissions by world region in the period 2000-2050 under the four scenarios (Unit: Tg yr^{-1} SO_2)

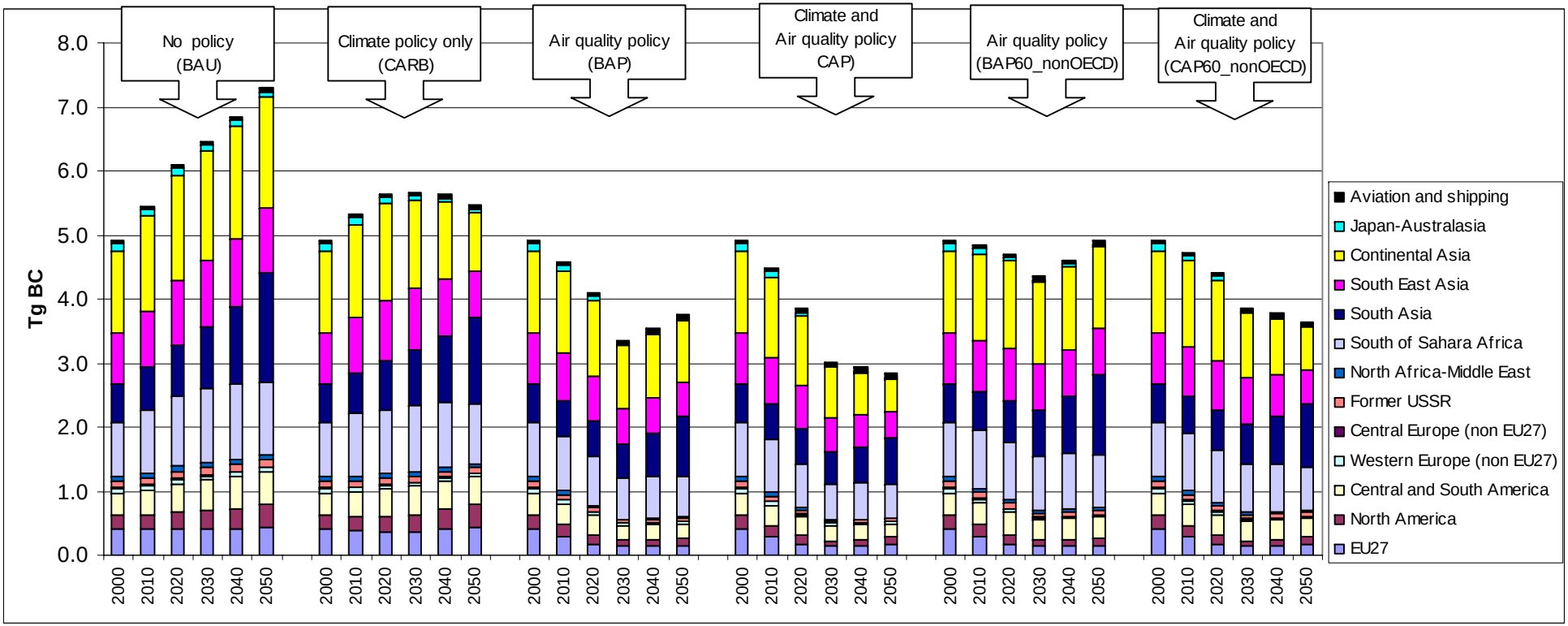

Figure 10: Black carbon emissions by world region in the period 2000-2050 under the four scenarios (Unit: Tg yr^{-1} BC)

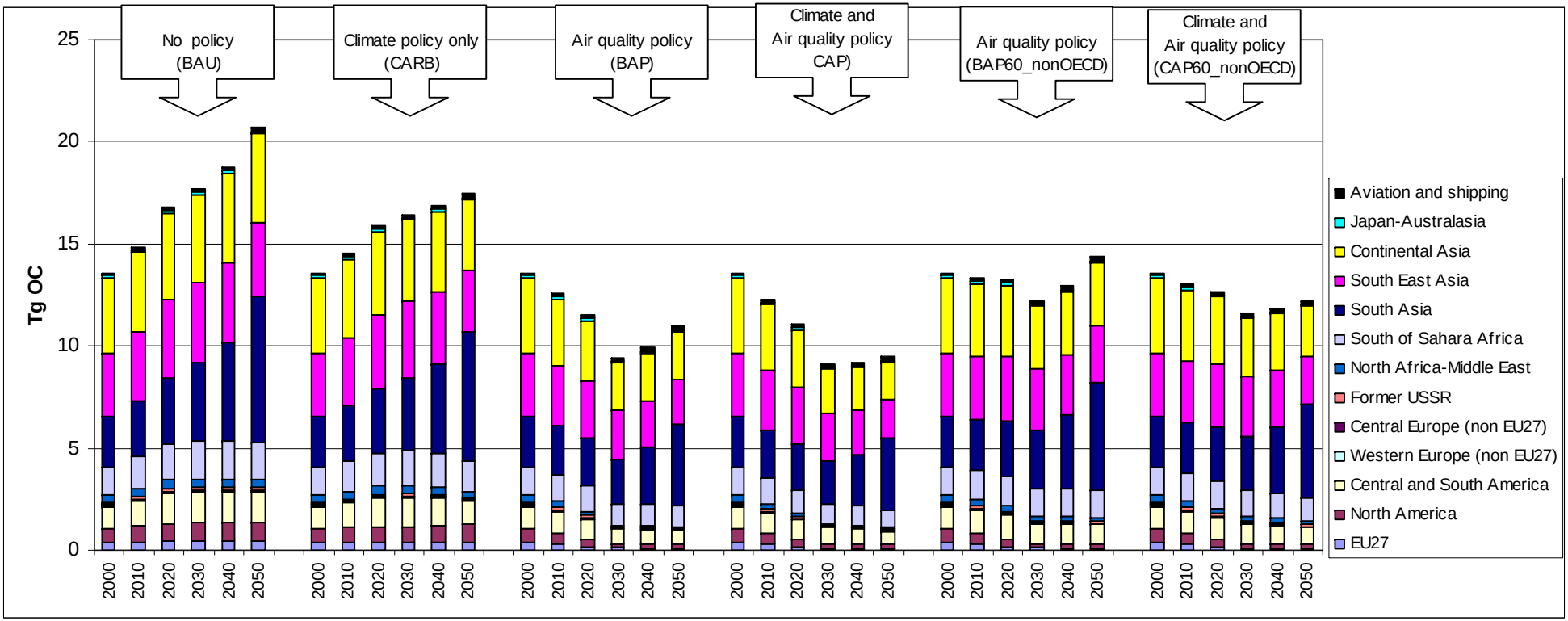

Figure 11: Organic carbon emissions by world region in the period 2000-2050 under the four scenarios (Unit: Tg yr^{-1} OC)

4. Results from the impact assessment

4.1 Surface and column concentrations for ozone and particulate matter

In Figure 12 (upper panels) we show the computed annual average surface concentrations for tropospheric O_3 and total aerosol (PM10) for the year 2000. Further we present the column aerosol loads for the sum of the major anthropogenic PM components SO_4, POM, and BC. Annual average ozone levels are between 30-50 ppbv in extended parts of the world, consistent with measurements [*Dentener et al,* 2006]. PM10 is very high over the source regions of natural aerosols (deserts in Africa and China, oceans). Also clearly shown are the elevated annual average PM10 concentrations over Eastern China (70->100 µg/m³). Over India we find concentrations between 40 and 60 µg/m³, whereas over the US and Europe annual average PM10 is in the range 20-30 µg/m³. The aerosol column of submicron aerosol (including SO_4, POM and BC , but disregarding sea-salt and mineral dust) shows elevated levels over Africa and South America (biomass burning), South-Eastern Europe and Middle East (industrial activities), India and China (mix of SO_4 and POM). The next panels in Figure 12 show the change in O_3 and PM loads for the BAU, CARB, BAP scenarios in he year 2030 and the BAU scenario for the year 2050, compared to the year 2000 base case. The results for the CAP scenario (not shown in Figure 12) lead in some regions to a further decrease of airpollution (compared to BAP), in other regions they are similar to BAP. (see also Figure 16). O_3 concentrations over the continents increase by 1-4 ppbv for the BAU-2030 scenario, and even up to 10 ppbv in India and south-east Asia. Over North-East China O_3 is decreasing due to the effect of titration by fresh NO emissions. The CARB scenario leads to a slight decrease (0 – 1 ppbv) in the annual average O3 concentration over most of the US, North Africa and the Mediterranean, whereas over central Europe and the north-East of the US the concentrations increases by 1 – 2 ppbv, caused by decreased O3 titration.

NO_x air pollution control (BAP and CAP scenarios) generally reduces O_3 levels by ca. 2-4 ppbv (up to 8 ppbv over the Mediterranean), except in Central Europe where due to less titration O_3 increases. The increase in O_3 over South East Asia for BAP and CAP is due to agriculturally related emissions.

Under the BAU scenario, aerosol (PM10) concentrations at the surface increase by 10-30 µg/m³ in large parts of Asia, and by 2-5 µg/m³ in North America. Noticeable is the significant reduction in aerosol levels over North America and Europe for the CARB scenario compared to BAU. In Europe aerosol concentrations remain almost the same for BAU and reduce by 5–10 µg/m³ under CARB. In China, aerosol loads increase dramatically; by up to 50 µg/m³ under BAU, and somewhat less under CARB. The BAP (and CAP, not shown) scenarios lead to a strong reduction in the PM10

surface concentration by often more than 10 μg/m³ in large regions of the world, except for China. Note that, although PM10 is presented here, the predominant part of the calculated changes in anthropogenic particulate matter for the scenario studies is in the PM2.5 size fraction.

Under BAU, a small decrease of the aerosol column is obtained only over Europe, whereas reductions of industrial SO_2 emissions lead to much larger and more widespread decrease under CARB. As it is the case for the surface concentrations, worldwide reductions of aerosol columns are obtained under BAP and CAP (see section 4.5)...

The BAU-2050 scenario shows the same geographical pattern as BAU-2030, but with an additional 1 – 2 ppbV increase in O_3 and 5 – 10 μg/m³ in PM10 over the polluted regions, compared to 2030.

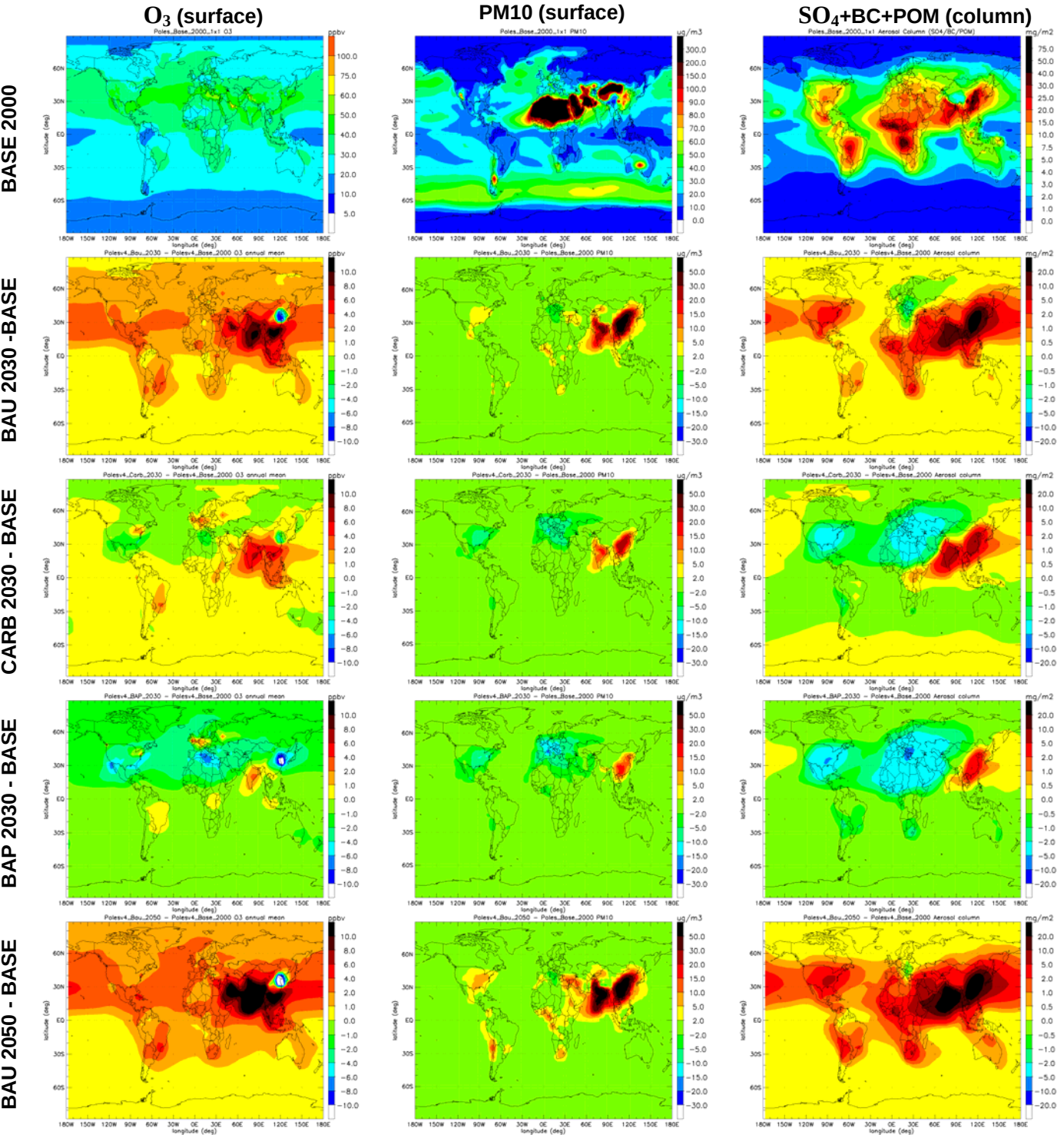

Figure 12: Concentrations of ozone [ppbv] and PM10 [µg/m³], and aerosol column [mg/m²] for the year 2000 (base), and the change for scenario's BAU, CARB, BAP in the year 2030 and BAU in the year 2050.

4.2 Effects of ozone on vegetation

Atmospheric ozone is a damaging component to vegetation. Air pollution-induced damage to crops (yield reduction as well as deteriorating crop quality) is an issue of concern in world regions where the expanding economy has lead to an increased emission of air pollutants in general and ozone

precursors in particular. There are several indicators for estimating damage to crops. Here we use the widely used cumulative indicator AOT40 (summing up calculated hourly ozone concentrations above 40 ppbv during local daytime), to assess the damage to wheat, which is worldwide one of the most important crops. For estimating the risk to crops, AOT40 is usually accumulated over a 'standard' growing season period of 3 months. For this global study we evaluate the maximal case, by considering the maximum 3-months AOT40 occurring during the year at each grid cell, irrespective of the wheat growing season. The relative yield loss is calculated using a generic wheat exposure-response relationship evaluated by Mills et al. (2007) Methodology and uncertainties are extensively discussed by Van Dingenen et al. (2008), and summarized in Annex 3.1.

Figure 13 and Table 3 show that wheat loss due ozone is occurring throughout the world: on average, in 2000 global wheat production is expected to be lower by 8% due to ozone. In the USA, Western Africa, Europe, and the Middle East, wheat losses up to 15% are calculated. First attempts to monetize crop losses (using 2000 market prices and production) indicates global economic damage of several billions US$ per year (Van Dingenen et al., 2008). Compared to the year 2000, crop losses increase by 2% globally and up to 8% regionally for BAU in 2030. They stabilize under CARB. Stringent air pollution mitigation (BAP, CAP) can reduce wheat crop losses by 4 to 5% globally. By 2050 under the BAU scenario, global crop losses increase by 3%, where as the CARB, BAP and CAP cases lead to decreases of 2% to 4% compared to present. Future work will evaluate the associated costs and consider other crops as well.

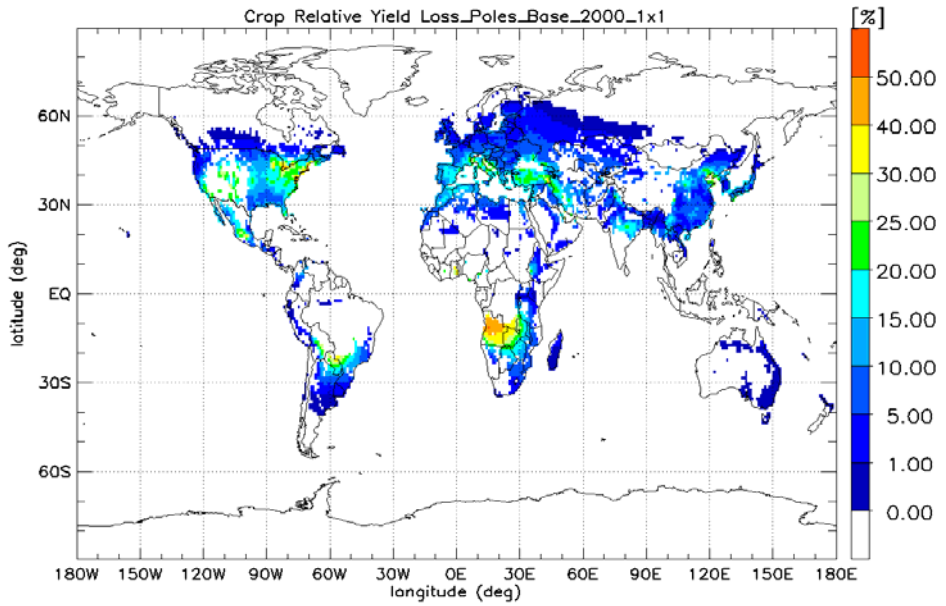

Figure 13: Wheat losses (% relative yield loss) due to damage by ozone in 2000.

Table 3: Regionally aggregated relative yield loss (RYL) for wheat [%].

	Base-2000	Bau-2030	Carb-2030	BAP-2030	CAP-2030	BAP60-Non-OECD-2030	CAP60-Non-OECD 2030	Bau-2050	Carb-2050	BAP-2050	CAP-2050
CANADA	3	3	2	2	2	2	2	3	2	2	2
USA	14	17	11	7	4	8	5	17	7	8	3
C. AMERICA	12	17	11	7	5	10	6	18	7	8	4
S. AMERICA	6	8	7	6	6	7	6	8	6	6	6
N. AFRICA	8	10	7	3	2	4	3	11	4	4	1
W. AFRICA	15	16	15	14	14	15	14	17	15	14	13
E. AFRICA	3	4	3	3	2	3	3	6	3	3	2
S.AFRICA	18	20	19	18	18	19	18	20	18	18	17
OECD EUROPE	9	10	7	4	3	5	4	11	6	5	3
E. EUROPE	8	9	7	5	4	5	5	10	6	5	4
FORMER USSR	4	4	3	2	2	3	2	4	2	2	2
MIDDLE EAST	12	18	12	8	6	11	8	23	9	12	5
S. ASIA	8	16	12	8	6	11	8	22	10	11	5
E. ASIA	7	12	10	5	4	8	6	11	7	5	3
S. E. ASIA	5	13	9	5	4	9	6	16	7	6	2
OCEANIA	0	0	0	0	0	0	0	0	0	0	0
JAPAN	8	13	9	3	1	6	3	14	4	3	-1
NH	8	10	7	5	4	6	4	11	5	5	3
SH	8	9	9	8	8	9	8	10	8	8	8
World	8	10	8	4	3	7	5	11	6	6	4

4.3 Effects of nitrogen deposition on vegetation

Deposition of reactive nitrogen induces a cascade of environmental effects (Dentener, 2006; Galloway, 2004). Since the net primary production of most terrestrial ecosystems is limited by nitrogen availability, deposition of reactive nitrogen (Nr) may enhance ecosystem productivity with possible consequences for the global carbon cycle. On the other hand eutrophication by Nr can cause acidification, an imbalance in nutrient cycling leading to a change of ecosystem diversity, as indicated by the exceedence of critical loads. In fresh water and coastal regions, nitrogen inputs can lead to noxious and toxic algal blooms, increased turbidity, and disruption of ecosystem functioning, shifts in food webs and loss of fish stocks. Nitrogen deposition to coastal waters leads to de-nitrification and enhanced emissions of N_2O, which is in turn a strong greenhouse gas and perturbs the chemistry of the stratosphere.

In this work we focus on the potential risk that natural ecosystems receive nitrogen from deposition above a threshold 1000 $mg(N)m^{-2}yr^{-1}$ ("critical load"). According to our calculations, currently (year 2000) ca. 18 % of the global natural ecosystems receives nitrogen deposition in excess of this threshold. These numbers are increasing to 22 % for the BAU and CARB scenarios in 2030 and stabilizing around 17 % and 19 % for the BAP and CAP scenario in 2030. As shown in Figure 14, the regions currently most affected are the United States (40% of the vegetation, and reducing to 20 % under BAP/CAP), Western Europe (40%), Eastern Europe (50%), South Asia, East Asia, and South

East Asia (20-40%), and Japan (60%). The considerable NO_x emission reductions in the BAP and CAP scenarios are partly off-set by increasing NH_3 emissions. In South and East Asia, NH_3 emissions are even increasing more strongly than the NO_x emissions reduce. As a result the fraction of ecosystems at risk for a too high nitrogen deposition does not dramatically change, indicating the important role of agriculture for N emissions and deposition. The combined air pollution and climate scenario CAP is standing out in reducing nitrogen deposition most in 2030 and 2050.

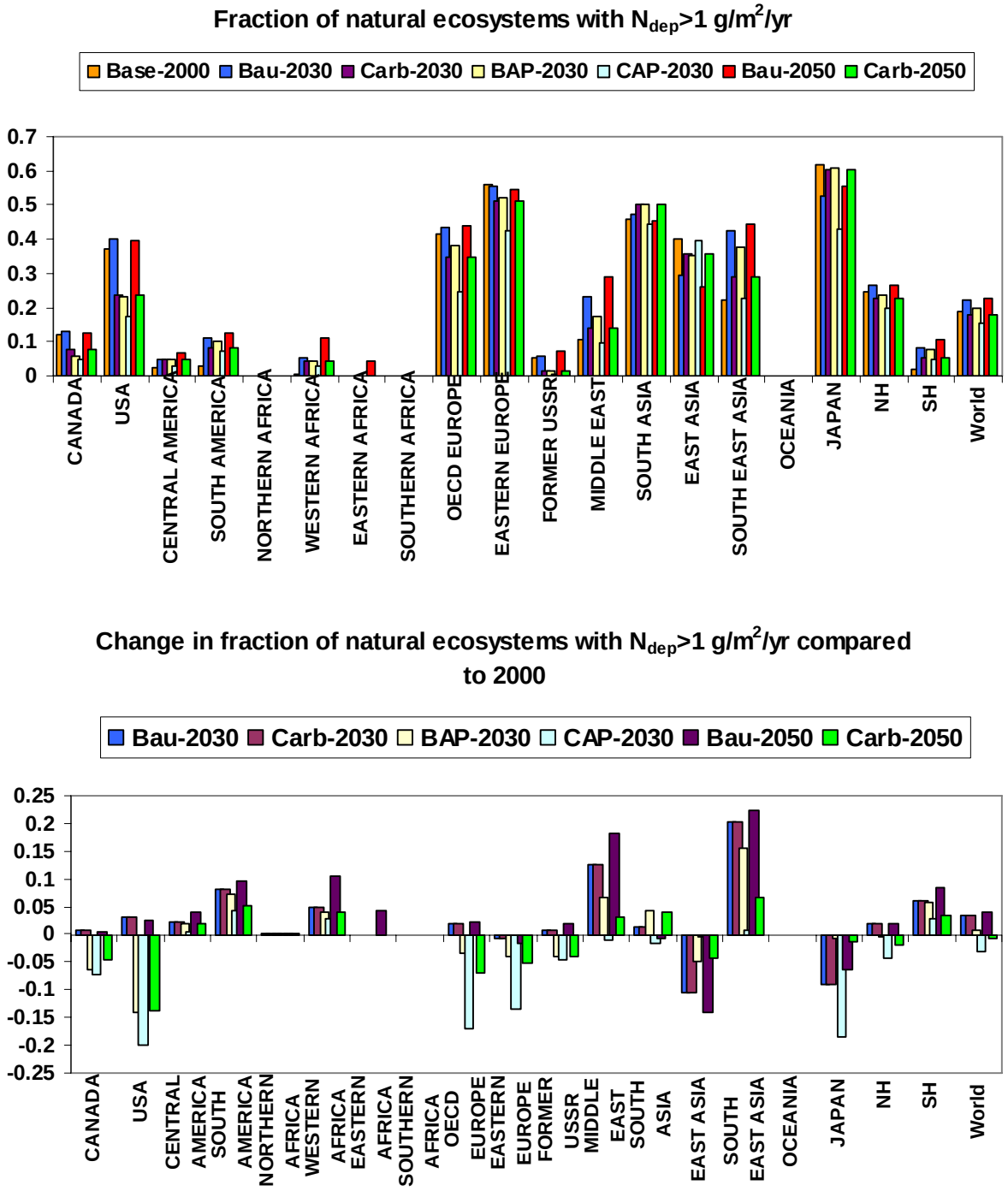

Figure 14: (a) Fraction of natural ecosystems (%) exposed to nitrogen deposition above 1 g/m²/yr and (b) the change compared to the year 2000.

4.4 Effects of PM and O_3 on human health.

There is ample epidemiological evidence that particulate matter (PM) and ozone negatively impact on human health. We evaluate the loss of statistical life expectancy (LLE) for the base year 2000 and the scenarios, following dose response relationships given by Pope (2002) and the methodology recommended by WHO (2004). We consider only anthropogenic aerosol (discriminating urban and rural concentrations) and ozone above a threshold of 35 ppbv. In the following we focus on the role of particulate matter (PM10) since the impacts of O_3 are calculated to be relatively small (see Annex 3.2). We consider the effects of anthropogenic PM10 (i.e. the sum of sulphate, nitrate, ammonium, black carbon and primary organic carbon). Important to mention is that, in line with WHO (2004), we assume that the relative risk function for PM10 is constant above 100 μg/m³, which means that there would be no health gains reducing PM10 concentrations from e.g. 150 μg/m³ to 100 μg/m³, clearly a disputable assumption (see World Bank report, 2007). Details are given in Annex 3.2. Figure 15 shows global maps for the (changes of) LLE [months] for PM10. The calculated LLE takes into account the combined acute and long term PM10 induced mortality. In Annex 3.2 we also give an example of the results of an alternative method to compute LLE, using a method proposed by the Worldbank [2004], using a counterfactual concentration, below which it is assumed that there is no health effect. The World Bank method leads to about 30 % lower values compared to the method of WHO.

In North-East United States and Europe in 2000 (Figure 15, and 16a), LLE for PM ranges between 6-24 months. In India, and especially China, these losses amount to up to 36 months. We note that the PM10 LLE follows mostly the anthropogenic PM10 (as well as PM2.5) patterns, slightly modified by the risk function. For loss of life expectancy due to anthropogenic PM10 typical values range between 2.5 and 3.5 month/(10 μg/m³ increment). Worldwide population-weighted LLE for anthropogenic PM10 is 11 months in the year 2000. The calculated value for OECD Europe is 8.6 months. The PM LLE for Europe is very similar to earlier calculations of IIASA (2005).

Serious further loss of LLE is expected under BAU, ranging from additional 1-4 months loss in the USA, up to 12 months additional loss in China, India and the Middle East. In Europe the situation remains rather constant (< 1 month additional loss). As could already be inferred from the trends in the PM concentrations, carbon reduction policies only (CARB compared to BAU) lead to a gain in life expectancy (for PM) of up to 4 months in parts of the USA, Europe the Middle East and India. Substantial improvements could be achieved by introducing stringent air quality policies, leading to an

increase of the statistical life expectancy by >12 months in parts of India and China, and 4 months worldwide.

Figure 16a shows the LLE for particles averaged for world regions.

In Annex 3.2 we give the integrated life-years lost computed by multiplying the LLE with the regional population numbers. Worldwide about 5 10^9 life years are lost.

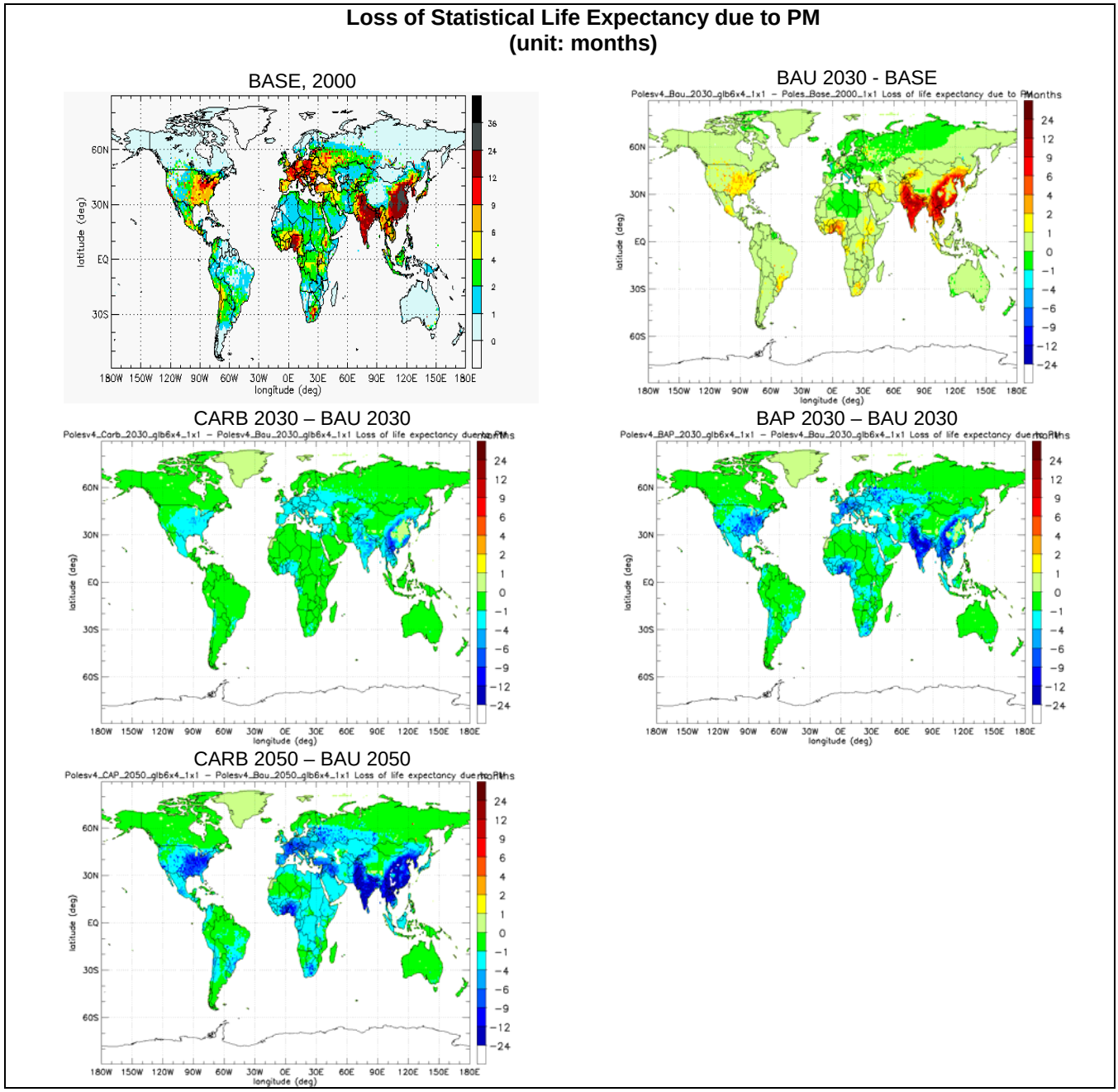

Figure 15: Loss of Statistical life expectancy (months) for anthropogenic PM10 (i.e. the sum of sulphate, nitrate, ammonium, black carbon and primary organic carbon) for the baseline and the change for four selected scenarios.

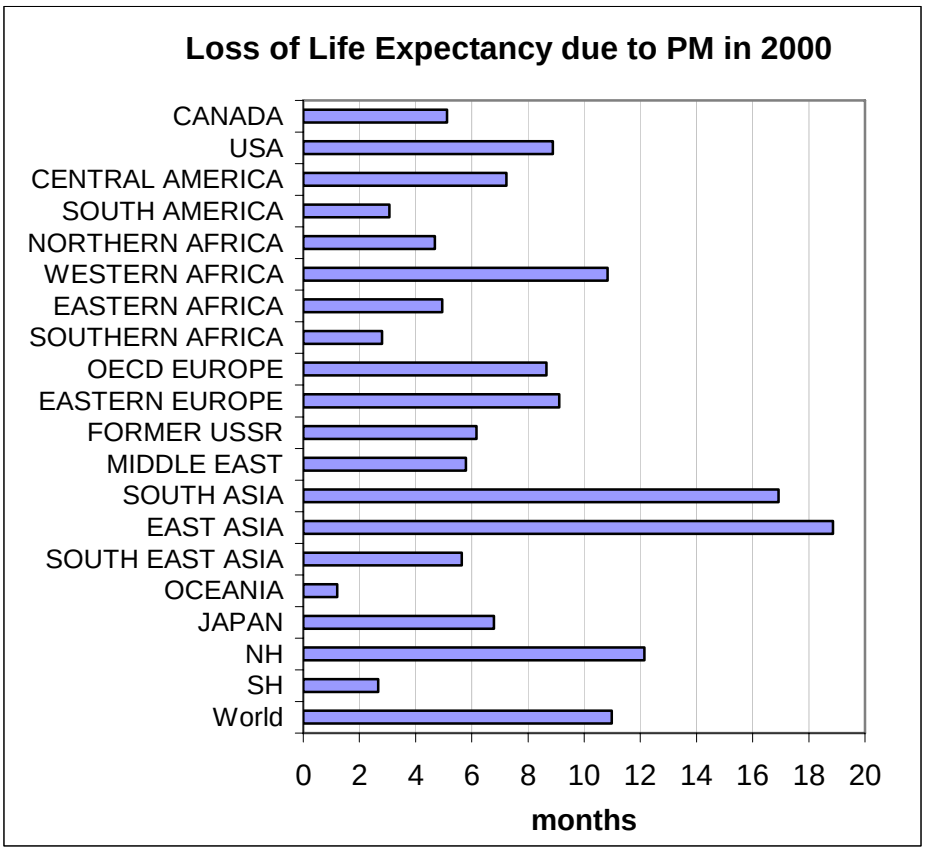

Figure 16a: Loss of Statistical life expectancy for PM10 (=i.e. the sum of sulphate, nitrate, ammonium, black carbon and primary organic carbon) for the baseline

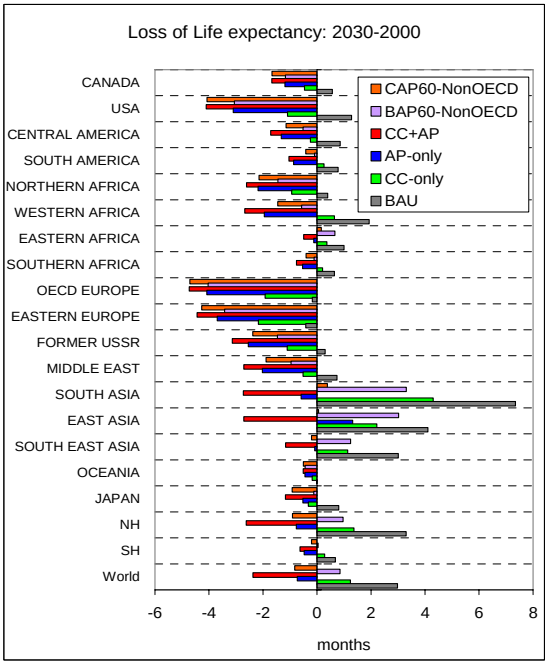

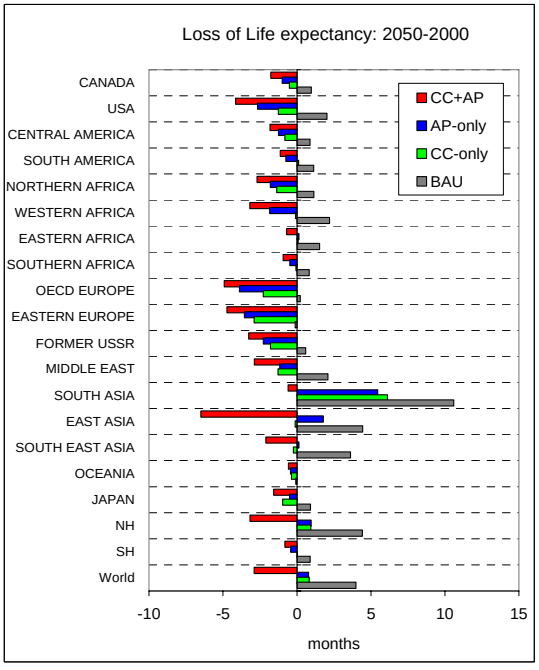

Figure 16 b and 16c: Change in the loss of Statistical life expectancy for PM10 (= i.e. the sum of sulphate, nitrate, ammonium, black carbon and primary organic carbon) for 2030 and 2050 compared to the baseline: population weighted regional averages. CC+AP=CAP; AP-Only=BAP; CC-only=CARB,.

4.5 Effects on climate: aerosol and ozone forcing

Whereas as the potential climate effects of long-lived greenhouse gases is commonly evaluated with Greenhouse Warming Potentials (GWP) over a time horizon of for instance 100 years, there is no accepted similar methodology available for the much shorter lived aerosols and ozone. Therefore, we evaluate in this section the instantaneous radiative forcing defined as the change in the energy balance at the top of the atmosphere (TOA), comparing the years 2030 and 2050 to the year 2000.

4.5.1 Ozone forcing

Ozone Radiative forcing was calculated off-line by utilizing radiative forcing computations presented by *Dentener et al.* [2005], and scaling them with the tropospheric column changes between 2030 and 2000 for the 4 scenarios. More details on the methodology are given in Annex 4. Comparing the ozone forcing with the changes in surface ozone in section 4.1 we see that the forcing maximizes in the (sub)-tropics above bright surfaces (Figure 17). Changes between 50-300 mW/m² are calculated for BAU and CARB, whereas air pollution controls also reduce the forcing by ozone by up to 200 mW/m² as annual average.

4.5.2 Aerosol forcing

Aerosol radiative forcing of the simulated monthly averaged aerosol burden was calculated using the off-line radiative transfer model described by *Marmer et al.* (2007), and is described in Annex A3.1. We consider the direct radiative forcing from the aerosol components SO_4, organic carbon (POM) and black carbon (BC). The indirect radiative forcing (change in cloud properties) is determined for SO_4. Like for ozone, we normalized the forcing into a radiative forcing efficiency (A3.1). Figure 18 shows the radiative forcing for the BAU scenario for the 3 components and the indirect forcing. It can be seen that the indirect and direct SO_4 forcing is negative with values between -1 and more than -5 Wm^{-2} over extended parts of the world. The forcing due to BC and POM is smaller, and more localized. The continental outflow regions into relatively clean marine air are dominating the indirect effect.

In Figure 19 we see that the total aerosol forcing is largely determined by the sum of direct and indirect SO_4 forcing- thus closely related to changes in emissions from fossil fuel combustion. . Forcings upto -20 Wm^{-2} are calculated comparing BAU2050-and 2000.

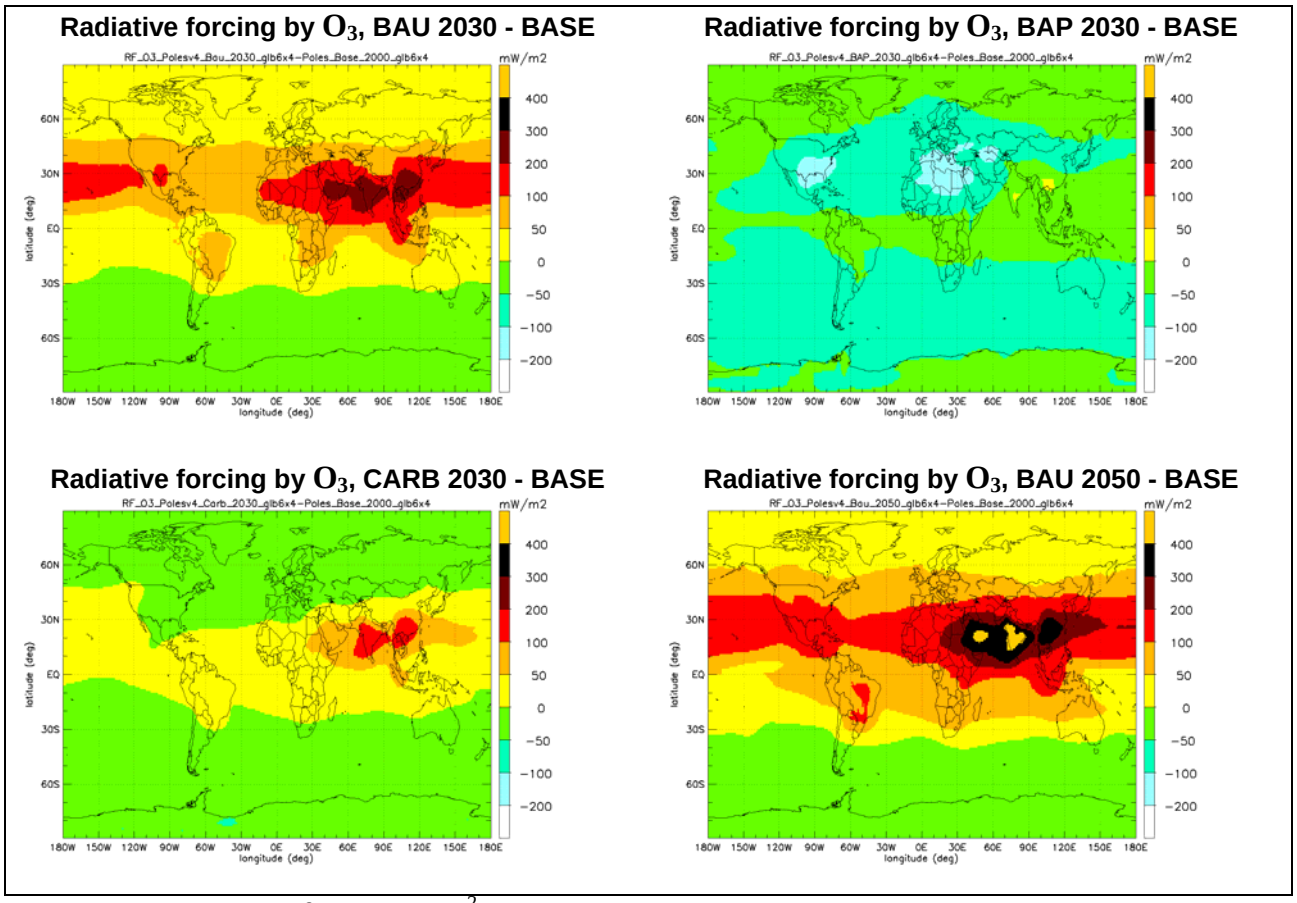

Figure 17: Radiative forcing.[Wm^{-2}] in 2030 and 2050 due to Ozone compared to 2000 Base Case for selected scenarios and time horizons.

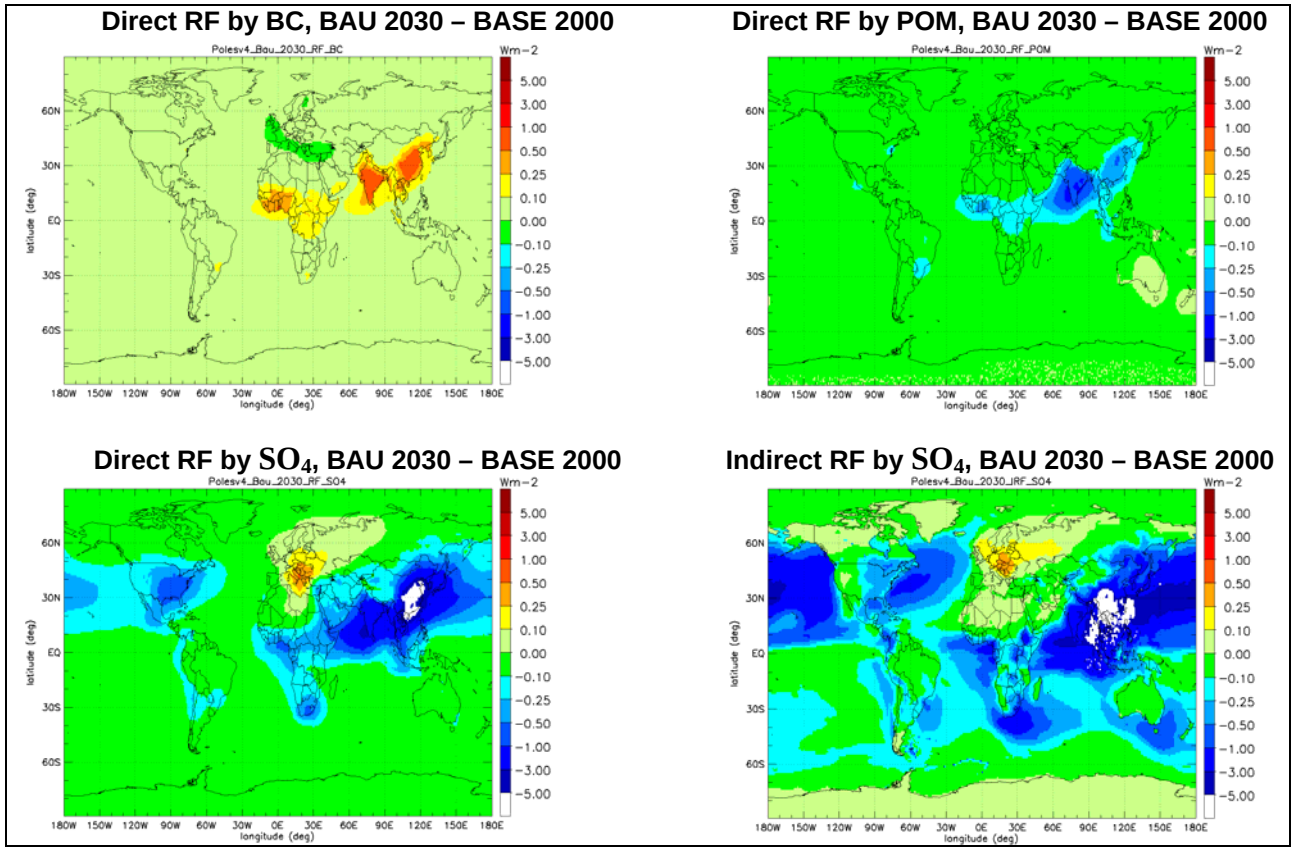

Figure 18: RF for BAU (comparing 2030 to 2000) for aerosol components and the IRF for SO_4.[Wm^{-2}]

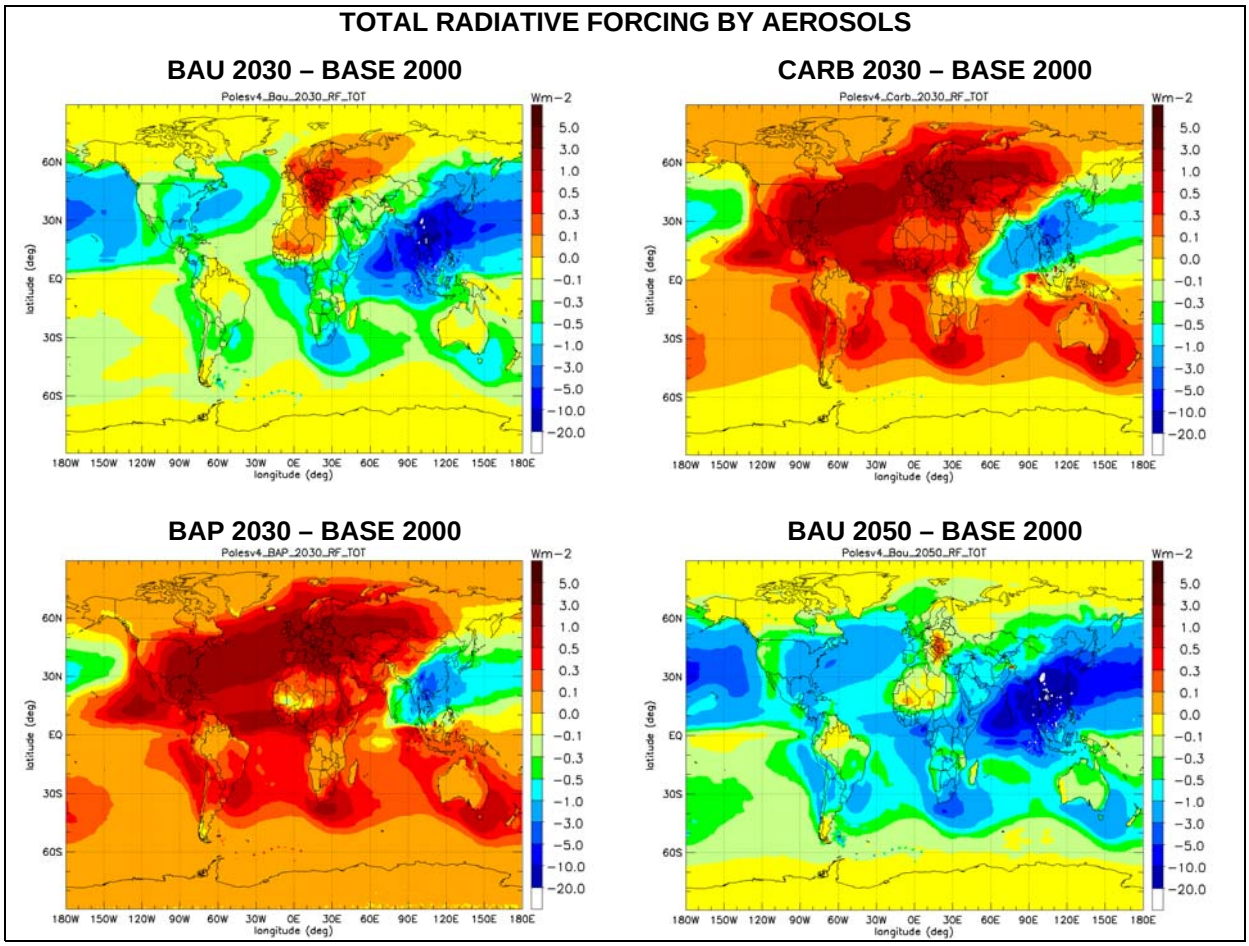

Figure19: Total of indirect and direct forcing [Wm-2] due to aerosol for selected scenarios and time horizons.

4.6 CH_4, CO_2, and N_2O concentrations pathway

As previously mentioned, in order to avoid expensive simulations over decadal time scales, we have performed all previous TM5 model simulations using the CH_4 mixing ratio for the year 2000, i.e. 1760 ppbv, whereas N_2O and CO_2 are not explicitly included in TM5. In order to assess the forcing due to a realistically changing CH4 concentration pathway, caused by emission trends and changes in the global OH concentrations, the following considerations are made.

Changes in NO_x, CO, and VOC emissions influence OH, but also the emissions and concentrations of CH_4 will cause a feedback on OH (*Prather*, IPCC-TAR, 2001). We use the TM5 CH_4 self-feedback factor (f=dln(LT)/dln(CH4); f=0.28, IPCC-TAR). Further we include natural CH4 emissions amounting to 300 Tg/yr, and changes in OH as resulting from the four scenario simulations with TM5. Further parameters to this model are: the atmospheric lifetime of OH (10 years), and the time constants for the loss of methane to soils and stratosphere (160 and 100 years, respectively). The resulting changes in CH_4 lifetime, comparing 2030 and 2000, (decreasing OH) amount to 0.8%, 1.2%, 4.5 %, and 1.7 % for the BAU, CARB, BAP, and CAP scenario respectively. Keeping natural methane

emissions constant, CH_4 levels increase to roughly 2050-2150 ppbv by 2030 for BAP and BAU, respectively, and 2200-2400 by 2050, whereas CARB and CAP lead to concentrations in the range 1800-1700 ppbv, by 2030, i.e. close to current levels, and 1670-1590 by 2050.

The resulting radiative forcing of CH_4 is calculated using the global approximations given in the IPCC TAR report (Table 6.2) and amount to 0.134, 0.017, 0.103 and -0.001 Wm^{-2}, for BAU, CARB, BAP and CAP, respectively in 2030, and 0.22, -0.032, 0.175 and -0.064 Wm-2 in 2050.

Higher methane concentrations lead to higher global ozone. Using an additional sensitivity simulation, we estimate that the additional forcing from increasing CH_4 on O_3 forcing amounts to ca. 0.05 Wm^{-2} for BAU in 2030, and less for the other scenarios, these forcings are included in the O3 forcing presented in the following section. The effect (i.e. an increase in surface ozone of 1.0 ppbv in annual mean ozone surface concentration due to the CH4 increase) has not yet been included in the assessment of impacts on vegetation and human health, presented earlier.

We evaluate the trend of CO_2 concentrations and radiative forcing using the CO_2 emissions as given in Figure 2, minus the CO_2 emissions captured, and without biofuel emissions (which we assumed to be CO_2 neutral). Net uptake of CO_2 by terrestrial ecosystems and oceans are in a first-order approximated by a CO_2 turnover time of 155 years, using the tabulated CO_2 emissions and abundances in the IPCC TAR report ("Bern-CC" model). CO_2 concentrations further increase to 404 (CARB), and 420 (BAU) ppmv in 2030, By 2050 the BAU CO2 concentrations further increase to ca. 490 ppmv, but level of at 397 ppmv for the CARB scenario. For completeness we also give in Figure 20 the same calculation using SRES-A2, and SRES-B2 CO2 emissions (Nakicenovic, 2000). The CARB and CAP scenarios stabilize at 415 and 400 ppmv in 2050 respectively (Figure 20b). Using the functional relationships for RF and CO_2 given in IPCC-TAR, the resulting CO_2 RF compared to 2000, amounts to 0.853, 0.54, 0.84, and 0.53 W/m² for BAU, CARB, BAP and CAP in 2030, respectively. For 2050 these numbers are 1.65, 0.47, 1.61, and 0.44 Wm^{-2}, respectively.

A similar approach is followed to calculate N_2O concentration pathways. We assume natural N_2O emissions of 18 Tg N_2O, and an atmospheric residence time of 130 years. N_2O mixing ratios increase from 316 ppbv in the year 2000 to 344 ppbv in 2030, and 365 ppbv in 2050. Calculated increased RF for BAU compared to 2000, amounts to ca. 0.08 W/m² in 2030, and 0.29 W/m² in 2050 , with minor differences among the 3 scenarios.

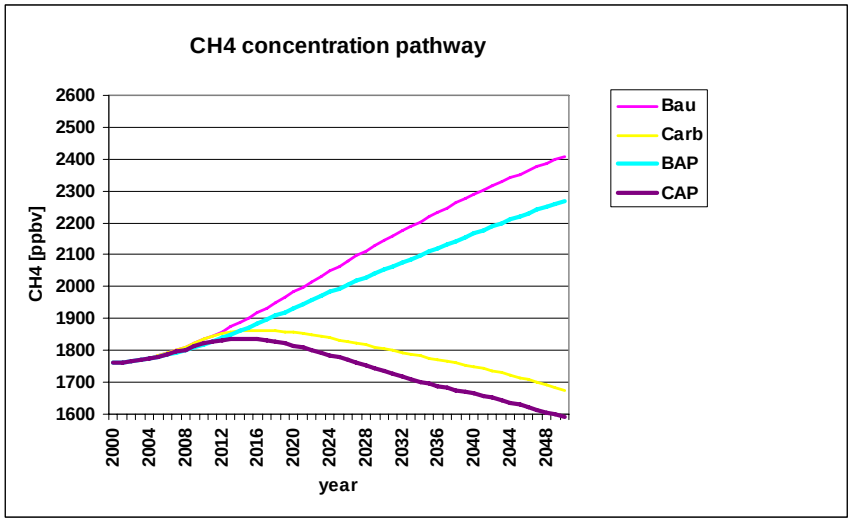

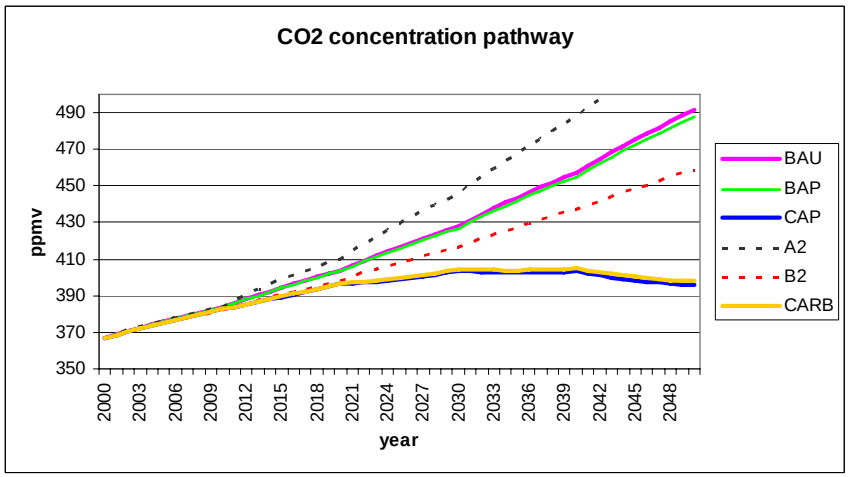

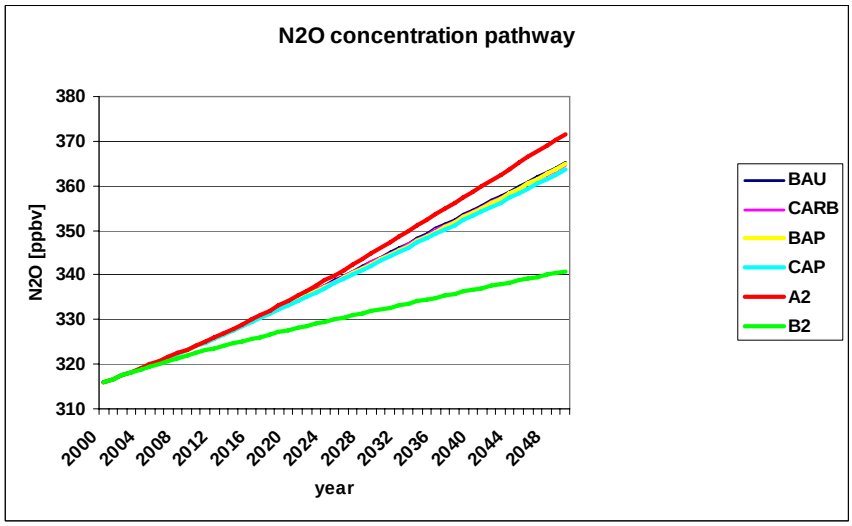

Figure 20: (a) Trend of CH_4 from 2000 to 2030 (b) trend of CO_2 from 2000 to 2050 (c) trend of N_2O from 2000 to 2050. The figure includes an estimate of concentrations of the IPCC SRES A2 and B2 scenarios using the same model.

4.7 Integrated radiative forcing and uncertainties

We use the global radiative forcings for aerosol, O_3, CH_4, N_2O, and CO_2 presented in the previous paragraphs, and calculate the overall RF as a measure of the net climate effect associated with the scenario. We tentatively assign the relative uncertainties listed in Table 4 to the global forcings, which are propagated in the estimate of the total global forcing as random errors (i.e. the square root of the sum of the quadratic errors).. We note here that these uncertainties are qualitatively consistent with those mentioned in the recent IPCC-AR4 report, but are a gross simplification of the real errors. For instance, this approach can not differentiate regional differences in errors.

As can be seen in Figure 21, the total forcing is mostly a balance of changes in aerosol and CO_2 concentrations, whereas changes in forcings from CH_4 N_2O, and O_3 have a smaller (but not negligible) impact. The trend and the uncertainty of the overall forcing are mostly determined by the highly uncertain indirect aerosol forcing. If we would disregard the indirect forcing, a consistent downward trend of radiative forcing would be predicted for the Carb/CAP scenarios.

Table 4: estimated uncertainty on each of the forcing agents

Component	Relative uncertainty
SO_4 direct RF	0.3
POM direct RF	0.3
BC direct RF	0.4
SO4 indirect RF	0.75
CH_4 RF	0.15
N_2O RF	0.3
CO_2 RF	0.1
O_3 RF	0.25

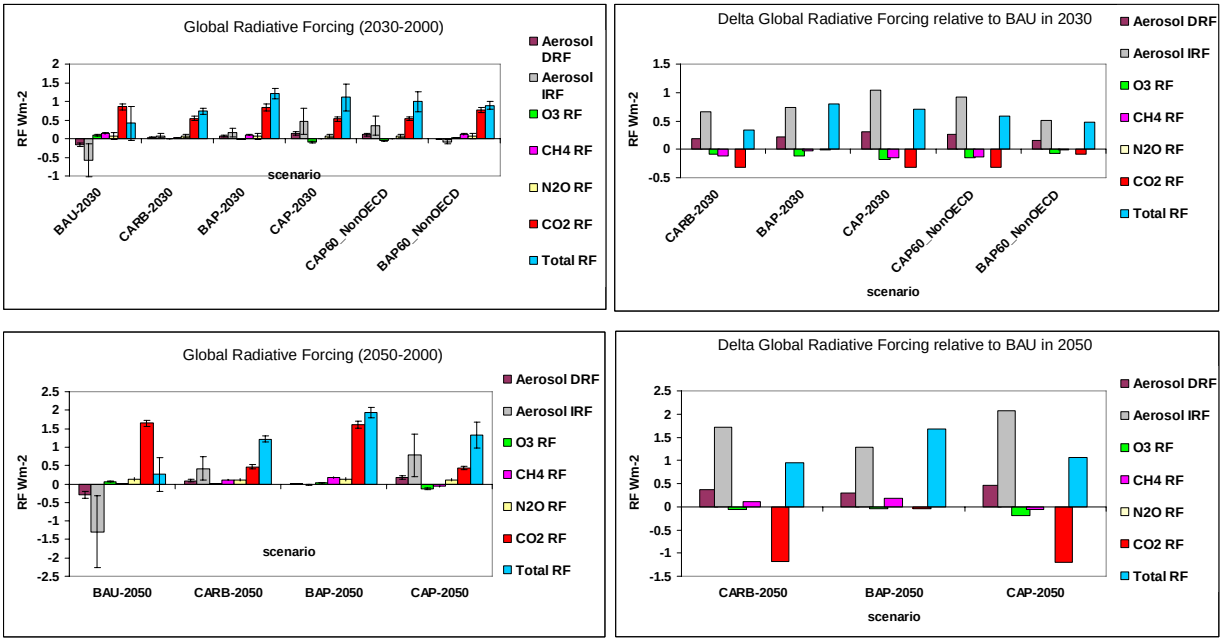

Figure 21. Global radiative forcings relative to the year 2000 for aerosols, GHG and total (left panels) for the year 2030 (upper) and 2050 (lower), and for each of the 3 emission reduction scenarios relative to BAU (right panels) for the year 2030 (upper) and 2050 (lower). DRF and IRF are direct and indirect forcing due to sulfate, organic and black carbon.

It is important to consider the time horizon for the scenario calculations. Comparing the impact of climate policy (CARB), air pollution policy (BAP) and combined climate and air pollution policy (CAP) to BAU (no further policy) shows that in 2030 all policies may lead to a net increase of the radiative forcing, with the climate dis-benefit being largest for BAP (0.8 Wm^{-2}), (highest AP control, no additional GHG control) and lowest for CARB (0.3 Wm^{-2}) (lowest AP control, highest GHG control). By 2050 the CARB/CAP scenarios lead to an additional increase of 1 Wm^{-2}, whereas BAP would give additional 1.7 Wm^{-2}. To avoid misinterpretation of these numbers, we emphasize again that the BAU scenario would lead to unacceptably high levels of air pollution. It also clearly shows the scope to limit undesirable increases of air pollution by implementing progressive climate policies. If developing countries do not implement the ambitious airquality targets, this may reduce the forcing by ca. 0.3 to 0.4 Wm^{-2}, at the expense of large exceedances of air quality targets.

The net effect of GHG policies (CARB and CAP) depends on the assumptions made on air pollution policies in place (BAU or BAP). With the very pessimistic assumption that air pollution emission factors would be constant from 2000 onwards (BAU), carbon policy (CARB) might increase radiative forcing in 2030 relative to BAU although the uncertainty range is near 100%. Given the more optimistic assumption on traditional air pollution policy in 2030 (BAP), adding GHG emission policies (CAP) might have a net positive effect on radiative forcing in 2030. In 2050 GHG policy always is expected to have a beneficial impact on radiative forcing (compared to no climate policy whatsoever) irrespective of whether combined with BAU air pollution control or BAP control measures.

5 Discussion and conclusions

In this work, scenarios have been explored ranging from the pessimistic assumption that no further climate and air pollution policy will be in place (BAU) to a scenario where climate and air pollution measures are integrated and implemented on the global scale (CAP). We also considered scenarios focusing on climate policy (CARB) and air quality policy only (BAP), and some variations on CARB and BAP, where air pollution emission controls in developing countries were assumed to be less ambitious.

The implementation of a global climate policy (CARB) results in substantial co-benefits in terms of reduced air pollutant emissions. This is due to fuel shift and decreased fuel demand, resulting in global emission reductions (compared to BAU) of SO_2 (-75% in 2050), CO (-35%); NO_x (-55%), NMVOC , NH_3, BC and POM (-25%)

On the other hand, the implementation of progressive emission abatement measures under air pollution policies (BAP scenario) has only a small impact on emissions of CH_4 (-3.5% in 2050 compared to BAU) and CO_2 (-1.5% in 2050 compared to BAU), but will reduce air pollution emissions globally by -35 to -70 %.

Comparing the additional benefits on air pollution of climate policy (CAP) relative to the case that only air pollution measures are implemented by 2030 (BAP), shows largest impact on SO_2 emissions, which further reduce by 45 Tg/yr (45%) in 2030, and 90 Tg/yr (75%) in 2050. For CAP60 vs. BAP60 the reduction in SO_2 emissions is even larger (60 Tg/yr in 2030, 120 Tg/yr in 2050) although the emissions obviously remain higher than in the BAP/CAP scenarios. Also for NOx (-26% in 2030, -42% in 2050), BC (-9% in 2030, -23% in 2050) and NMVOC (-4% in 2030, -20% in 2050) the co-benefits of climate policies for air quality are significant.

Calculation of environmental impacts of the series of scenarios shows major benefits for impacts on human health and avoiding damage to crops:

Comparing CARB to BAU in 2030 (the benefit of climate policy on air pollution) life expectancy increases by a global average of 1.7 months/person. Crop losses are reduced by 2.2 % worldwide.

Comparing BAP with BAU (the benefit of progressive air pollution policy), shows a worldwide benefit on life expectancy of global average of 3.7 months/person. Global crop losses due to ozone are reduced by 3.7 %.

Comparing CAP with BAP (the additional effect of climate policy compared to progressive air pollution policy) shows an additional benefit on life expectancy (global average) of 1.6 months/person. The relative yield losses of crops are additionally reduced by 0.9% worldwide.

In 2050 the life expectancy improves by 3.2 year/person for BAP, and additionally by. 3.7 (to 6.9) years/person if additionally climate policies are introduced. Crop losses decline by -4.7% (BAP) and additionally by -2 to -6.7 % (CARB), comparing to the business-as-usual case.

The benefits of the air pollution and climate policies on nitrogen deposition (as indicated by exceedance of critical loads) are relatively small, because of the important role of increasing agricultural NH_3 emissions that are counterbalancing the reduced NO_x emissions.

In general, it can be concluded that while climate change policies do have important co-benefits for air quality, they are alone not sufficient to solve air pollution problems and additional air pollution policies are also required.

Climate policies target at limiting long-term (2100) climate change. On the intermediate time-scales (2030-2050), however, there might be important trade-offs to be considered in climate and air pollution policies, since reducing particulate matter and precursor (especially sulfur) emissions, is likely to lead to a net positive radiative forcing and a warming of climate.

The net effect of GHG policies (CARB and CAP) depends on the assumptions made on air pollution policies in place (BAU or BAP). With the rather pessimistic assumption that emission factors would be constant from 2000 onwards carbon policy (CARB) might increase radiative forcing in 2030 compared to BAU. Assuming a more optimistic traditional air pollution policy in 2030 (as in BAP), additional GHG emission reductions as in CAP might lead to a net reduction in radiative forcing (compared to BAP already in 2030. Hence in 2030 the impact depends on the exact development of the emission controls in place for traditional air pollutants and will also depend on the extent of the GHG reductions and their indirect impact on air pollution emissions.

Taking a longer term perspective (the year 2050), the climate policy (CARB) or combined air pollution and climate policy (CAP) might lead to substantially smaller net increase of instanteneous radiative forcing than the air pollution scenario alone (i.e. 1 W m^{-2} versus 1.7 W m^{-2} relative to BAU).

Our analysis indicates that the reduction of air pollution, whether by air pollution or by climate policies, will lead to positive forcings and climate responses in the coming decades, a phenomenon now widely recognized in the scientific literature (i.e. Kloster et al, 2009; Andreae, 2007; Arneth et

al,2009; Bond 2007; Raes et al, 2009). The likely result of this is much accelerated increase of climate change in the coming decades, with possible consequences for adaptation of ecosystems and infrastructures. Current research focuses on identifying win-win strategies (i.e. reduction of Black Carbon, ozone, methane, and hydrofluorocarbons) that are beneficial for air pollution as well as climate (i.e. Dentener et al., 2005; Ramanathan and Xu, 2010)

References

Amann, M., W. Asman, I. Bertok, J. Cofala, C. Heyes, Z. Klimont, W. Schöpp and F. Wagner, Cost-effective emission reductions to meet the Environmental Targets of the Thematic Strategy on Air Pollution under different greenhouse gas constraints NEC. Scenario Analysis Report Nr. 5. IIASA, 2007.

Andreae, A., Atmospheric aerosols versus greenhouse gases in the twenty-first century, Phil. Trans. R. Soc. A, 365, 1915-1923, 2007.

Arneth, A., N. Unger, M. Kulmala and M. O Andreae, Clean the Air, Heat the Planet?, Science 326, :672-673, 2009.

Bergamaschi, P, C. Frankenberg, J.F. Meirink, M. Krol, F. Dentener, T. Wagner, U. Platt, J.O. Kaplan, S. Koerner, M. Heimann, E. Dlugogkencky, A. Goede, Satellite Chartography of Atmospheric Methane from SCIAMACHY Onboard ENVISAT: (II) Evaluation Based on Inverse Model Simulations, Journal of Geophysical Research, 112, D02304, doi:10.1029/2006JD007268, 2007.

Bond, T.C., 2007, Can warming particles enter global climate discussions?, Environm. Res. Lett. 2 045030 , 2007.

Boucher, O. and Lohmann, U.: The sulfate-CCN-cloud albedo effect- a sensitivity study with two general circulation models. Tellus. 47B, 281-300, 1995.

CEC, Impact Assessment accompanying the package of implementation measures for the EU's objectives on climate change and renewable energy for 2020. Commission Staff Working Document. SEC (2008) 85/3. Brussels, 2008.

Charlson, R.J., Schwartz, S.E., Hales, J.M., Cess, R.D., Coakely, J.A. Jr., Hansen, J.E., Hofmann, D. J.: Climate forcing by anthropogenic aerosols, Science, 255, 423-430, 1992.

Cohen, A. J., et al. "Urban air pollution." In M. Ezzati, A. D. Rodgers, A. D. Lopez, and C. J. L. Murray, eds. Comparative quantification of health risks: Global and regional burden of disease due to selected major risk factors, Vol 2. Geneva, World Health Organization, 2004.

De Meij, A., M. Krol, F. Dentener, V. E., E. Cuvelier, and P. Thunis, The sensitivity of aerosol in Europe to two different emission inventories and temporal distribution of emissions, Atmospheric Chemistry and Physics, Vol. 6, pp 4287-4309, 25-9-2006..

Dentener, F.J., and Crutzen P.J., Reaction of N_2O_5 on tropospheric aerosols: impact on the global distributions of NO_X, O_3 and OH, J. Geophys. Res., 98, 7149-7163, 1993.

Dentener F., Stevenson, D, Cofala, J., Mechler R., Amann, M., Bergamaschi P., Raes F., Derwent, R.G. The impact of air pollutant and methane emission controls on tropospheric ozone and radiative forcing: CTM calculations for the period 1990-2030, Atmospheric Chemistry and Physics, 5, 1731-1755, 2005.

Dentener, F., J. Drevet, J.F. Lamarque, I. Bey, B. Eickhout, A.M. Fiore, D. Hauglustaine, L.W. Horowitz, M. Krol, U.C. Kulshrestha, M. Lawrence, C. Galy-Lacaux, S. Rast, D. Shindell, D. Stevenson, T. Van Noije, C. Atherton, N. Bell, D. Bergman, T. Butler, J. Cofala, B. Collins, R. Doherty, K. Ellingsen, J. Galloway, M. Gauss, V. Montanaro, J.F. Müller, G. Pitari, J. Rodriguez, M. Sanderson, S. Strahan, M. Schultz, F. Solmon, K. Sudo, S. Szopa, O. Wild, Nitrogen and Sulphur Deposition on regional and global scales: a multi-model evaluation, Global Biogeochemical Cycles, 20, GB4003, doi:10.1029/2005GB002672, 2006 .

Doering, U, Janssens-Maenhout, G., van Aardenne, J., Pagliari, V., CIRCE project, report D3.3.1 – Scenarios of future climate change, 2009.

Edwards, J. M.,Slingo, A., Studies with a flexible new radiation code. I: Choosing a configuration for a large-scale model, Q.J.R. Meteorol. Soc., 122, 53 http://dx.doi.org/10.1002/qj.49712253107, 2006.

EEA. Emission Inventorty Guidebook. available via: www.eea.europa.eu/publications/EMEPCORINAIR4, 2006

Fischer, G., van Velthuizen, H., Nachtergaele, F., Medow, S.,Global Agro-Ecological Zones (Global – AEZ) [CD-ROM and web site. Available from: http://www.fao.org/ag/AGL/agll/gaez/index.htm], Food and Agricultural Organization/International Institute for Applied Systems Analysis (FAO/IIASA). Available from: http://www.iiasa.ac.at/Research/LUC/GAEZ/index.htm, 2000.

Fuhrer, J., Skärby, L., Ashmore, M.R., Critical levels for ozone effects on vegetation in Europe. Environmental Pollution 97, 91–106, 1997.

Galloway, J.M, F..J. Dentener, D. G. Capone, E. W. Boyer, R. W. Howarth, S. P. Seitzinger, G. P. Asner, C. Cleveland, P. Green, E. Holland, D. M. Karl, A.F. Michaels, J. H. Porter, A. Townsend, and C. Vorosmarty , Nitrogen Cycles: Past, Present and Future, Biogeochemistry, 70, 153-226, 2004.

Gauss, M., G. Myhre , G. Pitari, M. J. Prather, I. S. A. Isaksen, T. K. Berntsen, G. P. Brasseur, F. J. Dentener, R. G. Derwent, D. A., Hauglustaine, L. W. Horowitz, D. J. Jacob, M. Johnson, K. S. Law, L. J. Mickley, J.-F. Müller, P.-H. Plantevin, J. A. Pyle, H. L. Rogers, D. S. Stevenson, J. K. Sundet, M. van Weele, O. Wild, Radiative forcing in the 21st century due to ozone changes in the troposphere and the lower stratosphere, J.Geophys. Res., 108, D9, 4292, doi:10.1029/2002JD002624, 2003.

Haywood, J. and Boucher, O.: Estimates of the direct and indirect radiative forcing due to tropospheric aerosols: A review, Rev. Geophys., 38 (4), 513-543, 10.1029/1999RG000078, 2000.

Hertel, O., Berkowicz, R., Christensen, J., , Test of two numerical schemes for use in atmospheric transport-chemistry models, Atmos. Environ. 27A, 16, pp. 2591-2611, 1993.

Hess, M., Koepke, P., Schult, I. : Optical Properties of Aerosols and Clouds: The software package OPAC, Bull. Am. Met. Soc., 79, 831-844, 1998.

Holland, M., A. Hunt, F. Hurley, S. Navrud, P. Watkiss, Methodology for the Cost-Benefit analysis for CAFE: Volume 1: Overview of Methodology, AEA Technology, AEAT/ED51014/Methodology Issue 4 http://ec.europa.eu/environment/archives/air/cafe/pdf/cba_methodology_vol1.pdf, 2005.

Holtslag, A. A. M. and Moeng, C.-H.: Eddy diffusivity and countergradient transport in the convective atmospheric boundary layer, J. Atmos. Sci., 48, 1690–1698, 1991.

Houweling, S., F. Dentener, and J. Lelieveld, The impact of nonmethane hydrocarbon compounds on tropospheric photochemistry, J. Geophys. Res., 103, 10673-10696, 1998.

IIASA, M. Amann, I. Bertok, R. Cabala, J. Cofala, C.Heyes, F. Gyarfas, Z. Klimont, W. Schöpp, F. Wagner, A further emission control scenario for the Clean Air For Europe (CAFÉ) program, CAFÉ scenario analysis report 7, 2007.

IPCC-AR4: Climate Change 2007: The Physical Science Basis. Contribution of Working Group I to the Fourth Assessment Report of the Intergovernmental Panel on Climate Chang [Solomon, S., D. Qin, M. Manning, Z. Chen, M. Marquis, K.B. Averyt, M.Tignor and H.L. Miller (eds.)]. Cambridge University Press, Cambridge, United Kingdom and New York, NY, USA, 2007.

Kinne, S.; Schulz, M.; Textor, C.; Guibert, S.; Balkanski, Y.; Bauer, S. E.; Berntsen, T.; Berglen, T. F.; Boucher, O.; Chin, M.; Collins, W.; Dentener, F.; Diehl, T.; Easter, R.; Feichter, J.; Fillmore, D.; Ghan, S.; Ginoux, P.; Gong, S.; Grini, A.; Hendricks, J.; Herzog, M.; Horowitz, L.; Isaksen, I.; Iversen, T.; Kirkevåg, A.; Kloster, S.; Koch, D.; Kristjansson, J. E.; Krol, M.; Lauer, A.;

Lamarque, J. F.; Lesins, G.; Liu, X.; Lohmann, U.; Montanaro, V.; Myhre, G.; Penner, J.; Pitari, G.; Reddy, S.; Seland, O.; Stier, P.; Takemura, T.; Tie, X. An AeroCom initial assessment – optical properties in aerosol component modules of global models. *Atmos. Chem. Phys.* 6, 1777-1813, 2006.

Kloster, S., F. Dentener, J. Feichter, F. Raes, E. Roeckner, U. Lohmann, E. Roeckner, I. Fischer-Bruns, A GCM study of future climate response to air pollution reductions, Climate Dynamics, 34, 1177-1194, 2010.

Krol, M., Houweling, S., Bregman, B., van den Broek, M., Segers, A., van Velthoven, P., Peters, W., Dentener F., Bergamaschi P., The two-way nested global chemistry-transport zoom model TM5: algorithm and application. Atmos. Chem. Phys. 4, 3975-4018 – 2005.

Li, J., Wong, J., Dobbie, J.S., Chylek, P.: Parameterization of the Optical Properties of Sulfate Aerosols, Journal of the Atmospheric Sciences, 58, 193-209, 10.1175/1520-0469, 2001.

Louis, J. F.: A parametric model of vertical eddy fluxes in the atmosphere, Boundary LayerMeteor., 17, 187–202, 1979.

Marmer, E., Langmann, B., Hungershöfer, K., Trautmann, T.: Aerosol modeling over Europe 2: Interannual variability of aerosol short-wave direct radiative forcing, J. Geophys. Res., 112, D23S16,10.1029/2006JD008040, 2007.

Mechler, R., M. Amann and W. Schoepp. Methodology to Estimate Changes in Statistical Life Expectancy Due to the Control of Particulate Matter in Air Pollution. IIASA Interim Report IR-02-035, 2002.

Metzger, S., F. Dentener, J. Lelieveld', S. Pandis, Gas/aerosol partitioning I, a computationally efficient model, J. Geophysical Research, 107, 10.1029/2001JD001102, 2002.

Mills, G., Buse, A., Gimeno, B., Bermejo, V., Holland, M., Emberson, L., Pleijel, H.,.A synthesis of AOT40-based response functions and critical levels of ozone for agricultural and horticultural crops, Atmospheric Environment, 41, 2630-2643, 2007.

Myhre, C. E. L. and Nielsen, C. J.: Optical properties in the UV and visible spectral region of organic acids relevant to tropospheric aerosols. Atmospheric Chemistry and Physics, 4 (7), 1759-1769, 2004.

Nakicenovic N. et al. (ed.), Special Report on Emissions Scenarios 2000, Contribution to the Intergovernmental Panel on Climate Change, Cambridge University Press, Cambridge, UK, 2000.

Prather, M., D. Ehhalt, F. Dentener, R. Derwent, E. Dlugokencky, E. Holland, I. Isaksen, J Katima, V. Kirchhoff, P. Matson, P. Midgley, M. Wang, Chapter 4, Atmospheric chemistry and greenhouse gases, Chapter 4, in: Climate Change 2001: The scientific basis. Contribution of Working group 1 to the Third Assessment Report of the Intergovernmental Panel on Climate Change, edited by J.T. Houghton, Y.Ding, D.J.Griggs, M.Noguer, P.J. van der Linden, X. Dai, K. Maskell, C.A. Johnsson, Cambridge University Press, Cambridge, UK and New York, NY, USA, 881 p., 2001.

Ohara, T., Akimoto, H., Kurokawa, J., Horii, N., Yamaji, K., Yan, X., and Hayasaka, T.: An Asian emission inventory of anthropogenic emission sources for the period 1980–2020, Atmos. Chem. Phys., 7, 4419-4444, 2007.

Olivier, J.G.J., Van Aardenne, J.A., Dentener, F., Ganzeveld, L. and J.A.H.W. Peters, Recent trends in global greenhouse gas emissions: regional trends and spatial distribution of key sources. In: Non-CO2 Greenhouse Gases (NCGG-4), A. van Amstel (ed), page 325-330. Millpress, Rotterdam, ISBN 905966 043 9, 2005.

Peters, W., Krol, M.C., Bruhwiler, L., Dlugokencky, Dutton, G., Miller, J.B., Bergamaschi Peter, Dentener Frank, van Velthoven, P., Tans, P.P., Towards regional scale inversion using a two-way nested global model: Characterization of transport using SF6, J. Geophys. Res., D19134, doi:10.1029/2004JD005020, 2004.

Pope III, C.A., R.T. Burnett; M. J. Thun; et al., Lung Cancer, Cardiopulmonary Mortality, and Long-term Exposure to Fine Particulate Air Pollution http://jama.ama-assn.org/cgi/content/full/287/9/1132, JAMA, 287(9):1132-1141 (doi:10.1001/jama.287.9.1132), 2002

Putaud, J.-P. ,R. Van Dingenen, A. Alastuey, H. Bauer, W. Birmili, J. Cyrys, H. Flentje, S. Fuzzi, R. Gehrig, H.C. Hansson, R.M. Harrison, H. Herrmann, R. Hitzenberger, C. Huglin, A.M. Jones, A. Kasper-Giebl, G. Kiss, A. Kousa, T.A.J. Kuhlbusch, G. Loschau, W. Maenhaut, A. Molnar, T. Moreno, J. Pekkanen, C. Perrino, M. Pitz, H. Puxbaum, X. Querol, S. Rodriguez, I. Salma, J. Schwarz, J. Smolik, J. Schneider, G. Spindler, H. ten Brink, J. Tursic, M. Viana, A. Wiedensohler, F. Raes, A European aerosol phenomenology - 3: Physical and chemical characteristics of particulate matter from 60 rural, urban, and kerbside sites across Europe, Atmos. Envir., 44, , 1308-1320, 2010.

Raes, F. and Seinfeld, John H, New Directions: Climate change and air pollution abatement: A bumpy road. Atmospheric Environment, 43 (32). pp. 5132-5133. ISSN 1352-2310, 2009.

Ramanathan, V., and Y. Xu, The Copenhagen Accord for limiting global warming: Criteria, constraints, and available avenues, PNAS, www.pnas.org/lookup/suppl/doi:10.1073/pnas, 1002293107/-/DCSupplemental, 2010.

Russ, P., T. Wiesenthal, D. van Regemorter and J. Ciscar, Global Climate Policy Scenarios for 2030 and beyond. Analysis of Greenhouse Gas Emission Reduction Pathway Scenarios with the POLES and GEM-E3 models. JRC ITPS, Report EUR 23032 EN, 2007.

Russel, G., Lerner J., A new finite-differencing scheme for the tracer transport equation. J. Appl. Meteorol. 20, pp. 1483-1498, 1981.

Stevenson, D. S.; Dentener, F. J.; Schultz, M. G.; Ellingsen, K.; Van Noije, T. P. C.; Wild, O.; Zeng, G.; M. Amann; Atherton, C. S.; Bell, N.; Bergmann, D. J.; Bey, I.; Butler, T.; Cofala, J.; Collins, W. J.; Derwent, R. G.; Doherty, R. M.; Drevet, J.; Eskes, H. J.; Fiore, A.; Gauss, M. A.; Hauglustaine, D. A.; Horowitz, L. W.; Isaksen, I. S. A.; Krol, M. C.; Lamarque, J. F.; Lawrence, M. G.; Montanero, V.; Müller, J. F.; Pitari, G.; Prather, M. J.; Pyle, J. A.; Rast, S.; Rodriguez, J. M.; Sanderson, M. G.; Savage, N. H.; Shindell, D. T.; Strahan, S. E.; Sudo, K.; Szopa, S. Multi-model ensemble simulations of present-day and near-future tropospheric ozone. J. Geophys. Res.111, D8, D0830110.1029/2005JD006338, 2006.

Textor, C.; Schulz, M.; Guibert, S.; Kinne, S.; Balkanski, Y.; Bauer, S.; Berntsen, T.; Berglen, T.; Boucher, O.; Chin, M.; Dentener, F.; Diehl, T.; Easter, R.; Feichter, H.; Fillmore, D.; Ghan, S.; Ginoux, P.; Gong, S.; Grini, A.; Hendricks, J.; Horowitz, L.; Huang, P.; Isaksen, I.; Iversen, T.; Kloster, S.; Koch, D.; Kirkevåg, A.; Kristjansson, J. E.; Krol, M.; Lauer, A.; Lamarque, J. F.; Liu, X.; Montanaro, V.; Myhre, G.; Penner, J.; Pitari, G.; Reddy, S.; Seland, Ø.; Stier, P.; Takemura, T.; Tie, X. Analysis and quantification of the diversities of aerosol life cycles within AeroCom. Atmos. Chem. Phys., 6, pp 1777-1813, 2006. .

Tiedtke, M. 1989, A comprehensive mass flux scheme for cumulus parameterisation in large scale models. *Mon. Wea. Rev*. 177, pp. 1779–1800, 1989.

Twomey, Sean A.: Pollution and the Planetary Albedo, Atmos. Env. 8, 1251-1256, 1974.

Van Aardenne, J.A., F. Dentener, J.G.J. Olivier and J.A.H.W. Peter). The EDGAR 3.2 Fast Track 2000 dataset (32FT2000) http://www.mnp.nl/edgar/model/v32ft2000edgar/docv32ft2000, 2005.

Van Dingenen, R, F.J. Dentener, F. Raes, M.C. Krol, L. Emberson, J.Cofala, The global impact of ozone on agricultural crop yields under current and future air quality legislation, Atmos. Env, 43, 604-618, 2008.

van Vuuren, D. P., Isaac, M., Kundzewicz, Z., Arnell, N., Barker T., Criqui P., Bauer N., Berkhout F., Hilderink H., Hinkel J., Hof A., Kitous A., Kram T., Mechler R., Radziejewski M., Scrieciu S., Adaptation and Mitigation Strategies: Supporting European Climate Policy, 2009.

van Vuuren, D. P., den Elzen M. G. J., Lucas P. L., Eickhout, B., Strengers, B. J., van Ruijven, B. Steven Wonink & Roy van Houdt, 2007, Stabilizing greenhouse gas concentrations at low levels: an assessment of reduction strategies and costs, Climatic Change 81:119–159, 2007.

World Health Organization, 2004 "Health aspects of air pollution", WHO regional office for Europe, Copenhagen, 2004.

World Bank. The cost of pollution in China, Rural Development, Natural Resources and Environment Management Unit, The world Bank, Washington DC, 2007.

Annex 1: Definitions of geographic areas.

Table A1: Geographic areas identified in the scenario calculation

C_group_Poles	Country_code_A3	Name	EDGAR-POLES summary
	XXX	Oceans	
-	ATA	Antarctica	-
-	GRL	Greenland	-
AUT	AUT	Austria	EU27
BGR	BGR	Bulgaria	EU27
BLT	EST	Estonia	EU27
BLT	LTU	Lithuania	EU27
BLT	LVA	Latvia	EU27
BLX	BEL	Belgium	EU27
BLX	LUX	Luxembourg	EU27
BRA	BRA	Brazil	South America
CAN	CAN	Canada	North America
CHN	CHN	China	Asia
CHN	HKG	Hong Kong	Asia
COR	KOR	Korea, Republic of	Asia
DNK	DNK	Denmark	EU27
DNK	FRO	Faroe Islands	EU27
EGY	EGY	Egypt	Africa
ESP	ESP	Spain	EU27
FIN	ALA	Åland Islands	EU27
FIN	FIN	FinlanGd	EU27
FRA	AND	Andorra	EU27
FRA	FRA	France	EU27
FRA	MCO	Monaco	EU27
GBR	GBR	United Kingdom	EU27
GBR	GGY	Guernsey	EU27
GBR	IMN	Isle of Man	EU27
GBR	JEY	Jersey	EU27
GOLF	ARE	United Arab Emirates	Middle East
GOLF	BHR	Bahrain	Middle East
GOLF	IRN	Iran, Islamic Republic of	Middle East
GOLF	IRQ	Iraq	Middle East
GOLF	KWT	Kuwait	Middle East
GOLF	OMN	Oman	Middle East
GOLF	QAT	Qatar	Middle East
GOLF	SAU	Saudi Arabia	Middle East
GOLF	YEM	Yemen	Middle East
GRC	GRC	Greece	EU27
HUN	HUN	Hungary	EU27
IRL	IRL	Ireland	EU27
ITA	ITA	Italy	EU27
ITA	SMR	San Marino	EU27
ITA	VAT	Holy See (Vatican City State)	EU27
C_group_Poles	**Country_code_A3**	**Name**	**EDGAR-POLES summary**
JPN	JPN	Japan	Japan

MEME	ISR	Israel	Middle East
MEME	JOR	Jordan	Middle East
MEME	LBN	Lebanon	Middle East
MEME	PSE	Palestinian Territory, Occupied	Middle East
MEME	SYR	Syrian Arab Republic	Middle East
MEX	MEX	Mexico	South America
NDE	IND	India	Asia
NLD	NLD	Netherlands	EU27
NOAN	ESH	Western Sahara	Africa
NOAN	MAR	Morocco	Africa
NOAN	TUN	Tunisia	Africa
NOAP	DZA	Algeria	Africa
NOAP	LBY	Libyan Arab Jamahiriya	Africa
POL	POL	Poland	EU27
PRT	PRT	Portugal	EU27
RCAM	ABW	Aruba	South America
RCAM	AIA	Anguilla	South America
RCAM	ANT	Netherlands Antilles	South America
RCAM	ATG	Antigua and Barbuda	South America
RCAM	BHS	Bahamas	South America
RCAM	BLZ	Belize	South America
RCAM	BMU	Bermuda	South America
RCAM	BRB	Barbados	South America
RCAM	CRI	Costa Rica	South America
RCAM	CUB	Cuba	South America
RCAM	CYM	Cayman Islands	South America
RCAM	DMA	Dominica	South America
RCAM	DOM	Dominican Republic	South America
RCAM	GLP	Guadeloupe	South America
RCAM	GRD	Grenada	South America
RCAM	GTM	Guatemala	South America
RCAM	HND	Honduras	South America
RCAM	HTI	Haiti	South America
RCAM	JAM	Jamaica	South America
RCAM	KNA	Saint Kitts and Nevis	South America
RCAM	LCA	Saint Lucia	South America
RCAM	MSR	Montserrat	South America
RCAM	MTQ	Martinique	South America
RCAM	NIC	Nicaragua	South America
RCAM	PAN	Panama	South America
RCAM	PRI	Puerto Rico	South America
RCAM	SLV	El Salvador	South America
RCAM	TCA	Turks and Caicos Islands	South America
RCAM	TTO	Trinidad and Tobago	South America
RCAM	VCT	Saint Vincent and the Grenadines	South America
C_group_Poles	**Country_code_A3**	**Name**	**EDGAR-POLES summary**
RCAM	VGB	Virgin Islands, British	South America
RCEU	ALB	Albania	Other Europe
RCEU	BIH	Bosnia and Herzegovina	Other Europe

RCEU	HRV	Croatia	Other Europe
RCEU	MKD	Macedonia, the former Yugoslav Republic of	Other Europe
RCEU	MNE	Montenegro	Other Europe
RCEU	SRB	Serbia	Other Europe
RCZ	CZE	Czech Republic	EU27
RFA	DEU	Germany	EU27
RIS	ARM	Armenia	Russia+
RIS	AZE	Azerbaijan	Russia+
RIS	BLR	Belarus	Russia+
RIS	GEO	Georgia	Russia+
RIS	KAZ	Kazakhstan	Russia+
RIS	KGZ	Kyrgyzstan	Russia+
RIS	MDA	Moldova, Republic of	Russia+
RIS	TJK	Tajikistan	Russia+
RIS	TKM	Turkmenistan	Russia+
RIS	UZB	Uzbekistan	Russia+
RJAN	ASM	American Samoa	Oceania
RJAN	AUS	Australia	Oceania
RJAN	CCK	Cocos (Keeling) Islands	Oceania
RJAN	COK	Cook Islands	Oceania
RJAN	CXR	Christmas Island	Oceania
RJAN	FJI	Fiji	Oceania
RJAN	FSM	Micronesia, Federated States of	Oceania
RJAN	GUM	Guam	Oceania
RJAN	HMD	Heard Island and McDonald Islands	Oceania
RJAN	KIR	Kiribati	Oceania
RJAN	MHL	Marshall Islands	Oceania
RJAN	MNP	Northern Mariana Islands	Oceania
RJAN	NCL	New Caledonia	Oceania
RJAN	NFK	Norfolk Island	Oceania
RJAN	NIU	Niue	Oceania
RJAN	NRU	Nauru	Oceania
RJAN	NZL	New Zealand	Oceania
RJAN	PCN	Pitcairn	Oceania
RJAN	PLW	Palau	Oceania
RJAN	PNG	Papua New Guinea	Oceania
RJAN	PYF	French Polynesia	Oceania
RJAN	SLB	Solomon Islands	Oceania
RJAN	TKL	Tokelau	Oceania
RJAN	TLS	Timor-Leste	Asia
RJAN	TON	Tonga	Oceania
RJAN	TUV	Tuvalu	Oceania
RJAN	VUT	Vanuatu	Oceania
C_group_Poles	**Country_code_A3**	**Name**	**EDGAR-POLES summary**
RJAN	WLF	Wallis and Futuna	Oceania
RJAN	WSM	Samoa	Oceania
ROM	ROU	Romania	EU27
ROWE	CHE	Switzerland	Other Europe
ROWE	GIB	Gibraltar	Other Europe

ROWE	ISL	Iceland	Other Europe
ROWE	LIE	Liechtenstein	-
ROWE	NOR	Norway	Other Europe
ROWE	SJM	Svalbard and Jan Mayen	-
RSAM	ARG	Argentina	South America
RSAM	BOL	Bolivia	South America
RSAM	BVT	Bouvet Island	South America
RSAM	CHL	Chile	South America
RSAM	COL	Colombia	South America
RSAM	ECU	Ecuador	South America
RSAM	FLK	Falkland Islands (Malvinas)	South America
RSAM	GUF	French Guiana	South America
RSAM	GUY	Guyana	South America
RSAM	PER	Peru	South America
RSAM	PRY	Paraguay	South America
RSAM	SGS	South Georgia and the South Sandwich Islands	South America
RSAM	SUR	Suriname	South America
RSAM	URY	Uruguay	South America
RSAM	VEN	Venezuela	South America
RSAS	AFG	Afghanistan	Asia
RSAS	BGD	Bangladesh	Asia
RSAS	BTN	Bhutan	Asia
RSAS	LKA	Sri Lanka	Asia
RSAS	MDV	Maldives	Asia
RSAS	NPL	Nepal	Asia
RSAS	PAK	Pakistan	Asia
RSEA	BRN	Brunei Darussalam	Asia
RSEA	IDN	Indonesia	Asia
RSEA	IOT	British Indian Ocean Territory	Asia
RSEA	KHM	Cambodia	Asia
RSEA	LAO	Lao People's Democratic Republic	Asia
RSEA	MAC	Macao	Asia
RSEA	MMR	Myanmar	Asia
RSEA	MNG	Mongolia	Asia
RSEA	MYS	Malaysia	Asia
RSEA	PHL	Philippines	Asia
RSEA	PRK	Korea, Democratic People's Republic of	Asia
RSEA	SGP	Singapore	Asia
RSEA	THA	Thailand	Asia
C_group_Poles	**Country_code_A3**	**Name**	**EDGAR-POLES summary**
RSEA	TWN	Taiwan, Province of China	Asia
RSEA	VNM	Viet Nam	Asia
RSL	SVK	Slovakia	EU27
RUS	RUS	Russian Federation	Russia+
SMC	CYP	Cyprus	EU27
SMC	MLT	Malta	EU27
SMC	SVN	Slovenia	EU27

SSAF	AGO	Angola	Africa
SSAF	ATF	French Southern Territories	Oceania
SSAF	BDI	Burundi	Africa
SSAF	BEN	Benin	Africa
SSAF	BFA	Burkina Faso	Africa
SSAF	BWA	Botswana	Africa
SSAF	CAF	Central African Republic	Africa
SSAF	CIV	Côte d'Ivoire	Africa
SSAF	CMR	Cameroon	Africa
SSAF	COD	Congo, the Democratic Republic of the	Africa
SSAF	COG	Congo	Africa
SSAF	COM	Comoros	Africa
SSAF	CPV	Cape Verde	Africa
SSAF	DJI	Djibouti	Africa
SSAF	ERI	Eritrea	Africa
SSAF	ETH	Ethiopia	Africa
SSAF	GAB	Gabon	Africa
SSAF	GHA	Ghana	Africa
SSAF	GIN	Guinea	Africa
SSAF	GMB	Gambia	Africa
SSAF	GNB	Guinea-Bissau	Africa
SSAF	GNQ	Equatorial Guinea	Africa
SSAF	KEN	Kenya	Africa
SSAF	LBR	Liberia	Africa
SSAF	LSO	Lesotho	Africa
SSAF	MDG	Madagascar	Africa
SSAF	MLI	Mali	Africa
SSAF	MOZ	Mozambique	Africa
SSAF	MRT	Mauritania	Africa
SSAF	MUS	Mauritius	Africa
SSAF	MWI	Malawi	Africa
SSAF	MYT	Mayotte	Africa
SSAF	NAM	Namibia	Africa
SSAF	NER	Niger	Africa
SSAF	NGA	Nigeria	Africa
SSAF	REU	Réunion	Africa
SSAF	RWA	Rwanda	Africa
SSAF	SDN	Sudan	Africa
SSAF	SEN	Senegal	Africa
C_group_Poles	**Country_code_A3**	**Name**	**EDGAR-POLES summary**
SSAF	SHN	Saint Helena	Africa
SSAF	SLE	Sierra Leone	Africa
SSAF	SOM	Somalia	Africa
SSAF	STP	Sao Tome and Principe	Africa
SSAF	SWZ	Swaziland	Africa
SSAF	SYC	Seychelles	Africa
SSAF	TCD	Chad	Africa
SSAF	TGO	Togo	Africa
SSAF	TZA	Tanzania, United Republic of	Africa

SSAF	UGA	Uganda	Africa
SSAF	ZAF	South Africa	Africa
SSAF	ZMB	Zambia	Africa
SSAF	ZWE	Zimbabwe	Africa
SWE	SWE	Sweden	EU27
TUR	TUR	Turkey	Middle East
UKR	UKR	Ukraine	Russia+
USA	SPM	Saint Pierre and Miquelon	-
USA	UMI	United States Minor Outlying Islands	-
USA	USA	United States	North America
USA	VIR	Virgin Islands, U.S.	South America

Annex 2: Examples of coupling POLES and EDGAR data

A2.1 Power generation

The coupling of a POLES growth rate to the EDGAR data is illustrated for the power generation sector in Table A2-1. As the POLES sectoral information is less detailed than EDGAR, in particular for the fuels, aggregations were made and implied emission factors were derived accordingly.

The growth rates from the power generation sector were used also for the industrial production sector, assuming that the activity/emission trends in industrial production follows the combustion trends in that sector. The growth rates are entirely based on the economic dynamics of fuel costs and carbon taxes of POLES and the resulting fuel shifts an consumption.

Table A2-1: Allocation of POLES growth rates to the power generation sector

IEA_fuel	IEA_sector	POLES_sec	POLES_fuel	EDGAR ad_code	growth rate
ANTCOAL, BITCOAL, BKB, BROWN, COKCOAL, LIGNITE, PATFUEL, SUBCOAL, HARDCOAL	AUTOCHP	FINEL	COAL	ENE.AHP.BTC	FINEL.COAL
ANTCOAL, BITCOAL, BKB, BROWN, COKCOAL, LIGNITE, PATFUEL, SUBCOAL, HARDCOAL	AUTOELEC	FINEL	COAL	ENE.AEL.BTC	FINEL.COAL
ANTCOAL, BITCOAL, BKB, BROWN, COKCOAL, LIGNITE, PATFUEL, SUBCOAL, HARDCOAL	AUTOHEAT	FINEL	COAL	ENE.AHE.BTC	FINEL.COAL
ANTCOAL, BITCOAL, BKB, BROWN, COKCOAL, LIGNITE, PATFUEL, SUBCOAL, HARDCOAL	EPOWERPLT	FINEL	COAL	ENE.POW.BTC	FINEL.COAL
ANTCOAL, BITCOAL, BKB, BROWN, COKCOAL, LIGNITE, PATFUEL, SUBCOAL, HARDCOAL	EPUMPST	FINEL	COAL	ENE.PUM.BTC	FINEL.COAL
ANTCOAL, BITCOAL, BKB, BROWN, COKCOAL, LIGNITE, PATFUEL, SUBCOAL, HARDCOAL	MAINCHP	FINEL	COAL	ENE.CHP.BTC	FINEL.COAL
BLFURGS, COKEOVGS, ETHANE, GASWKSGS, MANGAS, NATGAS, NGL, OXYSTGS	AUTOCHP	FINEL	GAS	ENE.AHP.NGS	FINEL.GAS
REFINGAS, LPG	AUTOCHP	FINEL	OIL	ENE.AHP.NGS	FINEL.OIL
BLFURGS, COKEOVGS, ETHANE, GASWKSGS, MANGAS, NATGAS, NGL, OXYSTGS	AUTOELEC	FINEL	GAS	ENE.AEL.NGS	FINEL.GAS
REFINGAS, LPG	AUTOELEC	FINEL	OIL	ENE.AEL.NGS	FINEL.OIL
BLFURGS, COKEOVGS, ETHANE, GASWKSGS, MANGAS, NATGAS, NGL, OXYSTGS	AUTOHEAT	FINEL	GAS	ENE.AHE.NGS	FINEL.GAS
REFINGAS, LPG	AUTOHEAT	FINEL	OIL	ENE.AHE.NGS	FINEL.OIL
BLFURGS, COKEOVGS, ETHANE, GASWKSGS, MANGAS, NATGAS, NGL, OXYSTGS	EPOWERPLT	FINEL	GAS	ENE.POW.NGS	FINEL.GAS
REFINGAS, LPG	EPOWERPLT	FINEL	OIL	ENE.POW.NGS	FINEL.OIL
BLFURGS, COKEOVGS, ETHANE, GASWKSGS, MANGAS, NATGAS, NGL, OXYSTGS	EPUMPST	FINEL	GAS	ENE.PUM.NGS	FINEL.GAS
REFINGAS, LPG	EPUMPST	FINEL	OIL	ENE.PUM.NGS	FINEL.OIL
BLFURGS, COKEOVGS, ETHANE, GASWKSGS, MANGAS, NATGAS, NGL, OXYSTGS	MAINCHP	FINEL	GAS	ENE.CHP.NGS	FINEL.GAS
REFINGAS, LPG	MAINCHP	FINEL	OIL	ENE.CHP.NGS	FINEL.OIL
BLFURGS, COKEOVGS, ETHANE, GASWKSGS, MANGAS, NATGAS, NGL, OXYSTGS	MAINELEC	FINEL	GAS	ENE.PEL.NGS	FINEL.GAS
REFINGAS, LPG	MAINELEC	FINEL	OIL	ENE.PEL.NGS	FINEL.OIL
BLFURGS, COKEOVGS, ETHANE, GASWKSGS, MANGAS, NATGAS, NGL, OXYSTGS	MAINHEAT	FINEL	GAS	ENE.DHE.NGS	FINEL.GAS
REFINGAS, LPG	MAINHEAT	FINEL	OIL	ENE.DHE.NGS	FINEL.OIL
ANTCOAL, BITCOAL, BKB, BROWN, COKCOAL, LIGNITE, PATFUEL, SUBCOAL, HARDCOAL	ENUC	FINEL	COAL	ENE.NUC.BTC	FINEL.COAL
BLFURGS, COKEOVGS, ETHANE, GASWKSGS, MANGAS, NATGAS, NGL, OXYSTGS	ENUC	FINEL	GAS	ENE.NUC.NGS	FINEL.GAS
REFINGAS, LPG	ENUC	FINEL	OIL	ENE.NUC.NGS	FINEL.OIL
GASDIES, MOTORGAS	ENUC	FINEL	OIL	ENE.NUC.OPR	FINEL.OIL
GASDIES, MOTORGAS	AUTOCHP	FINEL	OIL	ENE.AHP.OPR	FINEL.OIL
GASDIES, MOTORGAS	AUTOELEC	FINEL	OIL	ENE.AEL.OPR	FINEL.OIL
GASDIES, MOTORGAS	AUTOHEAT	FINEL	OIL	ENE.AHE.OPR	FINEL.OIL
GASDIES, MOTORGAS	EPOWERPLT	FINEL	OIL	ENE.POW.OPR	FINEL.OIL
GASDIES, MOTORGAS	EPUMPST	FINEL	OIL	ENE.PUM.OPR	FINEL.OIL
GASDIES, MOTORGAS	MAINCHP	FINEL	OIL	ENE.CHP.OPR	FINEL.OIL
GASDIES, MOTORGAS	MAINELEC	FINEL	OIL	ENE.PEL.OPR	FINEL.OIL
GASDIES, MOTORGAS	MAINHEAT	FINEL	OIL	ENE.DHE.OPR	FINEL.OIL
GBIOMASS, SBIOMASS, BIOGASOL, INDWASTE, MUNWASTEN, MUNWASTER, CHARCOAL	AUTOCHP	FINEL	BIO	ENE.AHP.NSF	FINEL.BIO
GBIOMASS, SBIOMASS, BIOGASOL, INDWASTE, MUNWASTEN, MUNWASTER, CHARCOAL	AUTOELEC	FINEL	BIO	ENE.AEL.NSF	FINEL.BIO
GBIOMASS, SBIOMASS, BIOGASOL, INDWASTE, MUNWASTEN, MUNWASTER, CHARCOAL	AUTOHEAT	FINEL	BIO	ENE.AHE.NSF	FINEL.BIO
GBIOMASS, SBIOMASS, BIOGASOL, INDWASTE, MUNWASTEN, MUNWASTER, CHARCOAL	EPOWERPLT	FINEL	BIO	ENE.POW.NSF	FINEL.BIO
GBIOMASS, SBIOMASS, BIOGASOL, INDWASTE, MUNWASTEN, MUNWASTER, CHARCOAL	EPUMPST	FINEL	BIO	ENE.PUM.NSF	FINEL.BIO
GBIOMASS, SBIOMASS, BIOGASOL, INDWASTE, MUNWASTEN, MUNWASTER, CHARCOAL	MAINCHP	FINEL	BIO	ENE.CHP.NSF	FINEL.BIO
GBIOMASS, SBIOMASS, BIOGASOL, INDWASTE, MUNWASTEN, MUNWASTER, CHARCOAL	MAINELEC	FINEL	BIO	ENE.PEL.NSF	FINEL.BIO
GBIOMASS, SBIOMASS, BIOGASOL, INDWASTE, MUNWASTEN, MUNWASTER, CHARCOAL	MAINHEAT	FINEL	BIO	ENE.DHE.NSF	FINEL.BIO

For the sectors ‘production’ and ‘use other products’ (including solvents) growth rates for the emissions are scaled with the population growth rate. The population growth rate is taken from the ADAM project scenarios (van Vuuren et al., 2009).

A2.2 Agriculture

Trends in agriculture, land use and waste were also derived from the ADAM project with emission trends given by world region for a baseline scenario and a stabilization scenario (450 ppm) based on runs with the IMAGE model. For example, agricultural soils emissions follow ADAM growth rates of fertilizers and crop. In A2-2 the allocation of the respective ADAM scenario growth rates to all EDGAR sectors and substances are presented. For the sectors 'solid waste disposal' (main sector: waste) emissions of all components are scaled with the population growth rate, while emissions of 'waste water treatment' are scaled with growth rates of sewage. In the sectors 'agricultural soils' the emissions of the respective substances are scaled with the specific growth rates of the corresponding emitters, e.g. N_2O emissions are scaled with the growth rate of fertilizer combined with the growth rate of crop residues. Emissions of 'enteric fermentation' are scaled with the growth rates of the corresponding animals. Emissions of 'manure management' of the respective substances are scaled with the growth rates of animal waste. The emissions of 'agricultural waste burning' are scaled with the growth rates of CH_4 emissions from agricultural waste burning (ADAM). Indirect emissions are assumed constant in time.

Table A2-2: Allocation per sector and component of ADAM growth rates 450 & BASELINE scenarios

Substance	CIRCE-EDGAR Sectors	Based on ADAM 450 & baseline growth rates
NOx	Agricultural soils	NOx, N2O from fertilizer ADAM450/BASELINE and crop residues ADAM450/BASELINE
NOx	Agricultural waste burning	N2O, CH4 from agricultural waste burning ADAM450/BASELINE
NOx	Solid waste disposal	population from ADAM450/BASELINE
SO2	Agricultural waste burning	CH4 from agricultural waste burning ADAM450/BASELINE
SO2	Solid waste disposal	population from ADAM450/BASELINE
NMVOC	Agricultural waste burning	CH4 from agricultural waste burning ADAM450/BASELINE
NMVOC	Solid waste disposal	population from ADAM450/BASELINE
CO	Agricultural waste burning	CH4 from agricultural waste burning ADAM450/BASELINE
CO	Solid waste disposal	population from ADAM450/BASELINE
NH3	Agricultural soils	NH3, N2O fertilizers ADAM450/BASELINE+ NH3, N2O crops ADAM450/BASELINE
NH3	Agricultural waste burning	N2O, CH4 from agricultural waste burning ADAM450/BASELINE
NH3	Manure management	NH3, N2O animal waste ADAM450/BASELINE
NH3	Solid waste disposal	population from ADAM450/BASELINE
CH4	Agricultural soils	CH4 from ADAM450/BASELINE, wetland rice
CH4	Agricultural waste burning	CH4 from agricultural waste burning ADAM450/BASELINE
CH4	Enteric Fermentation	CH4 from ADAM450/BASELINE, animals
CH4	Manure management	CH4 from ADAM450/BASELINE, animal waste
CH4	Solid waste disposal	CH4 from ADAM450/BASELINE, landfills
CH4	Waste water treatement	CH4 from ADAM450/BASELINE, sewage
CO2	Agricultural soils	keep constant
CO2	Solid waste disposal	population from ADAM450/BASELINE
N2O	Agricultural soils	N2O fertilizers ADAM450/BASELINE+ N2O crop residue ADAM450/BASELINE
N2O	Agricultural waste burning	N2O, CH4 from agricultural waste burning ADAM450/BASELINE
N2O	Manure management	N2O animal waste ADAM450/BASELINE
N2O	Solid waste disposal	population from ADAM450/BASELINE
N2O	Waste water treatement	N2O from ADAM450/BASELINE ,domestic sewage
N2O	N2O Indirect emissions	constant
BC	Agricultural waste burning	CH4 from agricultural waste burning ADAM450/BASELINE
OC	Agricultural waste burning	CH4 from agricultural waste burning ADAM450/BASELINE
CO2	Agricultural waste burning	CH4 from agricultural waste burning ADAM450/BASELINE
NOx	Manure management	N2O animal waste ADAM450/BASELINE

In A2-3 an overview is given of the technical aspects of the calculation method for the different scenarios. Following abbreviations are used: "cst" is used as "constant", "AD" is used as "activity data", "EF" is used as "emission factor", "IEF" is used as "implied emission factor" and "E" is used as "emission".

Table A2-3: Overview of used CIRCE-EDGAR sectors and the coupling with growth rates based form POLES and ADAM for the BAU scenario

Business as usual				
Sector desricption	***CIRCE-EDGAR-BAU Acronyms***	***Activity Data (AD)***	***Emission Factor (EF)***	***Emissions (E) (kton)***
Agricultural soils	AGS	AD(x)=E(2005)/EF(2005)=cst01	EF(x)=E(x)/AD(2005)	EF(x) scaled with IMAGE-ADAMbaseline-BAU(x)
Agricultural waste burning	AWB	AD(x)=E(2005)/EF(2005)=cst02	EF(x)=E(x)/AD(2005)	EF(x) scaled with IMAGE-ADAMbaseline-BAU(x)
Production of chemicals	CHE	AD(x) scaled with POLES-FCCHI-BAU(x) as like IND	EF(x)=E(2005)/AD(2005)=cst11	E(x)=AD(x)*EF(2005)
Energy industry	ENE	AD(x) scaled with POLES-FINEL-BAU(x)	EF(x)=E(2005)/AD(2005)=cst12	E(x)=AD(x)*EF(2005)
Enteric Fermentation	ENF	AD(x)=E(2005)/EF(2005)=cst03	EF(x)=E(x)/AD(2005)	EF(x) scaled with IMAGE-ADAMbaseline-BAU(x)
Manufacturing industry	IND	AD(x) scaled with POLES-FC…-BAU(x)	EF(x)=E(2005)/AD(2005)=cst13	E(x)=AD(x)*EF(2005)
Production of iron & steel	IRO	AD(x) scaled with POLES-FCSTI-BAU(x) as like IND	EF(x)=E(2005)/AD(2005)=cst14	E(x)=AD(x)*EF(2005)
Manure Management	MNM	AD(x)=E(2005)/EF(2005)=cst04	EF(x)=E(x)/AD(2005)	EF(x) scaled with IMAGE-ADAMbaseline-BAU(x)
Non-energy use of fuels	NEU	AD(x) scaled with POLES-FCCHF-BAU(x)	EF(x)=E(2005)/AD(2005)=cst15	E(x)=AD(x)*EF(2005)
Production of non-ferrous metals	NFE	AD(x) scaled with POLES-FCOIN-BAU(x) as like IND	EF(x)=E(2005)/AD(2005)=cst16	E(x)=AD(x)*EF(2005)
Production of non-metallic minerals	NMM	AD(x) scaled with POLES-FCNMM-BAU(x) as like IND	EF(x)=E(2005)/AD(2005)=cst17	E(x)=AD(x)*EF(2005)
Fuel production & transmission	PRO	AD(x) scaled with POLES-PRT…-BAU(x)	EF(x)=E(2005)/AD(2005)=cst18	E(x)=AD(x)*EF(2005)
Production and use of other products	PRU	AD(x)=E(2005)/EF(2005)=cst05	EF(x)=E(x)/AD(2005)	E(x) scaled with population(x)
Residential combustion	RCO	AD(x) scaled with POLES-FC…(x)	EF(x)=E(2005)/AD(2005)=cst19	E(x)=AD(x)*EF(2005)
Oil refineries	REF	AD(x) scaled with POLES-PRTOIL-BAU(x)	EF(x)=E(2005)/AD(2005)=cst20	E(x)=AD(x)*EF(2005)
Application of solvents	SOL	AD(x)=E(2005)/EF(2005)=cst06	EF(x)=E(x)/AD(2005)	E(x) scaled with population(x)
Solid waste disposal	SWD	AD(x)=E(2005)/EF(2005)=cst07	EF(x)=E(x)/AD(2005)	E(x) scaled with IMAGE-ADAMbaseline-BAU(x)
Non-road transport excluding aviation and shipping	TNR	AD(x) scaled with POLES-FCOTT-BAU(x)	EF(x)=E(2005)/AD(2005)=cst21	E(x)=AD(x)*EF(2005)
Aviation	TNR.DAT & TNR.IAT	AD(x) scaled with POLES-FCART.OIL-BAU(x)	EF(x)=E(2005)/AD(2005)=cst22	E(x)=AD(x)*EF(2005)
Transformation industry	TRF	AD(x) scaled with POLES-PRT…-BAU(x)	EF(x)=E(2005)/AD(2005)=cst23	E(x)=AD(x)*EF(2005)
Road transport	TRO	AD(x) scaled with POLES-FCROT-BAU(x)	EF(x)=E(2005)/AD(2005)=cst24	E(x)=AD(x)*EF(2005)
Ships	TNR.SEA	AD(x) scaled with SEABUNKER_BAU_POLES(x)	EF(x)=E(2005)/AD(2005)=cst25	E(x)=AD(x)*EF(2005)
Waste Water Treatment	WWT	AD(x)=E(2005)/EF(2005)=cst08	EF(x)=E(x)/AD(2005)	EF(x) scaled with IMAGE-ADAMbaseline-BAU(x)

Annex 3: Effects of air pollutants on vegetation and health

A3.1 Ozone damage to crops (wheat)

a) Index and exposure-response function

The crop damage for wheat is calculated as a relative yield loss (RYL), for which an exposure-response function is available as a function of AOT40, the accumulated hourly concentration above a threshold of 40 ppbV during a 3 months growing season (Fuhrer et al, 1997; Mills et al., 2007).

$$\mathrm{AOT40} = \sum_{i=1}^{n} [O_3]_i - 40, [O_3]_i \geq 40\mathrm{ppbV},$$

$[O_3]_i$ = hourly ozone concentration, between 8 : 00 and 20 : 00 local time

RYL = 0.0161*AOT40 (ppm.h)

b) Crop distribution map

The gridded spatial crop distribution is based on the crop-specific Global Agro-Ecological Zones (GAEZ) suitability index, developed by Fischer et al. (2000). The crop suitability index (SI) is a modelled index, based on local soil and terrain properties, rainfall, temperature limitations, land use, … By lack of global gridded crop distribution maps based on observations, the GAEZ suitability maps are probably the best ones available to describe the spatial distribution of individual crops.

A3.2 Ozone and PM effects on human health

a) Indices used for the evaluation of the health impact.

The health impact of particulate matter for each scenario is calculated as a function of total anthropogenic PM10 (i.e. the sum of sulphate, nitrate, ammonium, black carbon and primary organic carbon). In other words, the reference level (or counterfactual value) is the natural background. In our assessment we distinguish urban and rural PM10 levels (see below).

The health impact of ozone is based on the indicator SOMO35 (sum of means over 35 ppbV). SOMO35 accumulates during one year the daily excess of the maximal 8-hourly average O_3 concentration over 35 ppbV. Hence, by definition, the indicator includes a reference level of 35 ppbV at which no health effect is assumed. For ozone, no difference is made between urban and rural concentrations.

b) Dose-response functions

The impact of each of both pollutants on health is expressed as a concentration-dependent proportionality factor (the relative risk function, RR) by which the baseline mortality rate μ_0 is multiplied. The baseline mortality rate is here defined as the mortality rate at the so-called counterfactual value, or reference level (i.e. PM10 = natural components, SOMO35 = 0 respectively). Taking into account that the actual mortality rate μ_a includes the effect of pollution, the baseline mortality rate is lower than the actual mortality rate, and is given by:

$\mu_0 = \mu_a / RR_i$ (i = O_3 or PM)

$RR_{PM} = e^{\beta_{PM} * \Delta PM}$

$\beta_{PM} = 0.0024$ (Pope et al., 2002; World Bank, 2007)

$\Delta PM = PM_{10} - PM_{10,natural}$, i.e. the PM10 concentration above the natural background

$RR_{O3} = e^{\beta_{O3} * \Delta O3}$
β_{O3} = 0.0007 (derived from the WHO (2004) recommended value of 0.003 per 10µg/m³ O_3, converted to the risk rate for 1 ppbV of O_3)
ΔO_3 = SOMO35/365, i.e. the average daily exceedance of the maximal 8 hourly average above 35 ppbV, averaged over 1 year, expressed in ppbV.

Compared to European and US studies we have to take into account the occurrence of very high PM10 levels in Asia, which lie outside the range of the Pope study. In fact, the Pope relative risk function reaches 1.38 at a concentration of 150 µg/m³, implying that 28 percent of deaths are premature deaths attributable to air pollution. This is clearly an implausible result. Cohen et al. (2004) dealt with this issue by assuming that the RR function becomes horizontal at approximately 100 µg/m³ of PM10. In our analysis we maintained this approach, although it implies no health benefit from a reduction of PM10 from 150 to100 µg/m³ (World Bank, 2007). Results from other approaches, like the one described in the World Bank 2007 report, are available, but not shown here.

As discussed by Holland et al. (2005) the short term ozone health effect on premature mortalities is considered to bring forward the moment of death with 3 to 18 months (central value 12 months) for persons who were already approaching decease. In other words, although ozone contributes to premature mortality, it is not the only cause of death and conversely, the benefit of reducing ozone through reducing short-term mortalities should be scaled down to reflect the limited responsibility of ozone in the cause of the mortalities. Life-table calculations assuming a 12 month lifetime reduction for each ozone-related mortality indicate that this reduces the O_3 contribution to the number of life years lost from a population with a factor 20 compared to a 100% responsibility assumption. Note that even under the latter assumption the ozone health effect in polluted areas is generally an order of magnitude lower than the PM health effect. Compared to reduction in PM levels, where long-term effects on mortality are calculated as a 100% PM effect, changes between the scenarios in the O_3 health effect can be considered to be negligible.

c) *Resulting change in statistical life expectancy (due to PM)*

The life expectancy reduction due to actual PM10 above their respective counterfactual levels is calculated from the evolving survival function over time of an initially 30-years-old cohort (year 2000) until death, according to the methodology applied in the CAFE assessment (Mechler et al., 2002). Younger cohorts are not followed since they were not addressed in the epidemiological studies.
The survival function indicates the percentage of a cohort alive after a time t has elapsed since the starting time. The function derives directly from age-dependent mortality rates (for details see Mechler et al., 2002). The baseline mortality rate $\mu_{0,}$ being a factor 1/RR lower than the actual mortality rate, leads to a higher statistical life expectancy than μ_a. The difference between the two life-expectancy calculations (baseline minus actual) yields the change in life expectancy caused by actual levels of PM10. Age-specific mortality rates for each country are available from the world population projections of the United Nations (UN, 2006). The UN prospects take into account that mortality rates at a given age tend to decrease in the future. As the UN prospects reach until 2050, we assume that the mortality rates remain constant after that.

d) *Urban versus rural population*

Because of the important contribution of traffic and households to emissions of particulate matter, urban areas experience significantly higher PM levels than the rural background. As the model resolution of 1°x1° can not resolve urban areas that extend over areas which are smaller than the grid cell area, we have to apply a sub-grid parameterization. The algorithm estimates the urban increment of (non-reactive) primary emitted anthropogenic black carbon and organic matter compared to the rural background. This is achieved by scaling the sub-grid emission strength of those compounds to urban and rural sub-grids within the native grid cell. The sub-grid is based on high-resolution

(2.5'x2.5') population dataset (CIESIN, university of Columbia) which subdivides the 1°x1° native TM5 grid in 24x24 subgrid cells. A subgrid cell is labelled as 'urban' if the population density exceeds 600/km², and 'rural' otherwise.

Let f_{UP} be the urban population fraction, defined as the fraction of the population within the 1°x1° gridcell which resides in the urban-flagged subgrid cells, and f_{UA} the urban area fraction, being the fraction of the 1x1 grid area occupied by the urban-flagged subgrid cells (in practice: the number of urban subgrid cells divided by 576, i.e. the total nr. of subgrid cells).

For convenience, we use in the following Black Carbon, but it holds also for particulate organic matter. Let E_{BC} be the emission strength of the anthropogenic BC of the whole native (1°x1°) grid cell. We make the assumption that the fraction $f_{UP}.E_{BC}$ is emitted from area $f_{UA}.A$ (A being the grid cell area) and $(1- f_{UP}).E_{BC}$ from area $(1- f_{UA}).A$.

In a simple box model approximation, under steady-state conditions, neglecting the transport of concentration of BC from neighbouring gridcells, the grid-average BC concentration can be written as:

$C_{BC} = \frac{E_{BC}}{\lambda}$ with λ = ventilation factor

Considering the urban and rural areas as sub-boxes of the native grid box, and assuming that the same ventilation factor λ is also valid for the urban and rural part of the grid cell (equivalent with the assumption that mixing layer height and wind speed are the same for all subgrid cells), the steady-state concentration in the urban sub-area can be written as:

$$C_{BC} = \frac{f_{UP}}{f_{UA}} \frac{E_{BC}}{\lambda} \text{ and } C_{BC} = \frac{(1 - f_{UP})}{(1 - f_{UA})} \frac{E_{BC}}{\lambda}$$

The ventilation factor λ, including an implicit correction factor for the non-zero background concentration in neighbouring cells, is obtained by taking advantage of the explicitly modelled gridcell concentration with the chemical transport model (C_{TM5}):

$$\lambda = \frac{E_{BC}}{C_{BC,TM5}}$$

Hence,

$$C_{BC,URB} = \frac{f_{UP}}{f_{UA}} C_{BC,TM5} \text{ and } C_{BC,RUR} = \frac{(1 - f_{UP})}{(1 - f_{UA})} C_{BC,TM5}$$

In order to avoid artificial spikes in urban concentrations when occasionally a very small fraction of the native grid cell contains a very large fraction of the population, we apply empirical bounds on the adjustment factors:

1) Rural Primary BC and POM *($C_{eq,RUR}$)* should not be lower than 0.5 times the TM5 grid average
2) Urban primary BC and POM should not exceed the rural concentration by a factor 5.

These assumptions are consistent with observations summarized in aerosol climatologies in Europe (e.g. Putaud et al. 2010).

In any case, the urban and rural adjustments for each of the primary components must fulfil the condition:

$$f_{UA}C_{URB} + (1 - f_{UA})C_{RUR} = C_{TM5}$$

The adjusted urban and rural concentrations of the primary emitted components can be cast in one 1°x1°-grid population-weighted average value:

$$C^{pop}_{BC,TM5} = f_{UP} \cdot C_{BC,URB} + (1 - f_{UP}) \cdot C_{BC,RUR}$$

After substituting $C_{BC,URB}$ and $C_{BC,RUR}$, the population-weighted concentration is expressed as a function of the area-weighted average concentration:

$$C^{pop}_{BC,TM5} = \left[\frac{(f_{UP})^2}{f_{UA}} + \frac{(1 - f_{UP})^2}{1 - f_{UA}} \right] \cdot C^{area}_{BC,TM5}$$

And similar for primary anthropogenic organic carbon.
All secondary components (sulfates, nitrates, secondary organic matter) and primary natural PM (mineral dust, seasalt) are assumed to be distributed uniformly over the native 1x1 gridcell.

Validation of the methodology:
We make use of a consolidated database of urban measurements established in the frame of the Global Burden of Disease project (courtesy Michael Brauer, 2010). Because the database contains exclusively urban measurements, we extract from the model the adjusted urban PM2.5, rather than the population-weighted average for the whole grid cell. The scatter plots show that on the average, the applied parameterization significantly improves the performance of the model compared to the non-adjusted PM2.5 concentration, although the scatter remains high. Reproducing the high variability of (primary) PM levels in the vicinity of its sources is beyond the scope and possibilities of the current global models, however we are confident that region-wide exposure estimates are improved by applying the methodology described above.

:

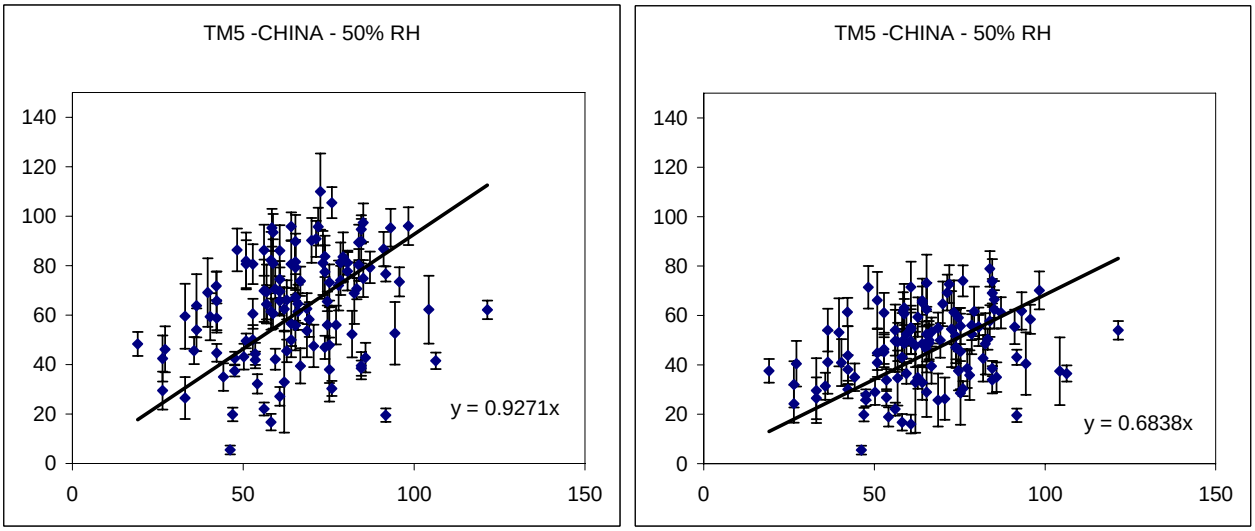

Figure A3.1 Comparison of measured (x-axis) and modeled data, with (left) and without (right) the urban increment methodology, measurements in abscissa.

e) Comparison of WHO and Worldbank methodology

In Table A3-1 we give a comparison of the above described WHO methodology for calculating LLE due to particulate matter, compared to the Worldbank methodology. The latter uses a modified risk-rate function as an alternative to the 'capped' WHO risk rate function in order to avoid unrealistically high PM-induced mortalities at extremely high PM loadings. The RR function is given by (World Bank, 2007):

$RR = \left(\frac{PM10}{CF} \right)^{\beta}$, $\beta = 0.073$, using a counterfactual concentration CF of 15 µg/ m³, or the concentration of natural aerosol (which ever is higher). We consider the BAU-2030 case, and the difference of BAU-2030 and Base-2000. LLE are in general smaller by ca. 30 %; in East Asia this is not the case since a limit value of 100 µg/m³ is not used in the Worldbank method.

Table A3-1 Loss of Life expectancy calculated with two different approaches for the risk rate function and counterfactual value

	LLE_pm (months) BAU 2030		Delta LLE BAU_2030-Base_2000	
Region	WHO	WB	WHO	WB
CANADA	5.7	3.1	0.6	0.5
USA	10.2	6.8	1.3	1.0
CENTRAL AMERICA	8.1	4.8	0.9	0.7
SOUTH AMERICA	3.8	2.1	0.8	0.6
NORTHERN AFRICA	5.1	1.7	0.4	0.1
WESTERN AFRICA	12.8	7.1	1.9	1.4
EASTERN AFRICA	5.9	3.6	1.0	0.7
SOUTHERN AFRICA	3.5	1.6	0.6	0.4
OECD EUROPE	8.5	6.1	-0.2	-0.2
EASTERN EUROPE	8.7	5.8	-0.4	-0.4
FORMER USSR	6.5	3.5	0.3	0.2
MIDDLE EAST	6.5	3.4	0.7	0.4
SOUTH ASIA	24.3	15.4	7.3	4.0
EAST ASIA	23.0	16.5	4.1	4.4
SOUTH EAST ASIA	8.7	5.4	3.0	2.3
OCEANIA	1.2	1.1	0.0	0.0
JAPAN	7.6	5.3	0.8	0.9
NH	15.5	10.2	3.3	2.4
SH	3.3	1.6	0.7	0.5
World	14.0	9.1	3.0	2.2

f) Calculation of integrated life years lost.

In TableA3-2 we give the integrated amounts of life years lost, calculated by multiplying the regional LLEs (months for a specific region) by the regional population numbers for the year 2000. We note that accuracy of these calculations could be improved by using scenario forecasts for population in the year 2030 and 2050, respectively, which would increase the numbers significantly.

Table A3-2: Population-integrated number of life years lost over an average lifetime above the age of 30 years. Numbers pertain to the population for the year 2000.

		Life years lost (million)										
	Population (million)	**Base-2000**	**Bau-2030**	**Carb-2030**	**BAP-2030**	**CAP-2030**	**BAP60 Non OECD 2030**	**CAP60 Non OECD _2030**	**Bau-2050**	**Carb-2050**	**BAP-2050**	**CAP-2050**
CANADA	29.7	13	14	12	10	9	10	9	15	11	10	8
USA	255.1	189	216	166	123	102	124	102	232	162	132	101
CENTRAL AMERICA	155.0	93	105	90	76	71	87	79	105	83	77	70
SOUTH AMERICA	326.1	83	105	90	60	55	81	72	114	86	63	53
NORTHERN AFRICA	136.6	53	58	43	29	24	37	29	66	38	33	23
WESTERN AFRICA	299.7	271	319	287	222	204	256	234	325	268	224	191
EASTERN AFRICA	186.4	77	92	83	75	69	87	79	101	78	79	66
SOUTHERN AFRICA	139.8	33	40	35	26	24	31	28	42	32	27	22
OECD EUROPE	338.5	244	239	190	129	111	131	112	250	180	135	106
EASTERN EUROPE	117.5	89	85	68	53	46	56	47	88	61	54	43
FORMER USSR	285.1	147	154	120	86	72	112	90	161	104	92	69
MIDDLE EAST	218.0	105	119	96	69	56	88	71	143	82	84	53
SOUTH ASIA	1,293.1	1,824	2,615	2,287	1,760	1,530	2,180	1,865	2,966	2,483	2,412	1,759
EAST ASIA	1,301.3	2,045	2,490	2,285	2,189	1,751	2,372	2,051	2,527	2,032	2,238	1,340
SOUTH EAST ASIA	439.5	207	317	248	204	164	252	199	339	198	212	130
OCEANIA	23.4	2	2	2	1	1	1	1	2	2	1	1
JAPAN	117.1	66	74	63	61	55	65	57	75	57	61	51
World	5,544.8	5,076	6,453	5,648	4,739	3,979	5,470	4,696	6,919	5,457	5,438	3,741

Table A3-3: Change in the population-integrated number of life years lost over an average lifetime above the age of 30 years

		delta life years lost compared to Base-2000									
	Population (million)	**Bau-2030**	**Carb-2030**	**BAP-2030**	**CAP-2030**	**BAP60-Non OECD_2030**	**CAP60-Non OECD_2030**	**Bau-2050**	**Carb-2050**	**BAP-2050**	**CAP-2050**
CANADA	29.7	1	-1	-3	-4	-3	-4	2	-1	-2	-4
USA	255.1	27	-23	-66	-87	-65	-86	43	-27	-57	-88
CENTRAL AMERICA	155.0	11	-3	-17	-22	-7	-15	11	-10	-16	-24
SOUTH AMERICA	326.1	21	7	-24	-28	-2	-11	31	3	-21	-31
NORTHERN AFRICA	136.6	4	-11	-25	-30	-16	-24	13	-16	-20	-31
WESTERN AFRICA	299.7	48	16	-49	-67	-14	-36	55	-2	-46	-80
EASTERN AFRICA	186.4	16	6	-2	-8	10	2	24	1	2	-11
SOUTHERN AFRICA	139.8	8	2	-6	-9	-1	-5	10	-1	-6	-11
OECD EUROPE	338.5	-5	-54	-115	-133	-114	-133	6	-64	-110	-139
EASTERN EUROPE	117.5	-4	-21	-36	-43	-33	-42	-1	-28	-35	-46
FORMER USSR	285.1	7	-26	-60	-75	-35	-56	14	-43	-54	-77
MIDDLE EAST	218.0	13	-9	-37	-49	-17	-34	38	-23	-21	-52
SOUTH ASIA	1,293.1	791	463	-63	-294	356	41	1,142	660	588	-65
EAST ASIA	1,301.3	445	240	144	-294	327	6	482	-13	193	-705
SOUTH EAST ASIA	439.5	110	42	-3	-42	46	-7	132	-9	5	-77
OCEANIA	23.4	0	0	-1	-1	-1	-1	0	-1	-1	-1
JAPAN	117.1	8	-3	-5	-11	-1	-9	9	-9	-5	-15
World	5,544.8	1,377	572	-337	-1,097	393	-380	1,843	381	362	-1,335

ANNEX 4: Calculation of Radiative Forcing for aerosols and ozone

A4.1 Radiative Forcing of aerosol

The aerosol radiative forcing is defined as the change in the energy balance at the top of the atmosphere (TOA). Atmospheric aerosols influence the radiative budget of the Earth-Atmosphere system in two different ways.
The direct forcing results from scattering and absorbing of the solar and thermal infrared radiation by aerosol particles, thereby altering the planetary albedo (Charlson et al., 1992).
In our study only the short wave spectrum 0.2-5 μm has been considered, since the anthropogenic aerosols are most efficient in scattering and absorbing the solar radiation in the submicron size range. We consider sulfate, black and organic carbon (BC and OC). The optical properties of sulfate, which mainly scatters shortwave radiation, are reasonably well known compared with other types of aerosols (Li et al., 2001). The optical properties of OC are not well established, the so far investigated organic acids are found to scatter solar radiation similar to sulfate (Myhre and Nielsen, 2004). Enhanced aerosol scattering of solar radiation back into space increases the planetary albedo and is therefore associated with cooling. BC is a strong absorber of solar radiation and is therefore associated with warming (Hess at al., 1998).
The indirect forcing results from modification of microphysical and radiative properties and lifetime of clouds by aerosols (Haywood and Boucher, 2000). In this study we have only considered the so far best established first indirect effect using the method described by Boucher and Lohmann (1995). This forcing results from the ability of the hydroscopic particles to act as cloud condensation nuclei thus altering the size, the number and the optical properties of cloud droplets (Twomey, 1974). More and smaller cloud droplets increase the cloud albedo which leads to cooling. While there are very large uncertainties associated with the estimates of the indirect effect the overall calculated magnitude matches the published literature range. The radiative forcing of the simulated monthly averaged aerosol burden was consequently calculated using the off-line radiative Transfer Model described by Marmer et al. (2007), using monthly average meteorological fields and surface characteristics retrieved from the ECMWF database for the year 2001. Radiative calculations are performed for the Base Case and for each scenario accordingly The difference in the net radiation at the top of the atmosphere between Base and each scenario yields the TOA radiative forcing. We assume externally mixed aerosols and calculate the forcing separately for each component. The total aerosol forcing is obtained by summing up these results. . To avoid further extensive radiative transfer calculation, we stored the monthly radiative forcing efficiencies for further use. Radiative forcing efficiency for SO4, POM, and BC are given in Figure A4.1

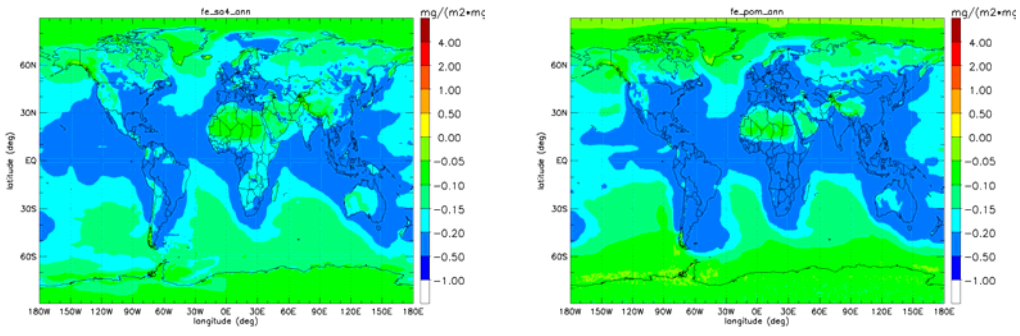

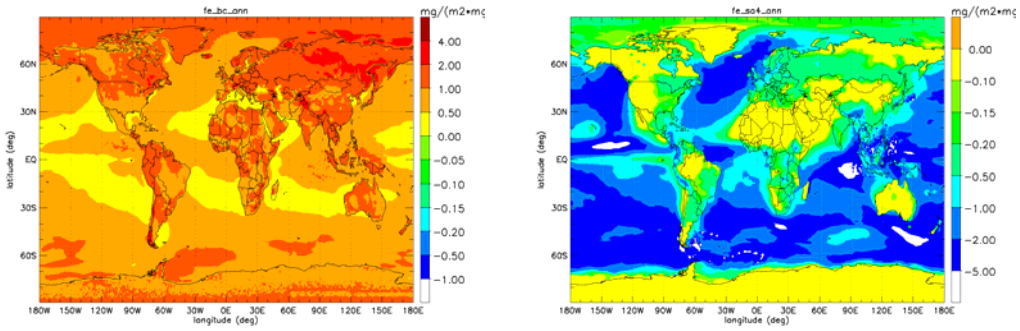

Figure A4.1 Annual average Radiative Forcing coefficients for SO4, Particulate Organic Matter, Black carbon, and the indirect forcing associated with SO4 [W/(m^2*mg).

A4.2 Radiative Forcing for ozone

Radiative forcing for ozone was approximated by using the forcings obtained for the scenario results by Dentener et al (2005), and scaling it with the ozone columns obtained in this study. The radiative transfer model in that study was based on Edwards and Slingo (1996), these forcings account for stratospheric adjustment, assuming the fixed dynamical heating approximation, which reduces instantaneous forcings by ~22%. The forcing calculations were performed by D. Stevenson (University of Edinburgh) in 2004, and provided as monthly averages. The resulting annual average forcing efficiency is given in Figure A4.2. We note the highest radiative forcing per Dobson unit (a commonly used measure of column integrated ozone) in the tropics, especially over bright surfaces. The resulting efficiencies are comparable to the forcing efficiencies calculated by Gauss et al. [2003].

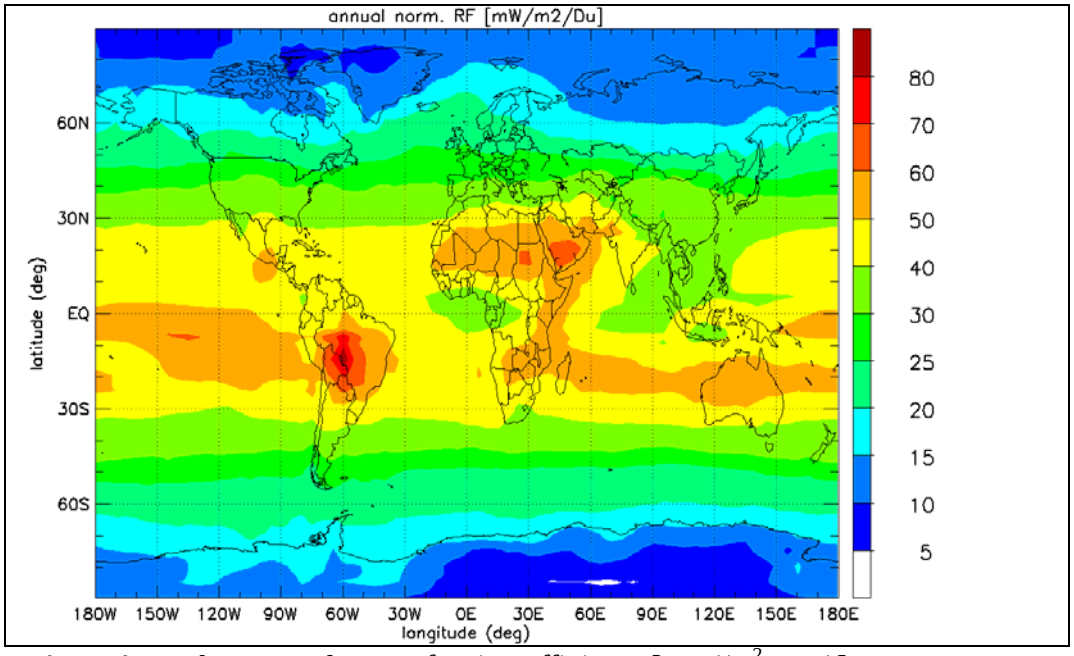

*Figure A4.2. Annual averaged ozone forcing efficiency[mW/(m^2*DU)]*

European Commission

EUR 24572 EN – Joint Research Centre – Institute for Environment and Sustainability
Title: Climate and Air Quality Impacts of Combined Climate Change and Air Pollution Policy Scenarios
Author(s): John van Aardenne, Frank Dentener, Rita Van Dingenen, Greet Maenhout, Elina Marmer, Elisabetta Vignati, Peter Russ, Laszlo Szabo and Frank Raes
Luxembourg: Publications Office of the European Union
2010 – 71 pp. – 21 x 29.7 cm
EUR – Scientific and Technical Research series – ISSN 1018-5593
ISBN 978-92-79-17454-4
doi:10.2788/33719

Abstract

This report describes an assessment of the co-benefits for air pollution of recently developed climate mitigation scenarios that inform the European Union policy making. The climate mitigation scenarios were obtained with the POLES equilibrium model for a business-as-usual and greenhouse gas reduction case. In the present work, these scenarios were expanded to air pollution emissions. For this purpose, growth rates of POLES relative to International Energy Agency (IEA) base-year activity data were used and combined with reduced emission factors representing new technologies and additional end-of-pipe abatements projecting future air pollution emission controls. To complete the emission inventory projections for the agriculture and land-use sectors, the base-year activity data of the United National Food and Agriculture Organisation (FAO) were combined with growing emission factors obtained from the IMAGE model. The resulting set of global -spatially and sector disaggregated- air pollution emissions were evaluated with the global chemistry transport model TM5, to calculate levels of particulate matter and ozone. Subsequently, air pollution impacts on human health, ecosystems and climate were evaluated.

The resulting set of four scenarios thus reflect various combinations of worldwide air pollution and climate policies: BAU ("no further climate and air pollution policies since the 2000 base-year"); CARB ("climate policy only"), BAP ("no further climate policy, but progressive air pollution policies, to address worldwide increasing levels of air pollution) and CAP ("combination of ambitious climate and air pollution policies").

The implementation of a global climate policy (CARB) has substantial co-benefits for reducing air pollutant emissions. Compared to BAU, in 2050 global emissions of SO2 are reduced by ca. 75 %, NOx by 55 %, CO (40 %) and other pollutants VOC, OC and BC) about 25% %. These emission reductions result from cleaner technologies and decreased fuel demand, and correspond to a CO2 emission reduction of more than 60 %. Advanced air pollution abatement technologies can obtain similar air pollutant reductions ranging between 35 % (NO_x), 45 % (OC, BC), 60 % (SO_2) and 70% (CO), however in this case the CO_2 emissions reach unabated levels of 55 Pg CO_2/yr. The combined air pollution and climate policy case (CAP) further reduces BAP air pollution emissions by 10-30 %. Noticeable are the decreases of methane emissions by ca. 60 %, which have important impacts on ozone air quality and climate.

The environmental benefits of the emission reductions are substantial. In 2050, average global life expectancy increases by 3.2 months/person for BAP (compared to BAU) and further increases by 3.7 to 6.9 months/person if additionally climate policies are introduced (CAP). Compared to 2000, only the CAP scenario leads to global improvement of life-expectancy (by about 3 months/person), while all other scenarios lead to higher particulate concentration and lower life expectancies, mainly driven by pollution developments in South and East Asia. These improvements in CAP are due to decreasing concentrations of primary (OC, BC) and secondary (SO_4, NO_3) aerosol. This work shows that combining air pollution and climate policies is in some regions the only way to stabilize or decrease the levels of air pollution and reducing impacts on human health. The global average life expectancy, however, masks large regional differences: e.g. current and future levels of air pollution in Asia are much larger than in Europe or the United States. Crop losses due to ozone are reduced by 4.7

% by implementing progressive air pollution policies, and could be reduced by another 2 %, by introducing additional climate policies.

Climate policies target at limiting long-term (2100) climate change. On the intermediate time-scales (2030-2050), however, there might be important trade-offs to be considered in climate and air pollution policies, since reducing particulate matter and precursor (especially sulfur) emissions, are likely to lead to a net positive radiative forcing and a warming of climate. Since reductions of particulate matter and ozone are necessary to protect human health and vegetation, combined air pollution and climate policies are more beneficial for both climate and air pollution than stand-alone policies. There is scope to preferentially mitigate emissions of Black Carbon and methane, which is beneficial for climate and human health.

The mission of the JRC is to provide customer-driven scientific and technical support for the conception, development, implementation and monitoring of EU policies. As a service of the European Commission, the JRC functions as a reference centre of science and technology for the Union. Close to the policy-making process, it serves the common interest of the Member States, while being independent of special interests, whether private or national.

JRC
EUROPEAN COMMISSION

LB-NA-24572-EN-C

ISBN 978-92-79-17454-4

Publications Office